The functional significance of the alternative first exons of the *Arabidopsis thaliana APT1* gene

by

Antonio Facciuolo

A thesis

presented to the University of Waterloo

in fulfillment of the

thesis requirement for the degree of

Master of Science

in

Biology

Waterloo, Ontario, Canada, 2009

Author's Declaration

I hereby declare that I am the sole author of this thesis. This is a true copy of the thesis, including any required final revisions, as accepted by my examiners.

I understand that my thesis may be made electronically available to the public.

Abstract

In plants, adenine nucleotides are essential for nucleic acid synthesis, as cofactors for biochemical reactions, and as precursors for the biosynthesis of the phytohormone cytokinin. Adenine nucleotides, such as AMP, are synthesized by the *de novo* synthesis pathway involving 10 sequential enzymatic reactions and 7 ATP/GTP molecules, and by the less energy-demanding salvage reactions. The enzymes catalyzing the latter route collectively make up the purine salvage pathway.

The predominant enzyme in purine salvage is adenine phosphoribosyltransferase (APT), which catalyzes the one-step conversion of adenine to AMP. Plant APTs are also thought to contribute to the metabolism of cytokinins by interconverting the physiologically active base forms into their inactive nucleotide forms. In *Arabidopsis thaliana* APT is encoded by a five-member gene family, where APT1 contributes 99% of the APT activity. The *APT1* gene has a six-exon gene structure that is present in *APT* genes of other organisms. Recently, expressed sequence tag (EST) collections have shown that the *APT1* locus gives rise to a second, longer transcript variant that contains an additional 5′ terminal exon. For the purposes of this research the longer isoform has been designated *APT1.1* and the shorter version, *APT1.2*. The aim of the first part of my thesis research was to determine the functional significance of these two transcript variants.

Semi-quantitative RT-PCR showed that *APT1.1* and *APT1.2* transcripts are equally abundant in leaf and floral organs. However, immunoblot analysis revealed that APT1.2 is constitutively expressed, while APT1.1 is subject to post-transcriptional regulation in both organs. Using recombinant APT1.1 protein, preliminary enzymatic assays showed this protein to

be very active on adenine substrates. Transgenic lines were constructed that either constitutively expressed the APT1.1 ORF fused to GFP protein, or that only expressed an Exon 1-GFP fusion protein from the native *APT1* promoter. In both plant lines GFP localization was observed in stationary punctate bodies in mesophyll cells, whereas constitutive expression of the APT1.1 ORF also showed co-localization of GFP with chlorophyll autofluorescence. Although the identity of these punctate-bodies is currently inconclusive, preliminary data using transmission electron microscopy show that these bodies may be localized in areas of the chloroplast devoid of chlorophyll. Finally, bioinformatic analysis of available plant ESTs predicts that many other plants species may contain a similar gene structure to *APT1* of Arabidopsis that gives rise to a cytosolic APT, and a chloroplast-localized APT.

Interestingly, the only phenotype previously identified as arising from APT1-deficiency was aborted pollen development in a point mutant annotated as *apt1-3*. Recently, a novel APT1-deficient mutant was recovered during a screen for mutants that were tolerant to chemically induced oxidative stress. The mutant, *oxt1*, contains a T-DNA insertion element between the first and second exon of *APT1* and surprisingly is as fertile as WT. Thus, the second part of this research was to determine the basis of fertility in the *oxt1* mutant. A genetic cross between these two mutants resulted in an F1 plant that is a developmental chimera of both mutants. The initial siliques on the plant were fertile like *oxt1*, whereas the later siliques on the plant were sterile like *apt1-3*. Measurements of adenine and cytokinin levels showed substantial alterations in these metabolite levels. Thus, these metabolites may be potential contributors to the diverse phenotypes observed in each mutant. The discovery and characterization of the unusual phenotype of *oxt1apt1-3* hybrids will lead the way in providing a model system to study changes in metabolite levels that contribute to the shift from fertility to sterility.

Acknowledgements

Surprisingly, this section is more difficult to write than any other section of this thesis, because it is hard to find the right words to capture my sincere gratitude.

First and foremost I must thank my supervisor, Barb Moffatt. She has been absolutely awesome to work with these past three years. Her patience, guidance, helpfulness, enthusiasm and motivation (especially during the writing of this thesis) was more than one can expect. Thank you, Barb.

I want to thank my committee members, Dr. Trevor Charles and Dr. Matt Smith for being part of this experience. I also would like to thank Dr. Simon Chuong for being there anytime I needed advice, help or a second opinion.

A BIG, HUGE thank you to my lab mates (in no particular order): Katja, Sarah, Ishari, Sang, Yong, Makoto, and Terry. You all are truly great friends and have been great to work with, share ideas, and have been there for me when I needed it. A special thanks to Andrew Doxey for all his help with the bioinformatics aspects of this project.

Last, but not least, I want to thank my family especially my parents for their constant support throughout all my years in university (both those that have past, and those yet to come). I don't want to leave out the help of my brothers, sister-in-law, aunts, uncles, cousins (especially Stella for helping with my references and abbreviations), and my two special nieces that have done everything in their power to distract me when I was trying to focus.

Table of Contents

List of Figures

List of Tables

List of Abbreviations

AAH	allantoate amidohydrolase
ADK	adenosine kinase
ADP	adenosine diphosphate
amiRNA	artificial microRNA
AMP	adenosine monophosphate
APT	adenine phosphoribosyltransferase
AT	3-amino-1,2,4-triazole
ATP	adenosine triphosphate
ATase	amidophosphoribosyltransferase
BA	benzyladenine
BSA	bovine serum albumin
BSO	buthionine sulfoximne
DEPC	dimethylpyrocarbonate
DTT	dithiothreitol
EDTA	ethylene diamine tetraacetic acid

EMS	ethyl methane sulphonate
EST	Expressed Sequence Tag
FSD3	Iron Superoxide Dismutase 3
GUS	β-glucuronidase
HEPES	4-(2-hydroxyethyl)-1-piperazinepropane-sulfonic acid monohydrate
HPLC	high performance liquid chromatography
IMP	inosine monophosphate
iP	isopenetyl-adenine
IPTG	isopropyl-D-thiogalactopyranoside
K_M	Michaelis-Menten constant
KOH	potassium hydroxide
LB	Luria-Bertani
MEP	methylerythriol phosphate
MES	4-morpholineethanesulfonic acid monohydrate
MS	Murashige and Skoog

MVA	mevalonate
PBS	phosphate buffered saline
PCD	programmed cell death
PMSF	phenylmethyl sulfonyl fluoride
PRPP	phosphoribosyl pyrophosphate
RT-PCR	reverse transcription Polymerase chain reaction
PVDF	polyvinylidene fluoride
Q-TOF	quadrupole time of flight
SDS	sodium dodecyl sulphate
TAE	tris-acetate-EDTA
TPP	thiamine pyrophosphate
TSS	transcription start sites
tZ	trans-zeatin
V_{max}	maximal velocity

Introduction

Arabidopsis as a model organism

Arabidopsis thaliana is a small, flowering plant belonging to the Brassicaceae family (Figure 1). This plant has become the most widely used model system to study many aspects of plant biology including genetics, molecular and cellular biology, plant anatomy, and plant physiology. Arabidopsis offers many advantages for molecular genetic research because of its completely sequenced diploid genome of 125 Mbp that has a low percentage of repetitive DNA, short exonic and intronic regions, and relatively small intergenic distances indicative of its compact, enriched regulatory regions (The Arabidopsis Genome Initiative, 2000). This small plant is inexpensive to grow and has a short generation time of approximately 6 weeks resulting in seed yields of approximately 10,000 seeds per plant. The ease by which a variety of mutant types can be generated is a particular strength: ethyl methane sulphonate (EMS) is commonly used to create single nucleotide polymorphisms, *Agrobacterium tumefaciens*-mediated T-DNA insertion for gene disruption, or transgenic silencing to reduce the expression of single or multiple genes. Furthermore, protoplast isolation protocols have been developed for transient gene expression studies. These advantages have drawn a large community of scientists to focus their research on Arabidopsis. The research outlined in this thesis examines the functional significance of alternative first exons in an adenine salvage gene involved in purine nucleotide biosynthesis.

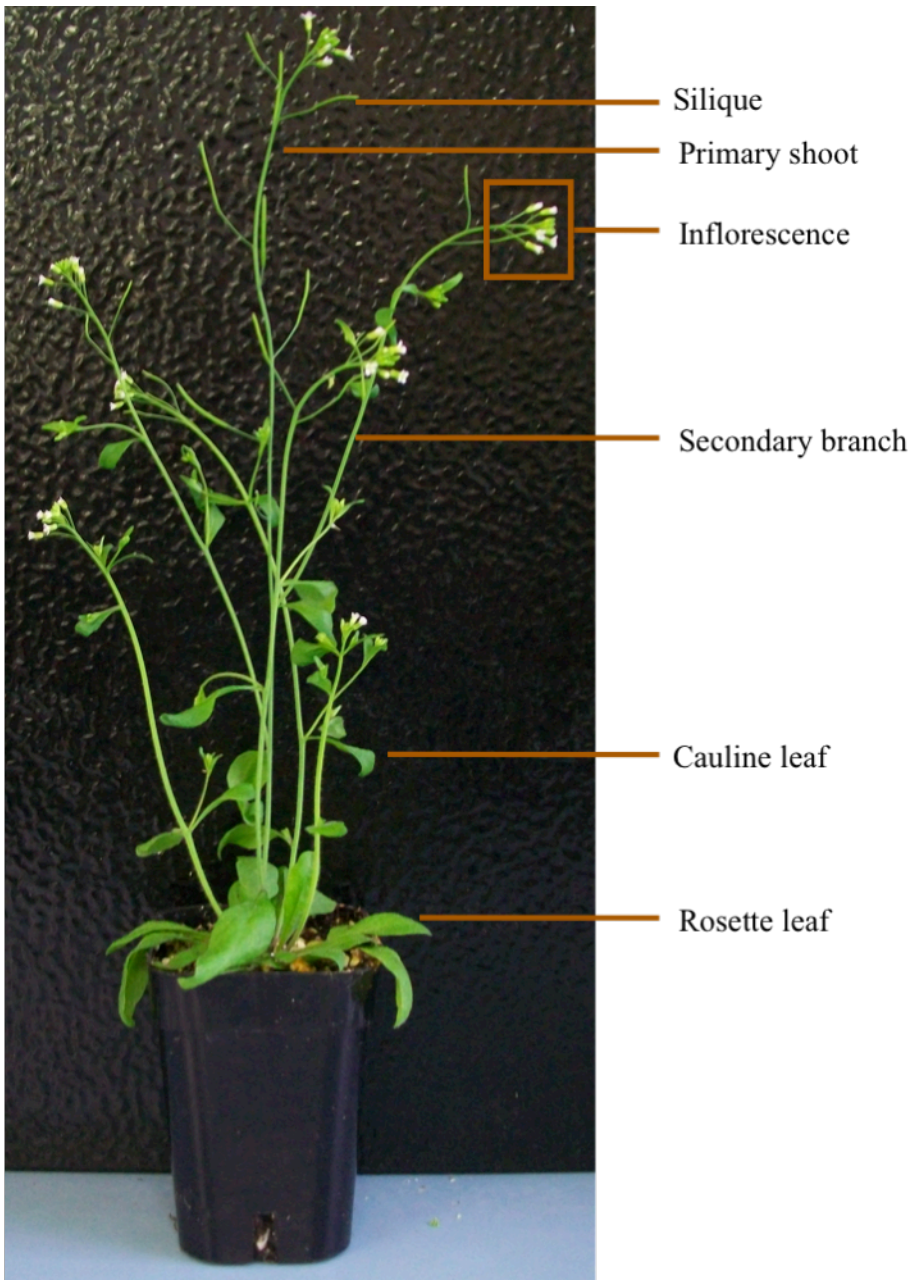

Figure 1. 5-week-old wild-type *Arabidopsis thaliana* plant. Image provided by Ishari Waduwara.

Biosynthesis of purine nucleotides

Purine nucleotides are essential to all cells as they serve as building blocks for nucleic acid synthesis, provide energy for biochemical reactions, and are precursors for a variety of cofactors (flavin adenine dinucleotide, adenine dinucleotide, and s-adenosylmethionine), B-class

vitamins, and in plants, the phytohormone cytokinin. The adenine nucleotides are of particular importance in that they are the major energy donors for innumerable biochemical reactions. The distribution of adenine nucleotides has been determined in wheat leaf protoplasts where 45% of cellular ATP is localized in chloroplasts with an equal proportion existing in the cytosol and the remaining 5% in the mitochondria (Stitt *et al*., 1982). The synthesis of adenine nucleotides is most relevant to the research described in this thesis.

de novo synthesis of adenine nucleotides

The enzymes involved in the *de novo* synthesis of purine nucleotides were first studied in *Escherichia coli*. Mutant strains deficient in each of the ten enzymatic reactions were recovered and used to identify purine biosynthetic enzymes in other species. The *de novo* synthesis enzymes from plants were identified by functional complementation of *E.coli* mutants (Senecoff and Meagher, 1993; Schnorr *et al*., 1994).

Purine nucleotides are synthesized from the amino acids glycine or glutamate, phosphoribosyl pyrophosphate (PRPP), and carbon dioxide (Zrenner *et al*., 2006) via the *de novo* synthesis pathway (Figure 2). This pathway involves a series of ten enzymatic reactions that lead to the synthesis of inosine monophosphate (IMP). Four additional reactions are required to produce ATP, which is then exported to the cytosol via an adenine nucleotide uniporter (Leroch *et al*., 2005). All the *de novo* enzymes in *E.coli* and plants are monofunctional, with the exception of one bifunctional enzyme in *E.coli*, whereas in most other eukaroytes (e.g. yeast, Drosophila, humans) these enzymes are present as mono-, bi- or trifunctional proteins (Smith and Atkin, 2002).

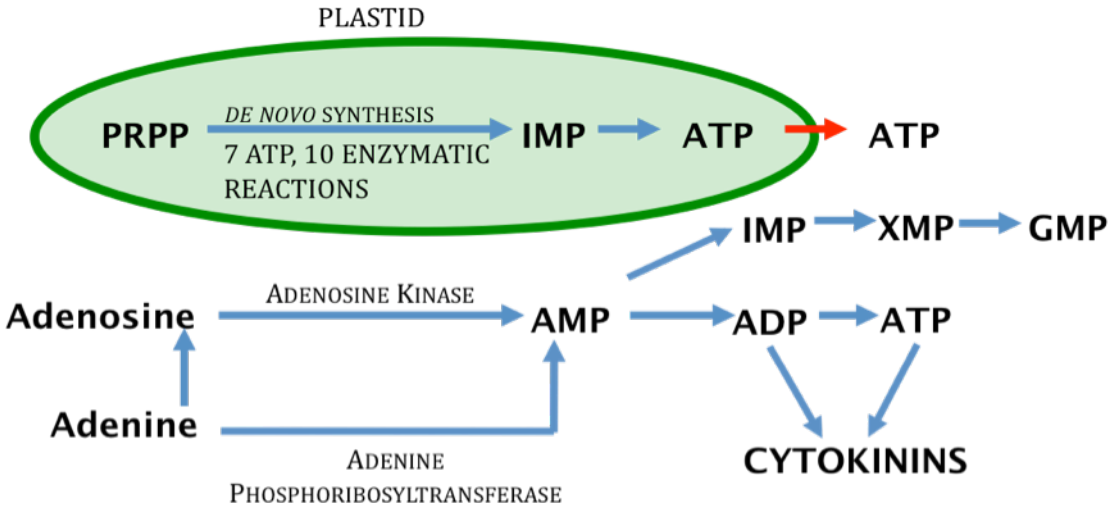

Figure 2. General schematic of purine nucleotide biosynthesis in plants. Adenine nucleotides are synthesized via two predominant routes, *de novo* synthesis and purine salvage pathways. The *de novo* pathway occurs in plastids and uses 7 ATPs and requires 10 enzymatic reactions to synthesize ATP. The salvage pathway exists in the cytosol and can be subdivided into two pathways. The predominant pathway is the one-step salvage of adenine to AMP; the secondary pathway involves the salvage of adenine to adenosine followed by phosphorylation to AMP. Purine nucleotides are subsequently used as energy donors for biochemical reactions, nucleic acid synthesis, synthesis of guanylate nucleotides, and as precursors for the plant phytohormone cytokinin. Image adapted from Zrenner *et al*. (2006).

Early studies of *de novo* synthesis focused on the subcellular localization of this pathway in root nodules of legume species. Initial studies pointed to plastid localization by the demonstration that PRPP amidotransferase activity (the first enzyme in *de novo* synthesis pathway) exists in plastid fractions of soybean nodules (Boland *et al*., 1982). To identify if the full complement of salvage enzymes were located within one organelle, cowpea and soybean nodules were subjected to subcellular fractionation on sucrose density gradients (Shelp *et al*., 1983; Boland and Schubert, 1983). These results showed that plastid fractions fed the purine precursor [^{14}C] glycine produced [^{14}C] IMP. In subsequent years, the subcellular localization of *de novo* synthesis in cowpea nodules was revisited (Atkins *et al*., 1997). Using subcellular fractionation on sucrose and percoll density gradients, plastid and mitochondrial fractions both

synthesized [1-^{14}C] IMP from [1-^{14}C] glycine. These results provided the first evidence that *de novo* synthesis may also reside in mitochondria of plant cells.

Further evidence to support compartmentalization of the *de novo* synthesis pathway came from the recovery of full-length cDNAs for *de novo* enzymes, coupled with bioinformatic analysis. Smith and Atkins (2002) showed that all ten Arabidopsis *de novo* cDNAs contain N-terminal plastid transit peptides. The sequences of *de novo* purine synthesis enzymes from other non-plant eukaryotic species do not contain apparent N-terminal leader sequences. Although, biochemical and bioinformatic analyses support the plastid localization, only two of the *de novo* purine enzymes have been localized by immunolocalization (Hung *et al*., 2004; Goggin *et al*., 2003). Interestingly, the fifth enzyme in the *de novo* pathway was shown to be dual localized to plastids and mitochondria, in cowpea nodules (Smith *et al*., 1998; Goggin *et al*., 2003). Future studies will have to experimentally identify the localization of all purine biosynthetic enzymes to verify the extent to which each purine biosynthesis enzyme occurs in each organelle or whether any of these particular enzymes possesses a dual function. Based on these early studies the general agreement is that non-legume plants compartmentalize the *de novo* pathway in plastids, whereas legume species have dual compartmentalization in plastids and mitochondria (Zrenner *et al*., 2006; Smith and Atkins, 2002).

Consistent with the bioinformatic analyses, non-plant eukaryotic *de novo* purine synthesis enzymes are localized in the cytosol. Gooljarsingh *et al* (2003) monitored the localization of human and *E.coli* GAR transformylase-GFP fusion proteins (the third enzyme in the *de novo* pathway) using confocal microscopy. In both *E.coli* and Cos-7 mammalian cells, GAR transformylase is present throughout the cytosol. A second study focused on the localization of

all six human *de novo* enzymes in HeLa cells (An *et al*., 2008). Interestingly, all six enzymes co-localized with each other in the cytosol forming a "purinosome" complex in response to low purine levels. This co-localization of *de novo* enzymes has yet to be demonstrated for any other organism.

Synthesis of adenine nucleotides by the salvage pathway

The synthesis of AMP by *de novo* synthesis is energetically expensive requiring ten enzymatic reactions and 7 ATP/GTP molecules. To overcome this high-energy demand, plant cells actively reuse purine bases produced from the degradation of nucleic acids, turnover of nucleotide cofactors or byproducts of metabolic reactions. The reuse of adenine bases is known as adenine salvage and can be further subdivided into two pathways (Figure 2). The first pathway involves the one-step conversion of adenine to AMP by adenine phosphoribosyltransferase (APT). The second is a two-step pathway in which adenine is converted to adenosine by adenine phosphorylase followed by phosphorylation to AMP by adenosine kinase (ADK).

APT's prevalence in purine salvage was first shown in *Acer pseudoplatanus* cell cultures where [8-^{14}C] adenine was recovered in the adenylate fraction with very little [8-^{14}C] adenine recovered as adenosine (Doree, 1973). The predominance of the one-step pathway is further supported in that APT and ADK activity are high in plants, yet adenine phosphorylase activity is low (Lee and Moffatt 1994; Moffatt *et al*., 2000; Ross, 1981). This evidence suggests that APT catalyzes the major route for adenine salvage, where ADK catalyzes the major route for adenosine salvage.

Purine salvage enzymes in plants contribute to both purine and cytokinin metabolism. The role of these enzymes is two-fold. They function in reducing intracellular accumulation of

adenine as well as the more obvious role in synthesizing adenine nucleotides. Much of the research on these enzymes has been focused on the importance of purine salvage activities in the maintenance of nucleotide pools during times of high demand such as seed germination or programmed cell death (Ashihara 1983; Stasolla *et al.*, 2005). In these and other tracer experiments the majority of [8-^{14}C] adenine was recovered in nucleotide fractions.

Adenine salvage enzymes are also thought to contribute to cytokinin interconversion. Cytokinins are plant growth regulators implicated in many aspects of growth and development (reviewed in Hirose *et al*., 2008). Structurally, cytokinins consist of an adenine moiety with either an isoprenoid or aromatic side chain conjugated at the N^6 position. Each of these two side chains further contains a number of derivatives adding to the diversity and modifying the functionality of these phytohormones. In Arabidopsis, the isoprenoid cytokinins are the major forms, in particular isopenetyl-adenine (iP) and its hydroxylated derivative trans-zeatin (tZ) (Sakakibara, 2006).

Cytokinins are further interconverted between bases, riboside and nucleotide forms. Although, only one enzyme in rice unequivocally catalyzes the conversion of the cytokinin nucleotide to its base form, there is growing evidence that purine salvage enzymes catalyze these interconversion reactions (Kurakawa *et al*., 2007). These cytokinin isoforms possess different binding affinities for cytokinin receptors indicating that the bases are the most physiologically active, with some residual activity in nucleosides, and very low levels of activity for nucleotides (Spichal *et al*., 2004). Therefore, APT and ADK activities theoretically contribute to reducing the abundance of active cytokinin bases and ribosides to the less active nucleotide form. In fact, it has been shown that APT purified to various degrees of homogeneity from wheat, peach, and

Arabidopsis can catalyze the interconversion of cytokinin bases to nucleotides (Chen *et al*., 1981; Lecomte and Le Floc'h, 1998; Moffatt *et al*., 1991) Interestingly, APT and ADK may also contribute to maintaining active cytokinin levels. As both purine enzymes synthesize AMP, the phosphorylated derivatives of this adenylate, may contribute the necessary precursors (ADP/ATP) for cytokinin biosynthesis (Kakimoto, 2001). The relative contributions of each purine salvage enzyme to cytokinin metabolism remains to be determined.

Purine salvage enzymes have long been assumed to reside in the cytosol. This localization is supported by a molecular analysis of these enzymes in Arabidopsis and the absence of apparent N-terminal leader sequences in recovered full-length cDNAs (Allen *et al*., 2002, Moffatt *et al*., 1994; Moffatt *et al*., 2000). To date, only two groups have localized purine salvage enzymatic activity outside the cytosol, and both instances are in plant species. Ashihara and Ukaji (1985) used subcellular fractionation to purify chloroplasts and mitochondria from spinach leaves. They showed that both fractions were able to catalyze the synthesis of [8-^{14}C]-AMP from [8-^{14}C] adenine and [8-^{14}C] adenonsine. A similar approach was used to localize APT activity in Jerusalem artichokes to mitochondria (Le Floc'h and Lafleuriel, 1983). No further studies have since shown non-cytosolic protein localization of these enzymes.

Adenine salvage by APT in Arabidopsis

Adenine salvage has been studied extensively in Arabidopsis since Moffatt and Somerville (1988) recovered the first APT-deficient plants based on their resistance to 2,6−diaminopurine. They isolated three point mutants, *apt1-1*, *apt1-2*, and *apt1-3,* which had 15%, 2%, and 1% residual APT activity, respectively. Surprisingly, the fertility of these plants correlates with the decrease in APT activity, where *apt1-1* has 2% of the seed production of wild

type and *apt1-2* and *apt1-3* are male sterile (Moffatt and Somerville, 1988). The male sterility in *apt1-3* is due to aborted pollen development shortly after meiosis (Moffatt and Somerville, 1988; Regan and Moffatt, 1990; Zhang *et al*., 2002). Three possible explanations were proposed for why APT deficiency leads to male sterility: insufficient ATP during microsporogenesis, accumulation of adenine leading to inhibition of methylthioadenosine nucleosidase or altered cytokinin interconversion during pollen development.

The effect of APT activity on cytokinin metabolism was tested in the most severe APT1-deficient mutant, *apt1-3*. Four-day old seedlings of WT and *apt1-3* were grown in liquid medium and fed the cytokinin benzyladenine [^{3}H]-BA. *apt1-3* plantlets metabolize 8-fold less BA than did WT plantlets (Moffatt *et al*., 1991). The apparent K_M of APT purified from Arabidopsis leaves was 4.5 μM for adenine versus 730 μM for the benzyladenine (BA) cytokinin, revealing its stronger binding affinity for adenine as compared to this particular cytokinin (Lee and Moffatt, 1993). Since this was above the physiological concentrations of cytokinins, it was difficult to conclude the extent to which APT acts on cytokinins *in vivo*. Despite conclusive evidence to support the role of reduced cytokinin or adenylate metabolism in male sterility, subsequent research focused on the *APT1* locus to gain further insight on its function in pollen development.

The full-length cDNA of *APT* was first recovered by Moffatt *et al* in 1992. Alignment of its predicted amino acid sequence with those of APTs from *E.coli*, Drosophila, hamster, human, and mouse showed these proteins to be highly conserved in both in their size and amino acid sequence. A promoter fusion with the β-glucuronidase-encoding (GUS) gene using the 950 base pair region upstream of the predicted transcriptional start site indicated that APT1 was expressed

constitutively in Arabidopsis plants (Moffatt *et al.*, 1994). The constitutive expression of the *APT* promoter was consistent with previous APT enzymatic assays that showed APT activity in leaves, flowers, stems, and buds (Lee and Moffatt, 1993). When expressed on a protein basis differences in expression are seen: relative to leaves APT activity is higher in buds (2.7-fold), stems (2.2-fold), and roots (3.9-fold).

With the increase in Expressed Sequence Tag (EST) collections and the availability of the complete Arabidopsis genome sequence, four additional *APT* genes were identified (*APT2*, *APT3*, *APT4*, and *APT5*). The amino acid sequence similarity among the five APTs is 89% (Allen *et al*., 2002). It is likely that these *APT* genes arose from genome duplication events as described by Blanc *et al* (2000). To date, APT4 and APT5 have not been investigated due to the minimal expression data available for these genes. As such, only the APT1, APT2, and APT3 isoforms will be discussed further.

To explore the kinetic properties of these APT isoforms Schnorr *et al*. (1996) recombinantly expressed APT1 and APT2 in *E.coli*. Based on their analysis APT1 and APT2 have similar apparent K_M values for adenine, while APT2 has a K_M 167-fold lower than APT1 for the cytokinin BA; the catalytic efficiency of APT1 is 180-fold higher than that of APT2. When BA is the substrate, APT2 was 250-fold more efficient than APT1. These results pointed towards a role of APT1 in adenine metabolism, and APT2 in the metabolism of cytokinins.

Allen *et al*. (2002) further compared the kinetic activities of these enzymes, this time including APT3. APT1, APT2, and APT3 have similar adenine K_M values but APT1 had a 31-fold higher adenine V_{max} than APT2, and 53-fold higher adenine V_{max} than APT3. This evidence

supports the model that APT1 is the predominant isoform acting on adenine in Arabidopsis; APT2 and APT3 had greater activity on cytokinins than did APT1.

The predominance of APT1 in adenine metabolism is consistent with the male sterility observed in the most APT-deficient mutant, *apt1-3*, that contains a point mutation at the splice donor site downstream of Exon 4 in *APT1* (Gaillard *et al*., 1998). Although the plant has two other functional APTs, APT2 and APT3, these isoforms are clearly not able to compensate for the loss of APT1 activity in *apt1-3*.

The subcellular localization of these three isoforms was also determined by Allen *et al*. (2002). Based on subcellular fractionation and immunoblotting analysis with isoform-specific peptide antibodies, APT1 and APT3 were localized to the cytosol; the results for APT2 were less conclusive but is likely cytosolic since it lacks an N-terminal transit peptide for chloroplast import.

In situ hybridization was used to address why the other APTs did not complement APT1 deficiency in pollen (Zhang, 2000). Consistent with previous data, APT1 was constitutively expressed with the highest level of expression in young buds. APT2 showed the strongest transcript levels in floral receptacles although the amount of signal was near background levels. This result is consistent with that obtained by Schnorr *et al* (1996) who found that APT2 could only be detected by primer extension assay in floral organs but not in leaves. APT3 transcripts were highest in ovaries. Interestingly, the transcript levels of all three APTs increase in *apt1-3* mutants flowers; the molecular mechanism of this increase remains unknown (Zhang, 2000).

Thus, based on these studies, APT1 appears to be the only isoform expressed in pollen. The timing of pollen abortion correlates with APT1's expression in both tapetal cells and

microsporocytes (Smith, 1997). Before meiosis APT1 expression increases in both these cell types, but immediately decreases soon thereafter. This correlation provides strong support for the importance of APT1 activity in pollen development.

Additional gene models for Arabidopsis *APT1*

Transcriptional profiling of Arabidopsis organs by EST analysis has revealed that a second, longer *APT1* mRNA arises from this locus (Figure 3). For the purpose of discussion, these two mRNAs and their corresponding protein products have been named APT1.1 to identify the longer isoform, and APT1.2 to identify the shorter isoform; APT1.2 is the form previously isolated by Moffatt et al (1994). When *APT1.2* was first reported it was shown to have a six-exon gene structure with a high sequence similarity to all other known APTs. The *APT1.1* mRNA differs from *APT1.2* by the presence of an additional 5′ terminal exon. This phenomenon of two transcripts arising from the same gene, yet containing different initiating exons is referred to as alternative first exons. For the purposes of clarity in discussing the alternative first exons of this gene, the first exon of *APT1.1* is designated as Exon 1 and the first exon of *APT1.2* is Exon 2. As seen in Figure 3, Exons 2 through 7 are common to both gene models and transcripts.

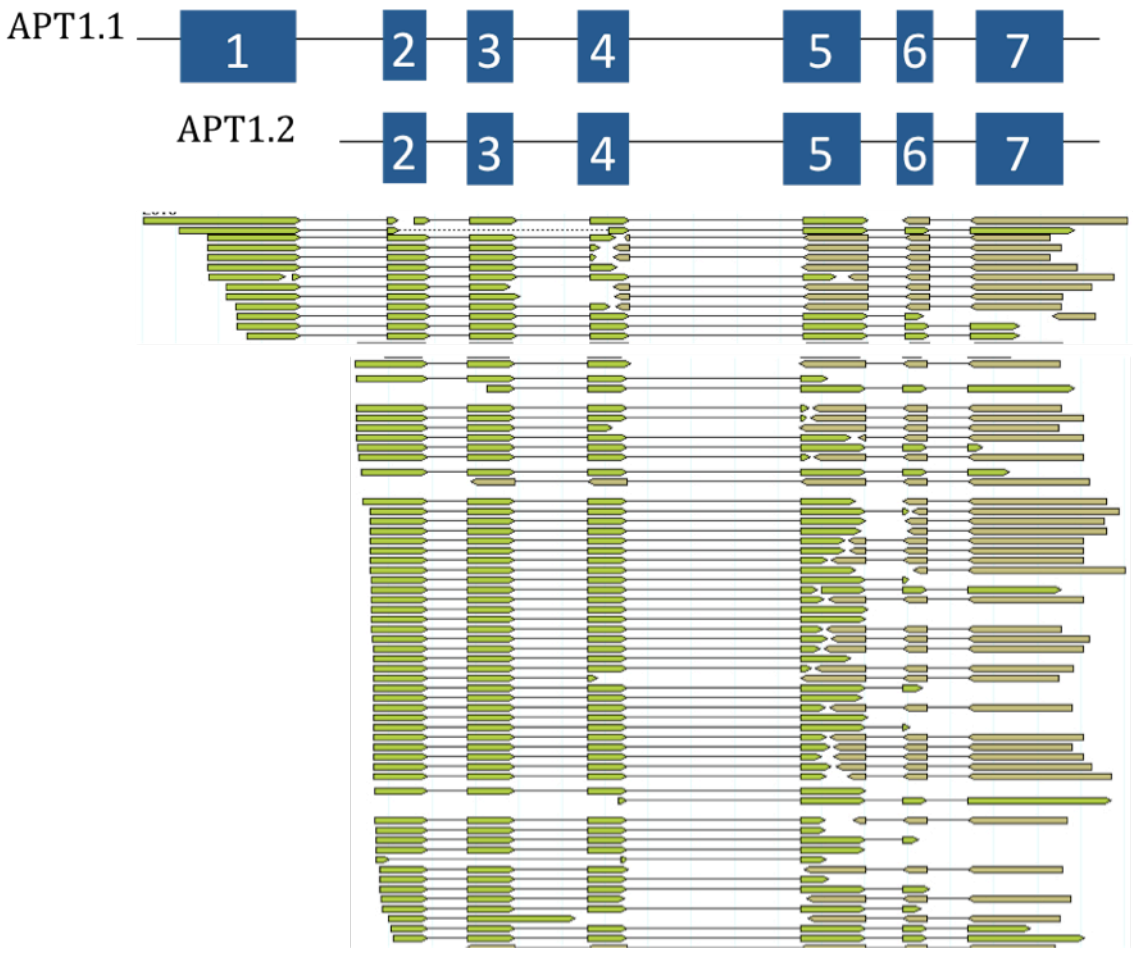

Figure 3. Predicted gene models of APT1.1 and APT1.2 based on EST collections. Two EST clusters are shown in green. The predicted gene models derived from each EST cluster is shown at the top with the blue boxes representing the exons. *APT1.1* has a seven-exon gene structure; *APT1.2* has a six-exon gene structure as identified by Moffatt *et al* (1992). The ESTs show that *APT1.1* and *APT1.2* have unique 5′UTR regions where that of *APT1.2* is located in the first intron. Image is modified from The Arabidopsis Information Resource website (http://www.arabidopsis.org).

Aside from their unique first exons, a second distinguishing feature between the *APT1.1* and *APT1.2* mRNAs is that each has a unique 5′ UTR region. As seen in Figure 4, the 5′ UTR of *APT1.2* resides in the first Intron where the 5′ UTR of *APT1.1* is upstream of the methionine codon of Exon 1.

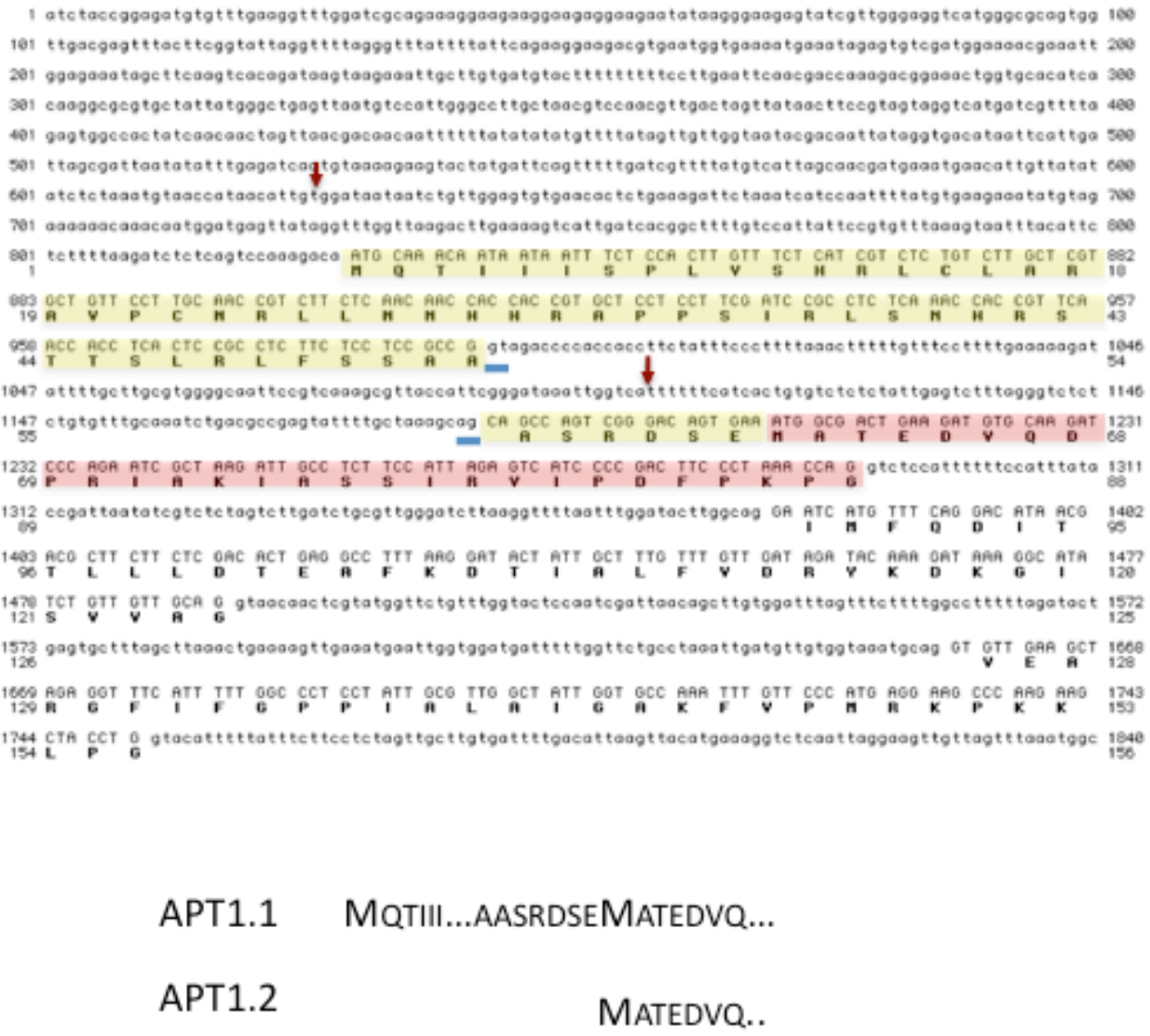

Figure 4. Partial genomic sequence of the *APT1* gene. Two mRNAs arise from the *APT1* gene in Arabidopsis. The *APT1.1* primary transcript initiates at the first red arrow and is spliced at the splice acceptor and splice donor sites underlined in blue, to remove the first Intron. The translation of this mRNA begins at Exon 1 (highlighted in yellow) and the resulting polypeptide includes the 6 amino acids adjacent to Exon 2 (highlighted in red). The *APT1.2* primary transcript initiates at the second red arrow with part of Intron 1 forming the 5´UTR. The translation of this mRNA initiates at Exon 2. Note that the APT1.2 polypeptide does not contain the 6 amino acids adjacent to Exon 2; these are only present in an APT1.1 polypeptide.

.

Interestingly, the distance between the transcriptional start sites (TSS) of *APT1.1* and *APT1.2* is approximately 478 base pairs. Bioinformatic analysis in humans shows that alterative first exons with TSS greater than 500 base pairs apart are unlikely to have one promoter direct the expression of both mRNAs (Kimura *et al*., 2006). This conclusion is consistent with the results of studies of the expression of alternative first exons in genes from humans (Kimura *et al*., 2006), rice, and Arabidopsis (Chen *et al*., 2007). Both studies found that the shorter mRNA is normally constitutively expressed, whereas the longer mRNA shows a spatial/temporal-specific expression in 52% of the human cases, 20-66% of the rice cases, and 5-18% of the Arabidopsis cases. The most plausible explanation for this occurrence is that the two transcripts are produced from two promoters. This would predict that *APT1.2* gene is constitutively expressed and *APT1.1* might exhibit spatial/temporal-specific expression. If this is true, the *APT1.1* promoter is presumed to be located upstream of its transcription start site (Figure 4), whereas the *APT1.2* promoter resides in the first intron and potentially further upstream.

The recovery of the *APT1.1* cDNA from both the RIKEN and CERES full-length cDNA clone collections indicates this is a functional mRNA. Both of these cDNA libraries were created by selecting for transcripts containing a 5′-guanidine cap, a hallmark of the 5′ end of mRNAs. This evidence initiated part of the research outlined in thesis: to identify if *APT1.1* produces a polypeptide and if so, what is its functional significance.

Chen *et al* (2007) highlight various alternative first exon genes in rice and Arabidopsis documenting the various roles of the first exon including being a transit peptide, adding or altering enzymatic activity, or controlling the spatial/developmental/temporal expression of the associated gene. Results of various subcellular localization prediction programs differ in their

proposed localization of APT1.1, although a chloroplast localization appears more frequently than others (Table 1). All the programs predict APT1.2 to be situated in the cytosol. As for differences in enzymatic activities, this cannot be predicted using bioinformatics thus this role for Exon 1 must be determined experimentally. Finally, the tissue sources for the ESTs were investigated to see if there was a bias in the tissues each mRNA was recovered from. Of the eighteen *APT1.1* ESTs, ten were obtained from floral organs, and the remaining were obtained from leaf tissue of young plantlets.

Table 1. Predictions of the subcellular localization of APT1.1 using bioinformatic tools. MitoProtII and TargetP are the only programs to predict both length and cleavage site of the proposed transit peptide (57 amino acids predicted by MitoProtII and 52 amino acids by TargetP). Date of access August 2009.

Program	Localization	Probability	Website	Reference
TargetP	plastid	0.881	http://www.cbs.dtu.dk/services/TargetP/	Emanuelsson *et al*., 2000
SubLoc	cytosol	0.74	http://www.bioinfo.tsinghua.edu.cn/SubLoc/	Hua and Sun, in press
iPSORT	mitochondrion	Above threshold of 6.21 (6.27)	http://hc.ims.u-tokyo.ac.jp/iPSORT/	Bannai *et al*., 2002
MitoProt II	mitochondrion	0.9953	http://ihg2.helmholtz-muenchen.de/ihg/mitoprot.html	Claros *et al*., 1996
Predotar	plastid	0.45	http://urgi.versailles.inra.fr/predotar/predotar.html	Small *et al*, 2004
PeroxP	Not in peroxisomes	N/A	http://www.plantenergy.uwa.edu.au/applications/suba/index.php	Emanuelsson *et al*., 2003
WoLFPSORT	plastid	0.86	http://wolfpsort.org/	Horton *et al*., 2007
MultiLoc	plastid	0.98	http://www-bs.informatik.uni-tuebingen.de/Services/MultiLoc/	Hoeglund *et al*., 2006

Novel *apt1*-deficient mutant is not male sterile

Concurrent with the discovery of the *APT1.1* isoform a novel *APT*1-deficient mutant was identified. This mutant was recovered by D. Falcone at the University of Massachusetts and named *oxidative stress tolerant 1* (*oxt1*). The *oxt1* mutant arose from a population of T-DNA mutagenized seeds that were plated on solid plant growth media supplemented with 3-amino-

1,2,4-triazole (AT) and buthionine sulfoximne (BSO) (Zhang *et al*., 2008). These compounds work synergistically to induce oxidative stress by inhibiting catalase activity and suppressing glutathionine biosynthesis, respectively (Zhang *et al*., 2008). WT seedlings exposed to these conditions initially show inhibited root growth; prolonged exposure results in chlorosis and death. Under these conditions *oxt1* exhibited 75% increased tolerance relative to WT (i.e. it shows symptoms on 75% higher concentration).

oxt1 was also tested for increased tolerance to other abiotic stresses such as temperature and drought. When *oxt1* mutants were grown at 28°C their dry mass was 1.5-fold greater than WT, indicating a higher rate of growth in these mutants. Moreover, *oxt1* mutants grown at 38°C for 5-days showed less anthocyanin production relative to WT plants. Increased drought resistance in WT and *oxt1* was tested by withholding water from 3-week-old plants. After 2 weeks 50% of WT plants died while all *oxt1* mutants survived (Sukrong *et al*., manuscript in prepartion).

Since *oxt1* exhibited greater stress tolerance, RT-PCR analysis was used to investigate the expression of select antioxidant defense genes. *oxt1* mutants have a higher expression of antioxidant defense genes in both non-stress and stress-induced conditions. During non-stress conditions three genes are up-regulated relative to WT: stromal ascorbate peroxidase, thylakoid ascorbate peroxidase, and catalase 3. Under stress-conditions these genes were further upregulated above the levels found in WT (Sukrong *et al*., manuscript in prepartion).

Subsequent map-based cloning revealed that *oxt*1 carries an uncharacterized T-DNA insertion immediately upstream of Exon 2 in *APT1* (D. Falcone, personal communication). APT activity was undetectable in *oxt*1 based on a spectrophotometric assay (D. Falcone, personal

communication). Despite their reduced APT activity, *oxt1* is completely fertile, unlike all previously characterized APT mutants. Dr. Falcone contacted Dr. Moffatt about collaborating on the analysis of the *oxt1* mutant's APT activity and stress tolerance.

Objectives of this Research

The research outlined in this thesis has three principal objectives:

1. The only evidence for the existence of *APT1.1* is based on EST collections. This research set out to initially address the following questions: Is the *APT1.1* transcript a functional mRNA; how does *APT1.1* transcript abundance compare to that of *APT1.2,* and does *APT1.1* give rise to a polypeptide?

2. The second objectives are to investigate whether APT1.1 is a functional enzyme and if so, to determine the functional significance of Exon 1 in APT1.1.

3. The *oxt1* mutant is APT1-deficient yet it is not male sterile. I did comparative analyses of *oxt1* and *apt1-3* to look for an explanation for their differing phenotypes.

Materials and Methods

Source of Chemicals and Reagents

All chemicals and reagents used were purchased from Sigma-Aldrich, Bioshop, or BioBasic, unless otherwise noted. Restriction enzymes were purchased from New England Biolabs or Fermentas.

Seed germination and plant growth

Seeds were sterilized in a 1.5 mL microfuge tube containing a maximum of 100 mg of seeds. The 1.5 mL microfuge tube was placed in a glass dessicator beside a 400 mL beaker containing 100 mL of Javex and 3 mL of concentrated HCl. The seeds were sterilized by chlorine gas for 2 hours. Sterilized seeds were stored afterward at room temperature away from direct light.

Sterilized seeds were grown on Murashige and Skoog (MS) solid medium in Petri plates. The medium was prepared using MS Salts and Gamborg's vitamins (Sigma), 2.56 mM 4-morpholine-ethanesulfonic acid monohydrate, 30 g/L sucrose, 0.8 g/L agar; the pH was adjusted to 5.8 using 1M potassium hydroxide (KOH). After stratification for 48 hours at 4°C in the dark, seeds were transferred to a 21°C growth chamber under 50 μEinsteins m^{-2} s^{-1} continuous fluorescent light. After 10-14 days the seedlings were transplanted into 4-inch deep plastic pots containing a 50:50 mix of "Sunshine LC1 mix" and "Sunshine LG3 Germination mix" soil (JVK, St Catharines, ON). Potted plants were grown in a 21°C growth chamber under 16-hour days and fluorescent lighting providing 120 μEinsteins m^{-2} s^{-1} fluorescent light.

Radiochemical assay of Adenine phosphoribosyltransferase enzyme activity

This assay was performed as described by Allen *et al* (2002). Crude protein extracts used for this assay were prepared on ice by grinding leaf tissue (50-100 mg) or flower tissue (30-70 mg) in 50 mM Tris-HCl buffer pH 8.8 at a ratio of 3 µL of buffer to 1 mg of tissue in glass homogenizers. The extracts were centrifuged at 13,200 rpm (18,500 x g) for 3 minutes to remove insoluble material and debris. The supernatant was assayed for enzyme activity. The general protein concentration recovered was 1-2 mg/mL for leaf extracts, 2-3 mg/mL for flower extracts. Note that desalting the protein extract through Sephadex G-25 beads (GE Healthcare) results in a 50% decrease in APT activity, and is not recommended.

The assay which measures the conversion of ^{3}H-adenine to ^{3}H-AMP was carried out in a final reaction volume of 100 µL containing 50 mM Tris-HCl pH 8.8, 15 mM NaF, 2.4 mg/mL bovine serum albumin (BSA), 10 mM NaN_3, 5 mM $MgCl_2$, 19 µM 5-phosphorylribose 1-pyrophosphate (PRPP), and 100 µM [2,8-^{3}H] adenine (40 Ci mmol^{-1}; MP Biomedicals Inc.). The 100 µM of adenine consisted of 0.2 µL of [2,8-^{3}H] adenine (initial concentration 25 µM) and 12.2 µL of 819 µM non-radioactive adenine resulting in 10 nmol of adenine per reaction. The PRPP had to be prepared fresh; all the other reagents were used from frozen stocks stored at −20^{o}C.

The reaction mixture was pre-warmed for 5 minutes at 37°C before plant crude protein extract was added and allowed to incubate at 37°C for 5 minutes. The reaction was stopped by adding 1 mL of ice-cold stop buffer (0.05 M NaOAc pH 5.0, 2.0 mM K_2HPO_4) followed by precipitation of ^{3}H-AMP with 200 µL of 0.5 M $LaCl_3$. Nucleotides were precipitated at 4°C for a minimum of 1 hour before being collected on a glass-fiber filter with pore size of 1.2 µM

(Fisherbrand, Cat.No. 09-804-24C), by vacuum filtration. The filter was placed in a scintillation vial containing 4 mL of Cytoscint (MP Biomedicals Inc.) and incubated for at least 1 hour before liquid scintillation counting (Model LS 1701, Beckman). Each sample was assayed in triplicate and in triplicate volumes (i.e. 2, 4, and 6 μL) to ensure the linearity of the assay. Activity was expressed as nmol of AMP mg of protein^{-1} min^{-1}. It should be noted that the assays performed in this thesis research were not linear at the highest volume. This issue was resolved for a short time by using a newly prepared stock of NaF, but later became an issue once again.

ADK Enzyme Assay

This assay was performed as described by Moffatt *et al*. (2000). Plant crude protein extracts for this assay were prepared on ice by grinding leaf tissue (80-100mg) in 100 mM HEPES buffer pH 7.2 at a ratio of 3 μL of buffer to 1 mg of tissue. The extracts were centrifuged at 13,200 rpm for 2 minutes. The supernatant was then desalted through Sephadex G-25 beads (GE Healthcare) that had been resuspended in 50 mM HEPES pH 7.2 (1 gm of beads per 5 mL of buffer). The concentration of the crude protein extract was generally 1.0-1.5 mg/mL as measured using Bio-Rad protein assay reagent (Bio-Rad). This extract was subsequently diluted to 0.1 mg/mL. Extracts of ADK-deficient mutants were not diluted.

This assay measures the conversion of ^{3}H-adenosine to ^{3}H-AMP. It was carried out in a final reaction volume of 50 μL containing 50 mM HEPES buffer pH 7.2, 4 mM ATP, 1 mM $MgCl_2$, 30 mM NaF, 2.5 μM deoxycoformycin (Warner Lambert), 1 mg/mL BSA, and 2 μM [2,8-^{3}H] adenosine (31.4 Ci mmol^{-1}; Sigma). The samples were processed as described for the APT assay with the exception that the reactions were carried out at 30°C. Activity was expressed as nmol of AMP mg of protein^{-1} min^{-1}.

RNA isolation, cDNA synthesis, and RT-PCR of *APT1, APT2, and APT3*

Plant tissue was homogenized using a mortar and pestle containing liquid nitrogen and quickly transferred to 1 mL TriPure Isolation Reagent (Roche Applied Science) in a 1.5 ml microfuge tube. After a five min incubation at room temperature, 200 µL of chloroform was added, the mixture was vortexed for 15 seconds, incubated for 15 minutes at room temperature and centrifuged at 13,200 rpm for 15 minutes at 4°C. To the aqueous phase an equal volume of isopropanol was added; the mixture was vortexed thoroughly and centrifuged at 13,200 rpm (18,000 rcf) for 15 minutes. The pellet was then washed with 1 mL of 75:25 ethanol:water and allowed to air dry for 10-15 minutes. The pellet was resuspended in 30 µL of dimethylpyrocarbonate (DEPC) treated water by heating at 60°C for 15 minutes. The RNA was stored at -80°C. Generally the yield was 30µg per 50 mg of leaves; 60µg per 30 mg of inflorescences.

Before cDNA synthesis 5 µg of RNA was treated with Turbo DNase I (Ambion) according to the manufacturer's instructions. All cDNA was synthesized with Invitrogen's SuperScript II reverse transcriptase using an anchor-dT primer at 42°C for 1 hour. The quality of cDNA synthesis and genomic DNA contamination was assessed by PCR amplification of 1 µL of cDNA with actin 2 intron-spanning primers (actin2F and actin2R) using the following cycle conditions: initial denaturation at 94°C for 3 min, 22 cycles of 94°C 30 seconds, 55°C 30 seconds, 72°C 1 min, and final elongation at 72°C for 10 minutes.

To measure the transcript abundance of the two *APT1* mRNA isoforms forward primers were designed to anneal within Exon 1 of *APT1.1* (AP186) and the 5′ UTR of *APT1.2* (187), which are unique to each gene (Appendix 3). The reverse primer (AB19754) annealed within

Exon 7, which is common to both isoforms. To ensure that each primer set was amplifying within its linear range a standard curve was developed by plotting the amount of cDNA amplified (determined by spot density analysis of the digitized image) against the number of cycles (20, 24, 28, 32, and 36) on a semi-log graph. The number of cycles to amplify was chosen by selecting a value midway in the linear range. Using these data, RT-PCR conditions for *APT1.1* and *APT1.2* were carried out as follows: 94°C 3 min, 30 cycles of 94°C 30 seconds, 55°C 30 seconds, 72°C 1 min, and final elongation at 72°C for 10 minutes. An equal volume of each PCR product was electrophoresed on a 1% Tris-acetate-EDTA (TAE) agarose gel at 100V for 16 minutes. The amount of PCR product in nanograms was measured using AlphaImager HP (Alpha Innotech) spot density software.

To measure the transcript abundance of *APT2* primers APT2L and APT2R were used; for APT3 the primers used were APT3RTFwd1 and AB11935. A standard curve was developed to determine the linear range for both primer sets as described above. The following cycle conditions were used for both primer sets: 94°C for 3 min, 30 cycles of 94°C 30 seconds, 55°C 30 seconds, 72°C 1 min, and final elongation at 72°C 10 minutes. The resulting PCR product was analyzed as outlined in the previous paragraph.

Western Blotting

Protein extracts were prepared by homogenizing 50-100 mg of leaf tissue or 50 mg of inflorescences in 100 μL 50 mM Tris-HCl pH 8.0 buffer (2 μL buffer per mg of fresh weight). The extracts were centrifuged at 13,200 rpm for 2 min to remove insoluble plant material and the supernatant saved. Protein quantification was determined by the Bradford protein assay (Bio-Rad) using BSA as the standard. These extracts were stored at -20°C.

After quantification of the protein sample, 20 μg of crude protein extract in 1X SDS-loading dye was electrophoresed on a 12.5% acrylamide separating gel layered with a 5% stacking gel. The samples and pre-stained protein ladder (Fermentas, PageRuler SM0671) were initially electrophoresed at 90 V for 20 minutes, after which the voltage was increased to 150 until the 18 kDa pre-stained marker ran off the gel. After electrophoresis, the gel was washed twice for 10 minutes in freshly prepared Bjerrum and Schafer-Nielsen transfer buffer (25 mM Tris, 190 mM glycine, 20% methanol, 0.05% (v/v) SDS). The polyvinylidene fluoride (PVDF) membrane was first soaked in methanol for 30 seconds then pre-soaked, along with the filter papers, in transfer buffer.

Electrophoretic transfer was carried out using Bio-Rad Trans-Blot SD at 20 V for 45 minutes followed by staining with Ponceau s (3% TCA, 0.2% w/v Ponceau s). This stain allowed for reversible detection of proteins on the membrane in order to estimate equal loading of each sample. After removing the stain by rinsing in water the membrane was blocked in polyvinyl alcohol (5 mg per 200 mL; MW 30-70,000) for 30 seconds followed by a quick wash in water (Miranda *et al*., 1993).

All further washes and antibody incubations were carried out in Phosphate-Buffered Saline solution with 1% (w/v) skim milk powder (Carnation) and 0.3% (v/v) Tween-20 (PBS/M/T). Incubation in primary antibody was for 2 hours at room temperature or overnight at 4°C using the following dilutions: anti-APT1 1:10 000, anti-ADK 1:3500, anti-SAHH 1:5000, anti-GFP 1:1000 (Invitrogen, Cat. No. A6455). APT1 antibody generation will be addressed in the following sections. Sang Lee generated the ADK antibody using full-length ADK1; SAHH

antibody was generated by Shira Davis (Biol 499 Senior Honours Project, University of Waterloo, 2009).

Washes after primary and secondary antibody consisted of two rinses with 10 mL of PBS/M/T followed by three, 10 minute washes in 20 mL PBS/M/T. Incubation in secondary antibody was for 1 hour at room temperature using a horseradish peroxidase-conjugated anti-rabbit IgG (1:10000; Jackson ImmunoResearch). Bound antibody was detected by incubating the membrane in 1 mL of homemade ECL detection reagent (1.25 mM luminol, 2 mM 4-IPBA, 100 mM Tris-HCl pH 8.8, 0.02% H_2O_2) (Haan and Behmann, 2007). The signal was imaged using a chemiluminescent gel documentation system (Model BIS303PC, DNR Bio-Imaging Systems). The system preset "ECL medium size blots" was selected, the detection period set between 0:20 sec to 1:00 min, and gain adjusted to be between 100 and 200.

Construction of transgenic lines

Unless otherwise noted, all the construction of all transgenic plants involved the following steps and cloning into the pSAT series of vectors (Tzfira *et al*., 2005). The ligation mixture was introduced into DH5α for plasmid propagation and colony screening. Plasmid isolated from the DH5α host was sequenced around the insert and junction regions.. The *promoter-insert-epitope tag-transcriptional terminator* fragment was subcloned into the pPZP-RCS2-bar binary vector and re-introduced into DH5α for plasmid propagation. This plasmid was transformed into the GV3101 *Agrobacterium tumefasciens* used to mediate stable transformation of the transgene into the Arabidopsis genome. As the pPZP-RCS2-bar binary vector contains the herbicide resistant gene *bar*, all transgenic lines are resistant to BASTA (Sigma) and Wipeout (Wilson Laboratories Inc.). Table 2 summarizes the transgenic lines constructed for this research

project. Further details on the generation of each construct will follow; primer sequences used in the cloning process can be found in Table 3.

Table 2. List of transgenic lines generated throughout this study.

Name	Genetic background (transgene)	Purpose
APT1::Ex1:GFP	WT (*APT1*::Exon 1:GFP)	Subcellular localization. Expression of Exon 1 from *APT1.1* promoter
APT1::Ex1-i-Ex2:GFP	WT (*APT1*::Exon 1-Intron 1-Exon2:GFP)	Subcellular localization of both isoforms. Expression of dual isoforms in the presence of Intron 1 and Exon 2
actP::APT1.1:2GFP	WT (actin promoter::APT1.1:GFP:GFP)	Subcellular localization of APT1.1 using full length open reading frame
actP::APT1.2:GFP	WT (actin promoter::APT1.2:GFP)	Subcelluar localization of APT1.2 using the full length open reading frame
ami1.1	WT (35S::ami1.1)	Silencing of *APT1.1* transcript by targeting its 5´UTR
ami1.2	WT (35S::ami1.2)	Silencing of *APT1.2* transcript by targeting its 5´UTR
APT1.1:StrepII	WT (35S::APT1.1:HA:StrepII)	APT1.1 fused to StrepII tag to purify interacting proteins
APT1.2:StrepII	WT (35S::APT1.2:HA:StrepII)	APT1.2 fused to StrepII tag to purify interacting proteins
*actP::*APT1.1	WT, *oxt1*, *apt1-3* (actin promoter::APT1.1 ORF) *oxt1* (see Appendix 4)	Complementation of *apt1-3* with APT1.1 isoform
actP::APT1.2	WT, *oxt1*, *apt1-3 (*actin promoter::APT1.2 ORF) *oxt1* (see Appendix 4)	Complementation of *apt1-3* with APT1.2 isoform

APT1::gAPT1:GFP	To be introduced into WT Arabidopsis	Expression of full length genomic *APT1* from 800 bp *APT1.1* promoter
APT1::gAPT1ΔIntron 1:GFP	To be introduced into WT Arabidopsis	Expression of full-length genomic *APT1* in the absence of Intron 1
APT1::gAPT1(stop codon mutations):GFP	To be introduced into WT Arabidopsis	Expression of full-length genomic *APT1* with stop codons introduced in Exon 1

Cloning of APT1-GFP fusion proteins

The *APT1*::Ex1:GFP clone was constructed by amplifying the segment of genomic DNA extending from 800 bp upstream of the transcriptional start site of the *APT1.1* promoter, through the 5′ UTR of *APT1.1*, and terminating at the end of Exon 1 using the primers AP185 and APex1R. This fragment was cloned into the *Age*I/*Bam*HI restriction sites of pSAT6 in-frame with eGFP sequence (strain #800, Tzfira *et al*., 2005). The resulting fusion gene was subcloned into the PI-*Psp*I restriction site of the pPZP-RCS2-bar binary vector.

The *APT1*::Ex1-i-Ex2:GFP clone was constructed by amplifying the same fragment that was used in the *APT1*::Ex1:GFP clone, with the addition of Intron 1 and Exon 2, using the primers AP185 and APex2R. This fragment was cloned into the *Age*I/*Bam*HI restriction sites of the pSAT6 vector in-frame with eGFP (strain #800, Tzfira *et al*., 2005) then further subcloned into the PI-*Psp*I restriction site of pPZP-RCS2-bar.

Construction of the *actP*::APT1.1:2GFP clone was a two-step process that involved cloning the actin promoter into a previously modified pSAT6-2eGFP vector (Sanghyun Lee, strain #1047) followed by the addition of the APT1.1 ORF. First, the actin promoter was subcloned from the pSAT7-actP-MCS-agsT vector (strain #1376) into the *Age*I/*Nco*I sites of the

pSAT6-2eGFP vector. In the second step, the *APT1.1* ORF (lacking the 5′ UTR) was amplified from WT cDNA using the primers AP181 and AB19750. This fragment was cloned into the *Nco*I site of the modified *actP*-pSAT6-2eGFP vector. This construct was further subcloned into the PI-*PspI* restriction site of pPZP-RCS2-bar.

Creating the *actP*::APT1.2:GFP clone was also a two-step cloning process. The actin promoter was first subcloned from the pSAT7-actP-MCS-agsT vector into the *Age*I/*Nco*I sites of pSAT6-eGFP vector (strain #800). The *APT1.2* ORF (lacking its 5′ UTR) was amplified from WT cDNA using primers APT cDNA and AB19750. The *APT1.2* ORF was cloned into the *Nco*I restriction site of the modified actP-pSAT6-eGFP vector and the resulting fragment was subcloned into the PI-*PspI* restriction site of pPZP-RCS2-bar.

Cloning of amiRNA constructs

Artificial microRNAs (amiRNAs) were designed using the online tool *WMD 2 – Web MicroRNA Designer* created by Schwab *et al*., 2005. The complete protocol can be found online; here I will briefly describe the design and cloning steps only. The online tool requires the user to enter a sequence of interest that is to be the target of the amiRNA. For this project, the 5′ untranslated regions for *APT1.1* and *APT1.2* were used, as they are unique to each transcript. The program outputs a ranked list of amiRNAs and their specific target regions. There is no guarantee regarding which amiRNA will be most efficient, although it is recommended to select the amiRNAs ranked at the top of the list. Once an amiRNA is selected the program designs a set of four overlapping oligonucleotides that are used in site-directed mutagenesis using the pRS300 plasmid as the initial template (primers are listed in Table 3). In this step the user is essentially replacing an amiRNA in the pRS300. The resulting amiRNA-producing fragment was cloned

into the *Eco*RI/*Bam*HI restriction sites of the pSAT4 vector under control of the constitutive 35S promoter. The fusion gene was subsequently subcloned into either the I-SceI or PI-*Psp*I restriction site of pPZP-RCS2-bar; ami1.1 was cloned into I-SceI, ami1.2 was cloned into PI-*Psp*I.

Cloning of APT1.1 and APT1.2 with StrepII epitope tag

The ORFs of *APT1.1* and *APT1.2* were amplified from WT cDNA using primer sets pXCS-Ex1F/pXCS-APT1R and pXCS-Ex2F/pXCS-APT1R, respectively. The PCR products were subsequently cloned into the *Hin*dIII/*Pst*I restriction sites of pXCS-HAStrep (Witte *et al*., 2004) in-frame with the StrepII tag. This design fuses the StrepII tag to the carboxy terminus of each ORF. The resulting plasmids were transformed into DH5α for plasmid propagation and screening. The fusion protein sequence was verified by DNA sequencing and the plasmid was transformed into the *A. tumefaciens* vector GV3101 MP90RK. It was essential to use this Agrobacterium strain as the ori_V on the pXCS vector is dependent on the *trf/tra* genes provided by GV3101 MP90RK to be functional (Koncz and Schell, 1986).

Cloning of APT1.1 and APT1.2 ORFs

The *APT1.1* coding region including its stop codon was amplified using primers AP181 and AB12380 and cloned into the *Nco*I/*Hin*dIII restriction site of the actP-pSAT4 vector (strain #1500). This places the ORF under the control of the actin promoter. The fusion gene was subcloned into the PI-*Psp*I restriction site of pPZP-RCS2-bar.

The APT1.2 coding region including the its stop codon was subcloned from a pET30a plasmid (strain #592) into the *Nco*I/*Hin*dIII restriction sites of the actP-pSAT6 vector (strain #1501). The fusion gene was subcloned into the I-*Sce*I restriction site of pPZP-RCS2-bar.

Table 3. DNA sequence of primers used in cloning and RT-PCR experiments outlined in this thesis.

Primer Name	Sequence (5′ to 3′)
AP185	5′-CAGACCGGTGAGTTTACTTCG -3′
APex1R	5′- TCAGGATCCAGGCGGAGGAG -3′
APex2R	5′- TCAGGATCCATGGTTTAGGGAAG -3′
AP181	5′- CTGCCATGGGAATGCAAACAATAATAATTTCTCC -3′
AB19750	5′- TAGCCATGGCAGCAGCCGACTTTACAAG -3′
APT cDNA	5′-TGCCATGGCGACTGAAGATGTGC-3′
miRAPT1Ex1A-I	5′-GATAATAATGGACAAAGCCGTGTCTCTCTTTTGTATTCC-3′
miRAPT1Ex1A-II	5′-GAGACGGCTTTTGTCCATTATTATCAAAGAGAATCAATGA-3′
miRAPT1Ex1A-IIIA	5′-GAGAAGGCTTTTGTCATTATTTTCACAGGTCGTGATATG-3′
miRAPT1Ex1A-IV	5′-GAAAATAATCGACAAAAGCCTTCTCTACATATATATTCCT-3′
miRAPT1Ex2A-I	5′-GATTTAGCAAAATACTCGGCGTGTCTCTCTTTTGTATTCC-3′
miRAPT1Ex2A-II	5′-GACACGCCGAGTATTTTGCTAAATCAAAGAGAATCAATGA-3′
miRAPT1Ex2A-III	5′-GACAAGCCGAGTATTATGCTAATTCACAGGTCGTGATATG-3′
miRAPT1Ex2A-IV	5′-GAATTAGCATAATACTCGGCTTGTCTACATATATATTCCT-3′
pXCS-Ex1F	5′- TCGAAGCTTATGCAAACAATAATA ATTTCTCC -3′
pXCS-APT1R	5′- AGCTGCAGAGCAGCCGACTTTACAAGAAC -3′
pXCS-Ex2F	5′- TCG AAGCTT ATG GCG ACT GAA GAT GTG C -3′
AB12380	5′- CCTAAGCTTCTCTTCCAGTTTC -3′

actin2F	5'- CCGATGGTGAGGATATTCAGCC-3'
actin2R	5'- TGTCACGGACAATTTCCCGTTCTGC-3')
AP186	5′-GTT TCT CAT CGT CTC TGT CTT GC-3′
187	5′-TCT CTG TGT TTG CAA ATC TGA CG-3′
AB19754	5′-CAA ATA GCG ACG TCT CTC C -3′
APT2L	5′-GAT GAG TGG GGT GAA GGA AAT AAA TGA -3′
APT2R	5′- ATG AAT CAT TCC ACA TGG AGC CAA TAG A -3′
APT3RTFwd1	5′-CATCTTGTTGTTCTCTTCGTCG -3′
AB11935	5′- AGC AAG CTT CAT CGG TAC TC-3′
apt1-exon1	5′-TAGCCATATGCAAACAATAATAATTTCTCC-3′
AB12380	5′-CCT AAG CTT CTC TTC CAG TTT C-3′
apt1-exon1 blunt	5′-ATG CAA ACA ATA ATA ATT TCT C-3′

Stable transformation of Arabidopsis using the floral dip method

The floral dip protocol is a simple method to utilize *Agrobacterium tumefaciens* to mediate the transformation of a transgene of interest into the Arabidopsis genome. The protocol outlined here is adapted described by Clough and Bent (1998). Briefly, the Agrobacterium GV3101 strain carrying the transgene of interest was used to inoculate 5 mL of Luria-Bertani (LB) Media supplemented with rifamycin (25 μg/mL), gentamicin (25 μg/mL), spectinomycin (100 μg/mL), and streptomycin (300 μg/mL). After incubation overnight at 28°C, this culture was used to inoculate 100 mL of LB media supplemented with the same antibiotics and

incubated for a second overnight at 28°C. The culture was centrifuged at 5500 rpm for 10 minutes, resuspended at an OD_{600} of 0.8 in 5% (w/v) sucrose, 0.05% (v/v) Silwett-L77 (Lehle Seeds, Cat. No. VIS-01) and placed in a tin foil baking dish (diameter 20 cm, depth 5 cm).

Approximately 100 seedlings were grown in 16 cm x 12 cm x 5.5 cm containers, for transformation. At approximately 4 weeks of age, when the plants had just developed a primary shoot with a few flowers, the flowers were submerged in Agrobacterium solutions prepared as described above; the plants were gently agitated for 5 seconds. After dipping the plants were placed in a growth tray, covered with plastic dome to maintain high humidity, and kept at room temperature away from direct sunlight for 24 hours. After this time, the dome was removed and the plants were transferred back to the growth chambers until seed set. After 2 to 3 weeks the plants were allowed to dry out for harvesting of seeds.

The resulting T1 seeds were sown on soil at a high density and maintained in growth chambers. T1 transformants carrying a Basta resistance gene were selected based on their ability to grow following foliar application of the commercial herbicide "Wipeout" (0.067% (v/v); Wilson Laboratories Inc). At 14 days, plants were sprayed with Wipeout once a day, for five continuous days. Transformants make healthy true leaves in these conditions while non-transformed seedlings turn yellow and die. The Basta-resistant T1 plants were transplanted into individual pots for seed set.

Genomic DNA extraction and genotyping of the *apt1-3* allele

Leaf tissue was first homogenized in 50 µL extraction buffer (0.2 M Tris-HCl pH 7.2, 0.25 M NaCl, 0.025 M EDTA, 0.5% (w/v) SDS). After homogenization 350 µL of extraction buffer was added before vortexing for 5-10 sec. The homogenate was centrifuged for 1 min at

14,000 rpm. The resulting supernatant, 300 µL, was transferred to a new tube and an equal volume of isopropanol was added to precipitate DNA by inverting the mixture multiple times. After a 2 min incubation period at room temperature the DNA was pelleted by centrifugation at 14,000 rpm for 5 min. The pellet was allowed to air dry before resuspension in 50 µL of TE buffer (10 mM Tris-HCl pH 7.5, 1mM EDTA).

The WT *APT1* gene contains three *Bst*NI restriction enzyme sites. The mutation of a single nucleotide within the *Bst*NI site in the *apt1-3* allele does not allow the *Bst*NI enzyme to recognize this site thus yielding restriction fragments that are different from those of the WT gene (Gaillard *et al*., 1998). The appropriate region of the *APT1* gene was PCR amplified using the APT Forward and AB19754 primers using the cycle conditions: 94°C 4:00 min, 36 cycles of 94°C 30 sec, 52°C 30 sec, 72°C 1:15 min, and final elongation of 72°C 10 min. One half of the PCR reaction was used for the restriction enzyme digest using *Bst*NI for 2h at 60°C. *Bst*NI digestion of the WT PCR product produces fragments of 80, 343, 461 and 479 bp; similar digests of the corresponding PCR fragment from an *apt1-3* mutant produces fragments of 80, 363, and 940 bp. These were most easily detected by electrophoresis of the complete digest on a 1% TAE agarose gel.

Affinity purification of StrepII-tagged proteins

StrepII-tagged proteins and their associated protein interactors were isolated using the following protocol that was adapted from Witte *et al*., 2004. One gram of leaf tissue was homogenized in liquid nitrogen and resuspended in 2 mL Ex-Strep buffer: 100 mM Tris-HCl pH 8.0, 5 mM EDTA, 200 mM NaCl, 10 mM dithiothreitol (DTT; from a 100 mM stock solution), 0.5% (v/v) Triton X-100, 10% (v/v) glycerol, 1 mM phenylmethyl sulfonyl fluoride (PMSF;

prepared fresh as a 100 mM stock in methanol), and 200 µL of protease inhibitor cocktail (Roche). The protease inhibitor cocktail is provided as a tablet; 1 tablet was dissolved in 1 mL of sterile water and 100 µL was added per mL of Ex-Strep buffer.

The homogenate was centrifuged at 4°C for 20 minutes, at 20,000 g. Before incubation with the StrepTactin Macroprep beads (Novagen), 40 µL of resin per purification was centrifuged at 700 g for 30 seconds to pellet the beads and allow removal of storage buffer in the supernatant fraction. The beads were washed once with 1X PBS and 2X with Ex-Strep buffer. The beads where incubated with the supernatant by end-over-end mixing for 15 minutes at 4°C. The mixture was centrifuged at 700 g for 30 seconds and the resin washed five times with 0.8 mL of W-Strep buffer: 100 mM Tris-HCl pH 8.0, 0.5 mM EDTA, 200 mM NaCl, 2 mM DTT 0.5% (v/v) Triton X-100, 10% (v/v) glycerol, 1 mM PMSF, and protease inhibitor cocktail (100 µL per mL of W-Strep buffer; Roche). After the final wash the resin was resuspended in 20 µL 2X SDS loading buffer and boiled for 6 minutes to aid the dissociation of StrepII tag from the strepavidin beads. The boiled mixture was placed on ice for 10 minutes to allow the beads to settle and facilitate the removal of the supernatant.

Protein concentration was not determined for any of the extractions as the protein was eluted directly into SDS loading dye. However, over-expressed StrepII fusion protein is easily detected by less sensitive staining methods such as Coomassie staining. If the intended purpose is to excise polypeptides for mass spectrometry analysis it is recommended to use either silver staining or Sypro Ruby Gel Protein Stain (Invitrogen). Polyacrylamide gels were stained with Sypro Ruby according to the manufacturer's instructions. Briefly, the gel was incubated twice in 100 mL fixative solution (50% methanol, 7% acetic acid) for 30 min. The gel was moved into a clean container and stained with 60 mL of Sypro Ruby gel stain overnight. The next day, the gel

was placed in a new container and washed with 100 mL Wash solution (10% methanol, 7% acetic acid) for 30 min. This was followed with two washes in MilliQ water for 5 min after which the gel was viewed and imaged using a 300 nm UV transilluminator.

Cloning and over-expression of recombinant APT1.1 and APT1.2 proteins

Recombinant APT1.1 and APT1.2 were expressed in *E. coli* using Novagen's pET28 and pET30 vectors. These vectors fuse six histidine residues (6xHIS) at the carboxy terminus of the of protein product providing a small and highly specific epitope tag for protein purification. The small size of the 6xHIS helps alleviate concerns of the tag interfering with protein folding and protein activity. A second feature of the pET system is the ability to control expression of the recombinant protein using isopropyl-D-thiogalactopyranoside (IPTG). IPTG induces expression of the T7 RNA polymerase gene contained in DE3 lysogens, leading to synthesis of the fusion protein.

The *APT1.2* ORF was cloned into the *Nco*I/*Hin*dIII restriction sites of pET30a (Antonio Facciuolo, Biol 499 Senior Honours Project, University of Waterloo, 2007). The ligation mix was transformed into DH5α (strain #591) and once the desired clone was identified it was introduced into the expression host BL21(DE3)pLysS (strain #601).

The *APT1.1* ORF was amplified from WT cDNA using the primers apt1-exon1 and AB12380. This fragment was cloned into the *Nde*I/*Hin*dIII restriction sites of the pET28a vector. The plasmid was transformed into DH5α (strain #1304) and the BL21(DE3)pLysS expression host (strain #1305). The *APT1.1* ORF was also amplified from WT cDNA using the primers apt1-exon1 blunt and AB12380. This fragment was subsequently cloned into the *Eco*RI/*Hin*dIII sites of pET30a. The recombinant APT1.1 was recovered from the expression hosts

BL21(DE3)pLysS and CodonPlus BL21(DE3)RIPL creating strains #601 and #1305. APT enzymatic assays on the APT1.1-6xHIS recombinant protein presented in this thesis were derived from strain #601.

The APT1.1-6xHIS and APT1.2-6xHIS recombinant proteins were over-expressed and purified under the same conditions. First, each strain was used to inoculate a 5-10 mL overnight LB starter culture supplemented with kanamycin (50 μg/mL) and chloramphenicol (25 μg/mL). The starter culture was used to inoculate 250 mL LB media supplemented with the same antibiotics as above and incubated at 37°C until the OD_{600} reached 0.8. At this point T7 expression was induced by adding 0.2 mM IPTG; the culture was incubated at 28°C for 5 h. The cells were collected by centrifugation at 4°C at 5500 rpm for 15 min. The supernatant was discarded and the pellet flash frozen on dry ice for 10 min before being stored at -20°C.

Freshly prepared cells or frozen cell paste were placed on ice or kept at 4°C for the remainder of the purification protocol. The pellet was resuspended in 20 mL Binding Buffer (Table 4) plus 0.1% (v/v) Tween 20 to reduce the viscosity of the crude cell extract. The resuspended cells were lysed by sonicating 4X for 30 sec, with a 1 min rest period on ice between each sonication (Sonic Dismembrator 100, Fisher Scientific). This extract was centrifuged at 4°C 13,200 rpm for 30 min and the supernatant filtered through a 0.45 μm filter to remove cellular debris.

To capture 6xHIS-tagged proteins Novagen's Ni-NTA resin was used for column chromatography. The composition of each buffer can be found in Table 4. One mL of Ni-NTA resin was prepared by loading the column bed with 3 volumes of strip buffer followed by 3 volumes of water, 5 volumes of charge buffer, and 3 volumes of bind buffer at a flow rate of 0.5

mL/min. The protein extract was loaded on the column resin and the flow through passed over the column to maximize capture of 6xHIS protein. The column bed was washed with 10 volumes of bind buffer followed by 12 volumes of wash buffer, and eluted using 3 volumes of elution buffer. The purified protein was concentrated and dialyzed using a Centricon Centrifugal Filter Device with 10,000 MW membrane cut-off (Millipore). For enzymatic assays the protein was dialyzed in 50 mM Tris-HCl pH 7.5; for antibody generation the protein was dialyzed in sterile PBS.

Table 4. Buffers used in purifying 6xHIS recombinant protein by affinity chromatography

Buffer	Composition
Charge Buffer	50 mM $NiSO_4$
Strip Buffer	100 mM EDTA, 0.5 M NaCl, 20 mM Tris-HCl pH 7.9,
Bind Buffer	5 mM imidazole, 0.5 M NaCl, 20 mM Tris-HCl pH 7.9
Wash Buffer	60 mM imidazole, 0.5 M NaCl, 20 mM Tris-HCl pH 7.9
Elution Buffer	400 mM imidazole, 0.5 M NacCl, 20 mM Tris-HCl pH 7.9

APT1 polyclonal antibody generation

APT1.2-6xHIS recombinant protein was generated, purified, and dialyzed in sterile PBS buffer as outlined in the previous section. A white New Zealand rabbit was given four booster injections. The first booster consisted of 500 μg of recombinant protein in PBS mixed with an equal volume of Freund's complete adjuvant. The remaining three boosters were administered every 3 weeks and consisted of 300 μg of recombinant protein mixed with an equal volume of Freund's incomplete adjuvant.

Three weeks after the last booster injection the rabbit was bled and approximately 150 mL of blood was collected. To separate the blood from the antiserum, it was placed at 37°C for 2 hours to allow the blood to naturally clot. The clot was pelleted by centrifugation for 15 min at 1500 x g and the supernatant transferred to a new tube. The antiserum was aliquoted, flash frozen in liquid nitrogen, and stored at -80°C.

The APT1-antibody was tested for sensitivity and specificity by immunoblotting. To test for sensitivity, 10 ng, 1 ng, and 500 pg of APT1.2-6xHIS recombinant protein was probed with the APT1 antibody at a dilution of 1:5000 and 1:10,000 (Appendix 1). These blots showed that the antibody could detect 500 pg of protein at a dilution of 1:10,000. Next, specificity was tested by probing WT and an APT1-deficient plant extract (*oxt1*). Using a dilution of 1:10,000, an abundant polypeptide was detected in WT at 24 kDa representing APT1.2; a faint band was detected in the APT1-deficient mutant.

Chapter 1 - Results

Recovering *APT1.1* and *APT1.2* full-length cDNAs

The first objective of this research was to determine if *APT1.1* encodes a functional mRNA. The fact that full-length cDNAs for *APT1.1* have been previously recovered by selecting for mRNA species containing a 5′-guanidine cap indicates that it is a functional mRNA. Capped cDNAs can be found in the Ceres cDNA clone collection (NCBI AY084300) and the RIKEN Arabidopsis full-length cDNA clone collection (NCBI BP837943). I attempted to recover these full-length cDNAs from WT leaves using Ambion's RLM-RACE kit. The initial step in this technique involves treatment of total RNA with calf intestinal phosphatase. This step removes 5′ phosphate groups from all RNA species except for mRNAs, which have their 5′phosphate group protected from enzymatic cleavage by the 5′-guanidine cap. The second step uses tobacco acid pyrophosphatase to remove the 5′-guanidine cap exposing a 5′-phosphate group, allowing for a suitable substrate for ligation to a DNA adaptor, in a reaction mediated by RNA ligase.

The subsequent cDNA synthesis initiates from primers binding to the polyA tail and the adaptor; amplification by PCR provides sufficient template for DNA sequencing of specific cDNAs. RLM-RACE was successful in recovering the *APT1.2* full-length cDNA previously reported by Moffatt *et al*., 1994. No full-length cDNA was recovered for *APT1.1*.

It was possible that RNA secondary structure, particularly in the 5′ end of the mRNA limited recovery of the full-length transcript. The methods used by RIKEN involved the use of trehalose, an agent known to stabilize reverse transcriptase at high temperatures (Carninci *et al*., 1998; Seki *et al*.,1998) . Thus a higher temperature cDNA synthesis reaction was carried out at

and 42°C and 55°C using Roche's Transcriptor High Fidelity cDNA synthesis kit. Several different forward primers were used for the PCR amplification step, to determine the 5′ end point of the cDNA product. AP183 anneals to the reported 5′ terminal end of the transcript; AP184 anneals 100 base pairs into the 5′ UTR, and AP187 anneals 30 base pairs upstream of the start codon (Figure 5, Appendix 3). PCR amplification using AP183 was unsuccessful for cDNA synthesized at both temperatures; PCR amplification using AP184 and AP187 consistently yielded DNA fragments of the expected sizes (787 bp for AP184 and 737 bp for AP187). The identity of the smaller fragment in the AP184 reaction at 55°C was not determined. Based on the terminal end of the 5′ UTR of *APT1.1* may contain significant secondary structure that blocked my attempts to recover the full-length cDNA of *APT1.1* as reported by Ceres and RIKEN. However I was confident that their data were reliable and did not invest further effort in duplicating their results.

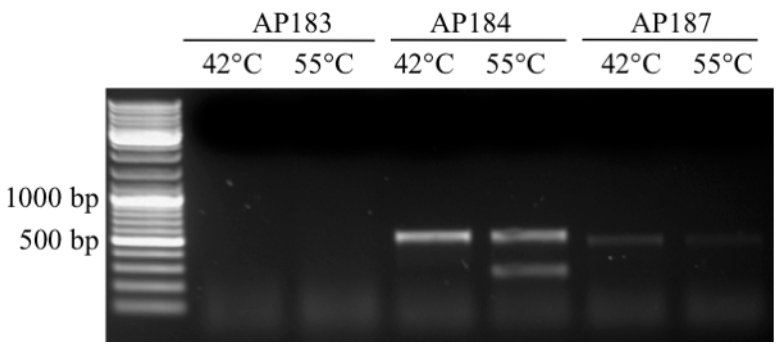

Figure 5. PCR primer walking along the *APT1.1* 5´UTR. RNA was extracted from leaf tissue and cDNA synthesized at 42°C and 55°C using Roche Transcriptor High Fidelity cDNA synthesis kit. Three forward primers were designed: AP183 to anneal to the 5´ end of the cDNA, AP184 to anneal 100 bp into the 5´ UTR, and AP187 to anneal 30 bp upstream of Exon 1. The reverse primer AB19754, anneals within the terminal exon, was used with all three forward primers.

Expression analysis of APT1.1 and APT1.2

The identification of two *APT1* transcripts in numerous expressed sequence tag collections along with the recovery of apparently full-length cDNAs lead to the second objective of this research: comparing the expression profiles of *APT1.1* and *APT1.2* in WT and the APT1-deficient mutants *oxt1* and *apt1-3*. The *oxt1* mutant contains a T-DNA insertion element between Exon 1 and Exon 2; *apt1-3* contains a point mutation in the Exon 4 splice junction. RT-PCR analysis was used to evaluate the impact of each of these mutations on the *APT1.1* and *APT1.2* transcript levels, as compared to the corresponding transcript levels in WT.

Semi-quantitative RT-PCR was carried out using forward primers specific to the 5´ UTRs of each transcript and a reverse primer, located in the terminal exon which is common to both *APT1.1* and *APT1.2* transcripts. Each primer's linear range was determined using WT cDNA as a template. Parallel reactions were initiated and starting at the 20th cycle, one reaction was stopped every 4 cycles, until the 44th cycle was reached. The amount of amplified product in each case

was quantified in nanograms using spot density analysis of the digitized image and the molecular weight markers as standards; the results were plotted against cycle number, on semi-log graph (Figure 6). Based on these data, I concluded that PCRs of 30 cycles were within the linear range for both reactions and would provide a meaningful relative abundance estimate.

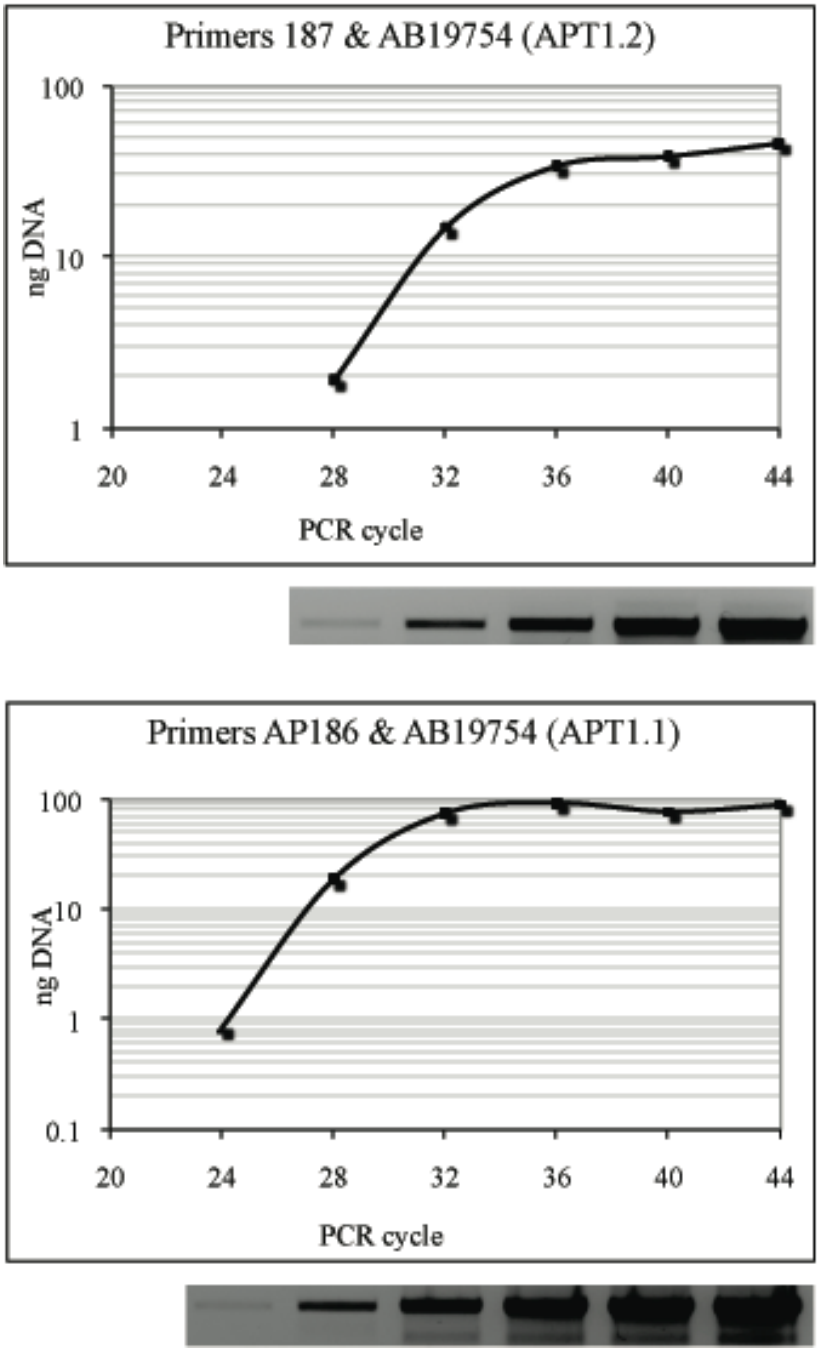

Figure 6. Linear range estimate of APT1.1 and APT1.2 primer sets for RT-PCR analysis. WT cDNA template was amplified by PCR for 20 through 44 cycles and electrophoresed on a 1% (w/v) TAE agarose gel. The gel image was digitized and each DNA fragment quantified, in nanograms, using spot density analysis. The nanograms of cDNA synthesized were plotted against the cycle number on semi-log graph paper. Thirty cycles were used for subsequent RT-PCRs using these primer pairs.

In WT, *APT1.1* and *APT1.2* transcripts were equally abundant in both expanded leaves (Figure 7A) and WT inflorescences (Figure 7B). *oxt1*, which contains a T-DNA insertion within Intron 1, lacked the expected *APT1.1* transcript in both leaves and inflorescences. A fore-shortened *APT1.2* transcript was present in both tissues of *oxt1*, in the same abundance as in WT.

Three distinct *APT1.1* and *APT1.2* related RT-PCR products were detected when mRNA from *apt1-3* leaves or inflorescences was used as a template. This was somewhat unexpected since *apt1-3* contains a point mutation in the splice junction of Exon 4 which was anticipated to trigger rapid turnover of both *APT1.1* and *APT1.2* transcripts. To identify the mRNA template of these products, each was gel purified and sent for sequencing. The results showed that the largest PCR product was amplified from an *APT1* transcript that had retained the third intron, consistent with the site of the *apt1-3* mutation. The second largest PCR product recovered from the *apt1-3* reaction was identical to the WT *APT1* product, consistent with there being some normal splicing of the primary transcript. The smallest PCR product was copied from an mRNA that was missing Exon 4. Thus, these RT-PCR results confirmed that Intron 3 splicing was abnormal in *apt1-3* resulting in the synthesis of aberrant transcripts. More importantly the analysis showed that *APT1.1* and *APT1.2* transcripts were present in approximately equal abundance in WT leaves and inflorescences. These transcripts were missing in the APT1-deficient mutants *oxt1* and *apt1-3*, consistent with the mutation each contains.

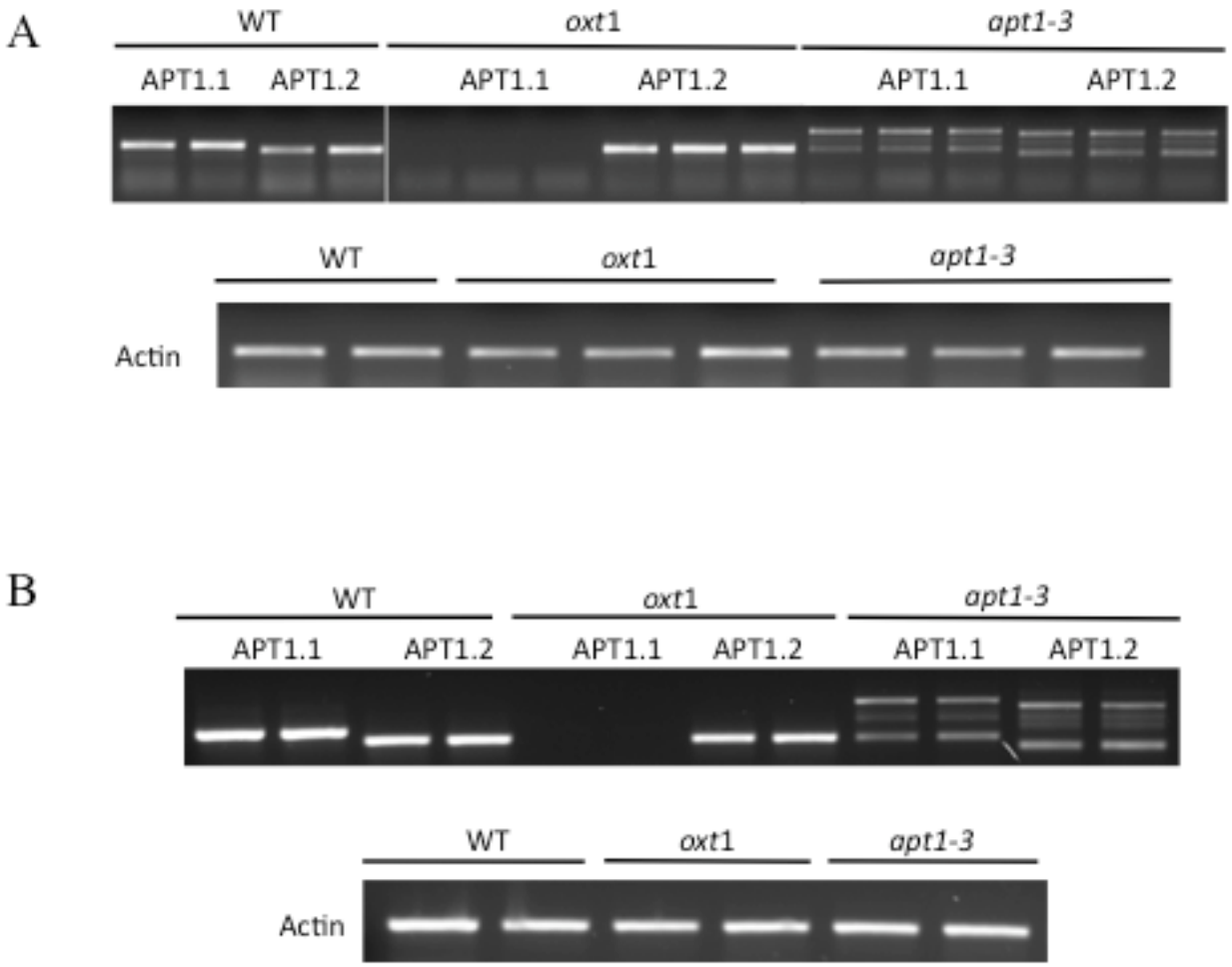

Figure 7. RT-PCR analysis of *APT1.1* and *APT1.2* in leaves and inflorescences. Transcript abundance was measured using forward primers specific to each transcript variant's 5′ UTR. The reverse primer, common to both transcripts, anneals with the terminal exon. WT organs showed equal expression of *APT1* isoforms in both leaves (A) and inflorescences (B). The *oxt1* mutants had no *APT1.1* product but did have an equal expression of *APT1.2* as in WT. *apt1-3* lines show three aberrant *APT1* transcripts. Actin was used as control to test that the same amount of cDNA was added to each PCR.

The next questions addressed were: are both APT1.1 and APT 1.2 transcripts translated in WT plants and if so, how do the protein and transcript abundances compare? This analysis was carried out by immunoblotting of crude extracts of leaves and inflorescences of four-week-old plants. APT1.2 was easily detected in WT leaves while APT1.1 was present at approximately one-tenth the level of APT1.2 (Figure 8, compare Lanes 5 and 6). APT1.2 was slightly more

abundant in inflorescences, than in leaves, while APT1.1 was undetectable (Figure 8, Lanes 7 and 8). Thus, although the *APT1.1* and *APT1.2* transcripts levels were similar in leaves, the immunoblots clearly showed that either the two transcripts were not translated with equal efficiency or that the APT1.1 protein is turned over more rapidly relative to APT1.2. APT1.1 transcripts were subject to post-transcriptional regulation that appeared to differ in extent, in leaves and inflorescences.

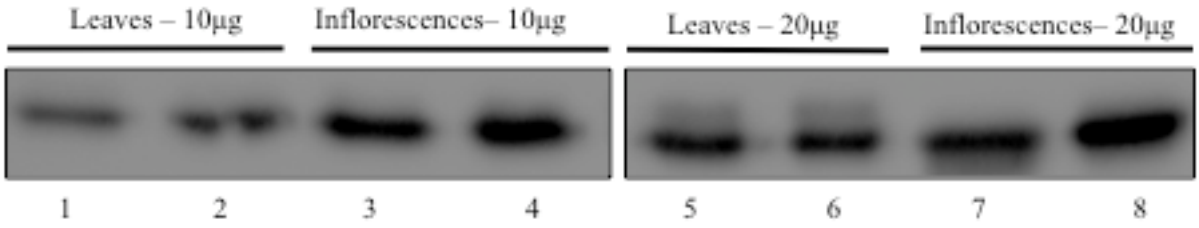

Figure 8. APT1.1 and APT1.2 protein abundance in WT leaves and inflorescences. Leaf and inflorescence protein extracts of 10µg and 20µg (with two biological replicates of each) were probed with rabbit anti-APT1 antibody; bound antibody was detected by anti-rabbit antibody conjugated to HRP. Polypeptides in lanes 1, 2, 3, 4, 7, and 8 are approximately 24 kDa. Polypeptides in lanes 5 and 6 are 24 kDa and 26 kDa, respectively.

A similar immunoblot analysis was carried out on leaf and floral extracts of the APT1-deficient mutants, *apt1-3* and *oxt1*. In *apt1-3*, expression of APT1.1 and APT1.2 was below the level of detection, which is consistent with the 1-2% residual APT activity in this mutant (Figure 9). In *oxt1*, a faint APT1.2 polypeptide was visible after a normal detection period (20 sec); this polypeptide became more apparent after a longer exposure (1 min 10 sec). Based on these data it was estimated that *oxt1* has about 1% of the APT1.2 present in WT leaves. No APT1 polypeptides were detected in *apt1-3* leaf and floral extracts even after long detection periods of the immunoblots (data not shown).

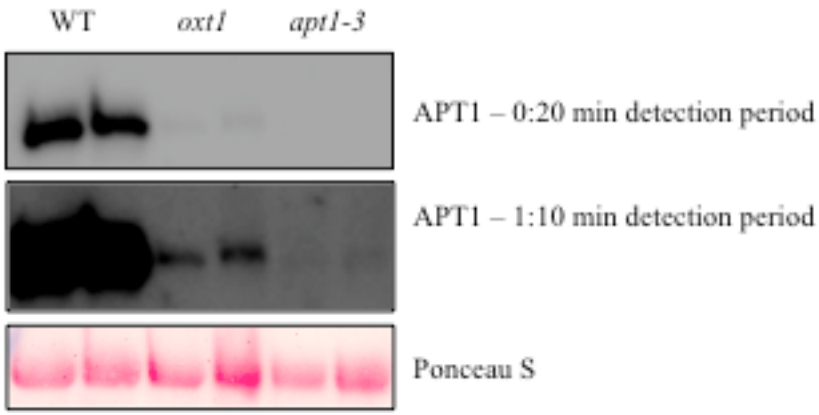

Figure 9. Abundance of APT1.1 and APT1.2 in WT and APT1-deficient mutants. Leaf protein extracts (20µg each lane) were probed with anti-APT1 antibody and bound antibody detected using a rabbit secondary antibody conjugated to HRP. The immunoblot was visualized for two different detection periods; only the longer detection period revealed APT1 in *oxt1*. The membrane was stained with Ponceau S to test for equal loading of samples.

The absence of an APT1.1 polypeptide in *oxt1* and *apt1-3* indirectly confirmed that the faint APT1.1 detected in WT leaves is indeed an APT1 protein. Its weak detection on initial immunoblots was not convincing that this polypeptide was APT1.1. Rather it could be regarded as a nonspecific target. To address this concern a direct approach was used to confirm that translation initiation occurs at Exon 1 *in vivo*.

APT1.1 coding capacity and regulation

Two transgenes were constructed to test whether the APT1 Exon 1 is translated *in vivo* and thus prove that *APT1.1* is a functional mRNA (Figure 10A). The first construct contained 800 base pairs upstream of the *APT1.1* transcriptional start site, plus the 5′ UTR and the first Exon, fused in-frame with GFP (*APT1*::Ex1:GFP). The second construct contained the same elements (*APT1* promoter region, 5′UTR , Exon 1) in addition to Intron 1, and Exon 2, again fused in-frame with GFP (*APT1*::Ex1-i-Ex2:GFP). The premise behind the design of these

constructs was that if translation initiation occurs at Exon 1 then a polypeptide of 32 kDa would be produced in *APT1*:Ex1:GFP plants (26 kDa GFP +7 kDa Exon 1) whereas translation of the second transgene would produce both a 36 kDa polypeptide (26 kDa GFP + 7 kDa Exon 1 + 3 kDa Exon 2) and a 29 kDa polypeptide (26 kDa GFP + 3 kDa Exon 2).

Each transgene was introduced into WT Arabidopsis and four stable T1 transformants for each construct were analyzed by immunoblotting. Crude leaf extracts were separated by electrophoresis through SDS-PAGE, blotted to membranes and probed for the presence of GFP. *APT1*:Ex1:GFP plants synthesized a polypeptide of 28 kDa, slightly smaller than the expected 32 kDa but larger than GFP alone (Figure 10B). The *APT1*::Ex1-i-Ex2:GFP plants were predicted to express two GFP-fusion polypeptides: the 36 kDa polypeptide initiated at Exon 1 and a 29 kDa polypeptide representing translation initiation at Exon 2. Interestingly, only the 29 kDa was detected in these plants.

Although the results were not exactly as anticipated, these immunoblotting data confirmed that translation initiated at Exon 1 and an *APT1.1* polypeptide is synthesized *in vivo* as observed in *APT1*::Ex1:GFP plants. In *APT1*::Ex1-i-Ex2:GFP plants only a polypeptide of 29 kDa was detected with the anti-APT1 antibody representing translation initiation occurring at Exon 2. In these same plants there was no detectable translation initiation of Exon 1.

These results showed that translation initiation at Exon 1 is greatly reduced by the presence of Intron 1 and Exon 2. Since these transgenes were expressed in a WT background, which has functional APT1 genes, it is evident that the inhibition of APT1.1 synthesis by Intron 1-Exon 2 occurred only when these elements are immediately downstream of Exon 1, as in the *APT1*::Ex1-i-Ex2:GFP transgene; this transgene did not affect expression of the WT gene.

Thus the *APT1*::Ex1-i-Ex2:GFP transgene mimicked expression of the WT *APT1* gene in leaves and inflorescences in that a polypeptide was initiated at Exon 2 (Ex2:GFP fusion) while the corresponding APT1.1 polypeptide was undetectable. To confirm this post-transcriptional effect I needed evidence that *APT1.1* and *APT1.2* transcripts are produced from the *APT1*::Ex1-i-Ex2:GFP transgene, and that the absence of APT1.1 protein was not an artifact of this particular transgenic construct.

RT-PCR was used to investigate the transcriptional products arising from the *APT1*::Ex1-i-Ex2:GFP transgene. RNA was extracted from the leaves of two independent homozygous *APT1*::Ex1-i-Ex2:GFP plant lines (2-2 and 2-4). Two forward primers were used for RT-PCRs specific to the 5′ UTR of *APT1.1* and *APT1.2*, respectively; the reverse primer was specific for the GFP open reading frame, which was located at the 3′ end of both transgenes. The selection of this reverse primer ensured that only *APT1* transcripts arising from the transgenes and not from the WT allele would be amplified (Figure 10C). This RT-PCR was not done semi-quantitatively as this was a test for the presence or absence of two transcriptional products; 36 PCR cycles were arbitrarily chosen. Amplification of the *APT1.1* transcript using these primers was expected to yield a product of 428 bp whereas amplification of the *APT1.2* transcript would yield a 360 bp fragment. Both of these products were detected in the *APT1*::Ex1-i-Ex2:GFP plants.

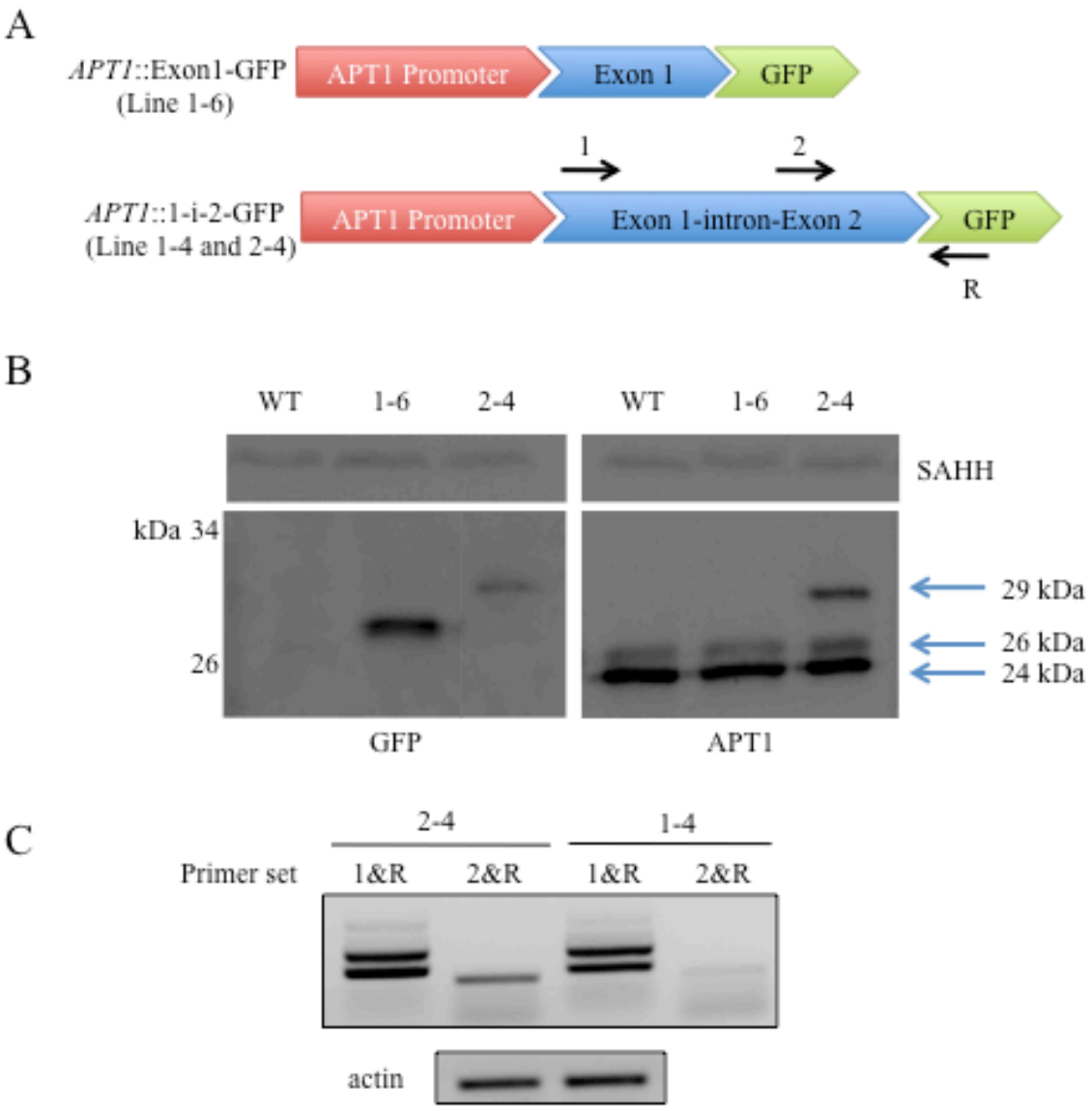

Figure 10. Transcript and protein products arising from *APT1*::Ex1:GFP transgenes. A, Schematic of *APT1*::Ex1:GFP and *APT1*::Ex1-i-Ex2:GFP transgenes. Arrows represent primers used for RT-PCR. B, Immunoblot analysis of GFP protein synthesized from the 1-6 line of *APT1*::Ex1:GFP and the 2-4 line of *APT1*::Ex1-i-Ex2:GFP. The left blot was probed with anti-GFP antibody; the right with anti-APT1 antibody, and the top blot with anti-SAHH antibody. In all cases bound antibody was detected using anti-rabbit antibody conjugated to HRP. SAHH was used to test for equal loading. C, RT-PCR analysis of *APT1*::Ex1-i-Ex2:GFP transgene. RNA used for cDNA synthesis was extracted from leaves of two independent lines (2-2 and 2-4). Forward primers used for RT-PCR were specific to each isoform's 5′ UTR. The reverse primer anneals within the GFP ORF and is common to both transcripts.

The RT-PCR detected a second, larger APT1.1 product arising from the *APT1*::Ex1-i-Ex2:GFP transgene. The size of this fragment, approximately 600 to 700 bp, was larger than the expected 428 bp fragment, but consistent with the size of the primary *APT1.1* mRNA (i.e. mRNA in which the intron was not spliced out; 648 bp). This fragment was not sequenced so this conclusion has yet to be to verified unequivocally.

Taken together with the immunoblot analysis these data showed that the *APT1.1* transcript is post-transcriptionally regulated while the *APT1.2* transcript is not. Assuming that the *APT1.1* and *APT1.2* transcripts arising from the *APT1*::Ex1-i-Ex2:GFP transgenes are of similar abundance as occurs from the WT gene, then the reduced APT1.1 protein levels must be a post-transcriptional effect. This post-transcriptional regulation could be acting on either the primary transcript or the processed mRNA. If the regulation is exerted on the primary transcripts then the targets of this process could be the 5′ UTR/Intron 1; if the regulation acts on the mRNA then the target must be the APT1.1 5′ UTR as this is the only difference between the two transcripts.

APT1.1 encodes an active enzyme

Having concluded that *APT1.1* is a functional mRNA whereby translation initiation can occur at Exon 1 the next question addressed whether the APT1.1 protein produced from this transcript is an active enzyme. The APT1.1 and APT1.2 ORFs were previously cloned into the pET28a and pET30a vectors in-frame with 6 histidine residues (APT1.1-6xHIS, APT1.2-6xHIS). The recombinant proteins were over-expressed in *E. coli* BL21(DE3)pLysS cells and purified by affinity chromatography using a Ni-NTA resin (Novagen). Purified recombinant protein was than dialyzed in 50 mM Tris-HCl, pH 8.8. The enzymatic activity of APT1.1-6xHIS and APT1.2-6xHIS was measured using a radiochemical assay that monitored the amount of ^{3}H-

adenine converted into ^{3}H-AMP (Table 5). Although the kinetic properties of these recombinant proteins were not determined, the results showed that APT1.1-6xHIS and APT1.2-6xHIS recombinant proteins were very active enzymes. APT1.1-6xHIS had 805-fold greater specific activity than WT extracts; APT1.2-6xHIS had 41-fold greater specific activity than WT extracts.

Table 5. Enzymatic activity for APT1.1-6xHIS and APT1.2-6xHIS recombinant proteins. Recombinant proteins were over-expressed in *E.coli* BL21(DE3)pLysS cells and affinity purified using Ni-NTA resin. Recombinant protein was dialyzed in 50 mM Tris-HCl pH 8.8 and APT activity measured using a radiochemical assay. Results are the average of two individual over-expression and purification experiments.

	Specific Activity nmol AMP mg protein^{-1} min^{-1}	**Standard Deviation (%)**	**Fold Increase over WT**
WT (crude extract)	5.43	21.1	-
APT1.1-6xHIS (purified protein)	4372	13.2	805
APT1.2-6xHIS (purified protein)	223	21.1	41

Subcellular localization of APT1.1 and the function of Exon 1

Given that both APT1 isoforms were very active enzymes, the question arose as to whether the proteins resided in the same subcellular compartments. One possibility was that Exon 1 encodes a transit peptide that compartmentalizes APT1 activity in a cellular location other than the cytosol. Bioinformatic analysis using TargetP predicts Exon 1 is a cleavable transit peptide that localizes APT1.1 to chloroplasts (Emanulesson *et al*., 2000; Nielsen *et al*., 1997). A

recent proteomic study of the plastid proteome supports this bioinformatic analysis as APT1.1 was identified in the chloroplast stroma (Sun *et al*., 2009).

To test this hypothesis 800 base pairs of the presumptive *APT1.1* promoter were used to direct the expression of an Exon 1 GFP fusion protein (*APT1*::Ex1:GFP). This transgene was introduced into WT Arabidopsis and four stable transformants were recovered. The localization of the GFP in leaves of four homozygous lines was observed using confocal microscopy. In leaves of 3-4 week-old plants, the GFP signals were strongest in epidermal cells and were localized in the cytosol. The GFP signals in the underlying mesophyll cells were contained in stationary punctate bodies of approximately 2 μm (Figure 11). GFP localization was also observed in nuclei, as expected, since this fusion protein is below the exclusion limit of the nuclear pore (28 kDa versus 70 kDa exclusion limit) (D'Angelo *et al*, 2009).

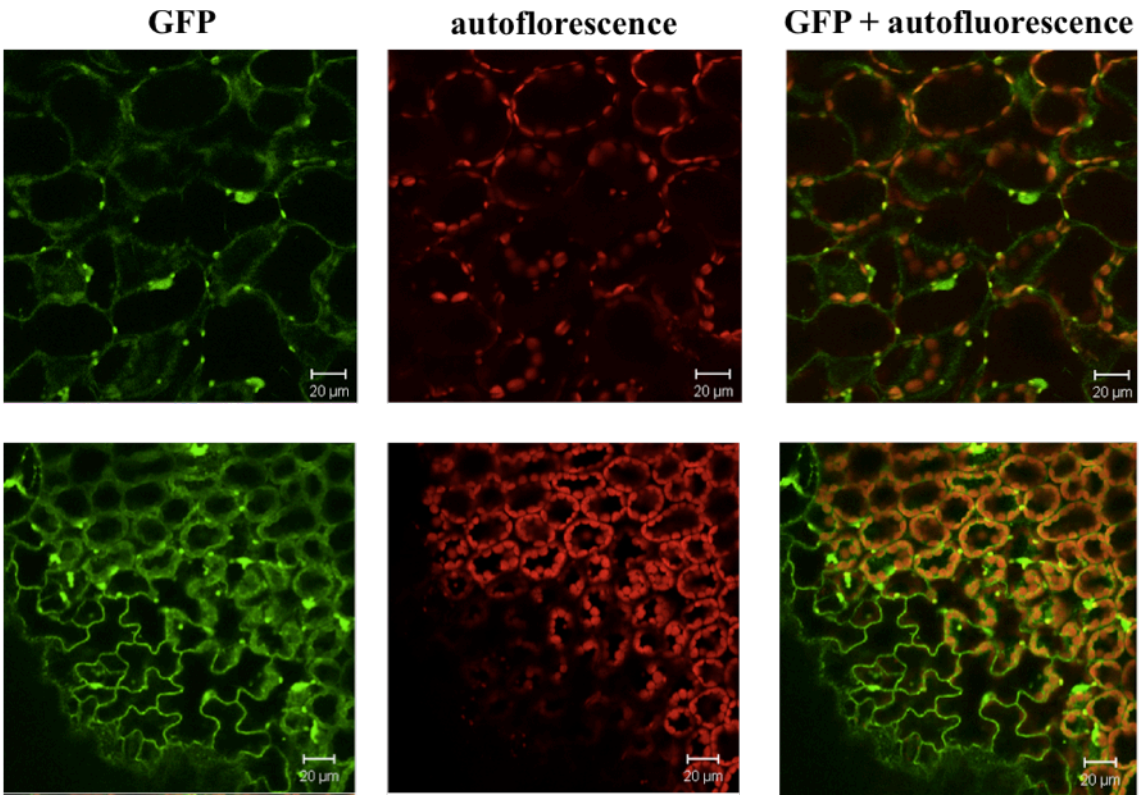

Figure 11. Confocal microscope analysis of *APT1*::Ex1:GFP transformants. Leaves were imaged using confocal laser scanning microscopy. Shown is the GFP signal (left), chlorophyll autofluorescence (middle) and a merged image of both fluorescent signals (right). The white scale bar represents 20 µm.

The identity of the punctate signals in mesophyll cells was investigated next. The punctate bodies did not consistently colocalize with chlorophyll autofluorescence, which would have indicated chloroplast localization. This might have been due to weak GFP expression from the native APT1.1 promoter. A count of 20 punctate bodies in the *APT1*::Ex1:GFP plants showed that these punctuate bodies were between 2 to 3 µm in diameter. In addition, these punctate bodies were stationary. This observation rules out the likelihood that these punctate bodies represent mitochondria or peroxisomes since those organelles are smaller (0.5µm to 1µm in diameter), and more dynamic in their movements (Logan and Leaver, 2000; Titorenko and Mullen, 2006).

With the hope that higher expression of GFP might give a more definitive signal a new construct was made using the actin promoter in place of the native *APT1* promoter. The open reading frame of APT1.1 was cloned in-frame with two tandem C-terminal GFP ORFs (*actP*::APT1.1:2GFP). The 5′ UTR of APT1.1 was not included in this construct. The presence of the second GFP ORF increased the size of the fusion protein to 78 kDa so that diffusion into the nucleus should be eliminated (D'Angelo *et al*, 2009). The *actP*::APT1.1:2GFP transgene was introduced into WT Arabidopsis and five stable transformants were examined by confocal microscopy. In all T1 lines there was a clear overlap of the GFP signal with chlorophyll autofluorescence (Figure 12). Once again, the stationary punctate bodies of 2 to 3 μm in diameter were observed at the mesophyll layer cells. Interestingly, these signals did not overlap with chlorophyll autofluorescence. As expected, no nuclear GFP signals were detected in these lines indicating that the nuclear localization seen in the *APT1*::Ex1:GFP plants was due to diffusion.

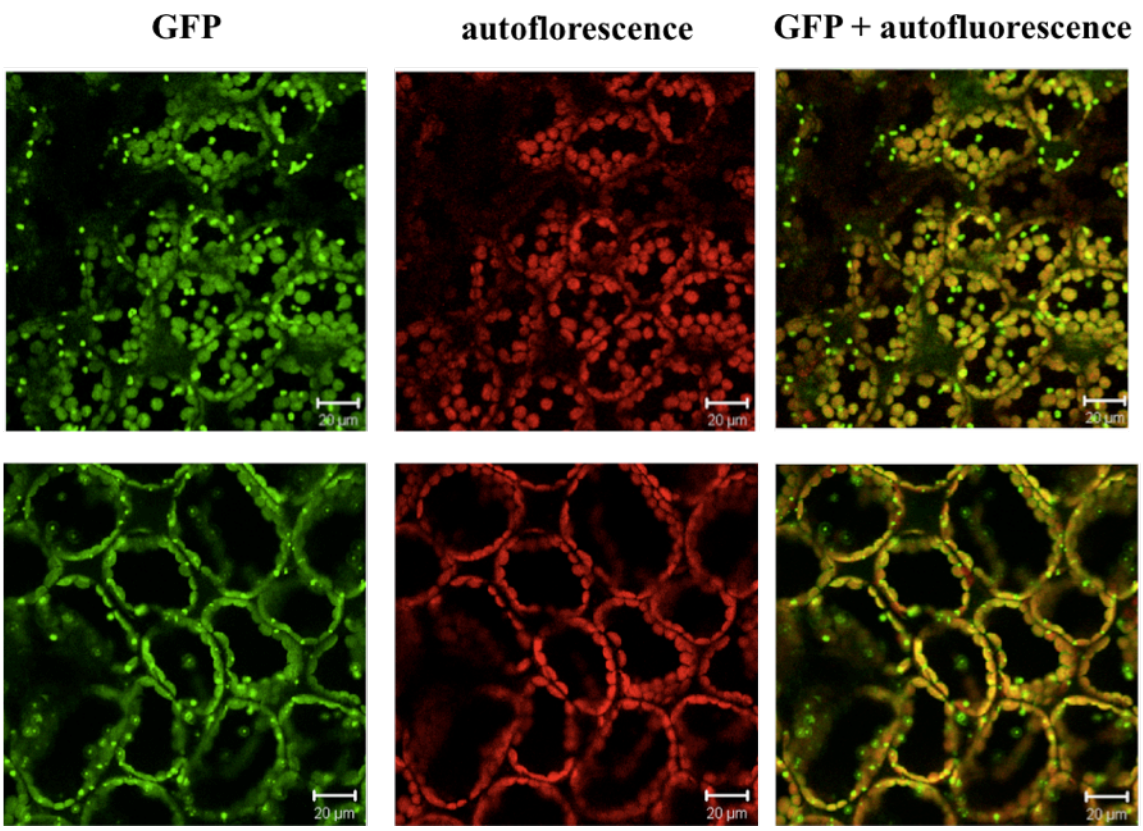

Figure 12. Confocal imaging of *actP*::APT1.1:2GFP translational fusions in Arabidopsis leaves. Top panel represents 3.5-week-old leaves, bottom panel represents 4.5 week old leaves of stable transformants. Confocal laser scanning microscope was used to separately capture GFP signals (left) and chlorophyll autofluorescence (middle). A merged image of both fluorescent signals is shown in the right panels.

Overall, these observations suggested that APT1.1 under the expression of the actin promoter is localized to chloroplasts with a secondary undefined punctate-like location. Furthermore, in *APT1*::Ex1:GFP-containing plant lines, Exon 1 alone was sufficient for targeting to the punctate bodies.

If Exon 1 is a transit peptide for chloroplast import, it might be expected to be proteolytically cleaved once it has accomplished its role in targeting and directing translocation of APT1.1 across the chloroplast envelope. Bioinformatic analysis of APT1.1 identifies Exon 1

as a chloroplast transit peptide that cleaves away all but eight amino acids. To address this issue, the size of the GFP fusion proteins in *APT1*::Ex1:GFP and *actP*::APT1.1:2GFP plants was estimated by immunoblotting. In the *APT1*::Ex1:GFP lines a polypeptide of 33 kDa was expected if Exon 1 was not cleaved (26 kDa GFP + 7 kDa Exon 1); cleavage of Exon 1 would release a 26 kDa GFP polypeptide. *actP*::APT1.1:2GFP plants should synthesize a 78 kDa polypeptide in the absence of cleavage (52 kDa GFP + 26 kDa APT1.1); if Exon 1 was cleaved, a 71 kDa protein would remain.

Immunoblot analysis was carried out on leaf extracts of these transgenic lines. In the four *APT1*::Ex1:GFP lines examined a polypeptide of 28 kDa was detected with the anti-GFP antibody. This is smaller than the complete Exon1-GFP fusion protein and is thus suggestive that APT1.1 is subject to proteolytic cleavage (Figure 10B). However, in the five *actP*::APT1.1:2GFP lines that were similarly analyzed, a polypeptide of 78 kDa was detected, which is consistent with no cleavage (Figure 13). Thus, these lines provided conflicting data regarding Exon 1 being subject to proteolytic cleavage. The fusion of Exon 1 alone with GFP showed that this protein was cleaved. However, when only the ORF was expressed, Exon 1 was not proteolytically cleaved.

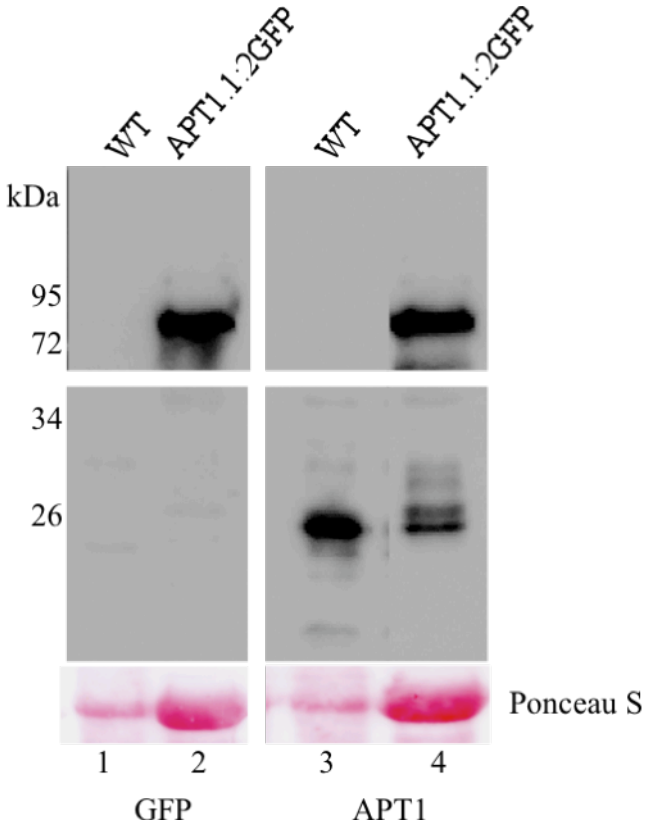

Figure 13. Immunoblot analysis of *actP*::APT1.1:2GFP containing plant lines. Crude leaf extracts (20 ug) of stable transformant Line #1 and WT inflorescences were probed with anti-APT1 antibody (right panels) and anti-GFP antibody (left panels). APT1.1:2GFP detected in lanes 2 and 4 migrated at 78 kDa, endogenous APT1.2 in lane 3 migrated at 24 kDa, and endogenous APT1.1 and APT1.2 in lane 4 migrated at 26 kDa and 24 kDa, respectively. Ponceau S staining shows equal loading of total protein.

Searching for protein-protein interactors of APT1.1 and APT1.2

Knowing that APT1.1 and APT1.2 were localized to different subcellular compartments raised questions regarding the function of each isoform. For example, are APT1.1 and APT1.2 differently localized because they function in metabolic pathways specific for distinct subcellular locations? To address this question, an attempt was made to identify potential protein-protein interacting partners for each isoform in the hopes that these might provide insight into their *in vivo* roles. Of the numerous methods available to detect protein-protein interactors, I chose to

express epitope-tagged versions of each APT isoform *in planta* and recover the tagged APT, along with its interactors, by affinity chromatography. To this end, *APT1.1* and *APT1.2* were cloned under the control of the Cauliflower Mosaic Virus 35S promoter with a C-terminal StrepII epitope tag (Witte *et al*., 2004). The StrepII tag is a small, eight amino acid peptide that is structurally similar to biotin. Assuming the StrepII tag does not interfere with APT1 protein interactions, the APT1-StrepII fusion can be captured along with its interactors, by chromatography on a strepavidin resin. The interactors can be separated by SDS-PAGE, and the identity of unique polypeptides identified by mass spectrometry.

Four stable APT1-StrepII transformants were used for protein extraction and purification along with a control line expressing an allantoate amido hydrolase (AAH)-StrepII fusion protein (Werner *et al*., 2008). The polypeptides recovered from APT1.1-StrepII and APT1.2-StrepII expressing lines were separated by SDS-PAGE, and visualized by Sypro Ruby Protein Gel Staining. Only one polypeptide was identified that interacted with APT1.1-StrepII, and was distinct from those in the control sample (Figure 14). This polypeptide was approximately 3 kDa larger than APT1.1-StrepII.

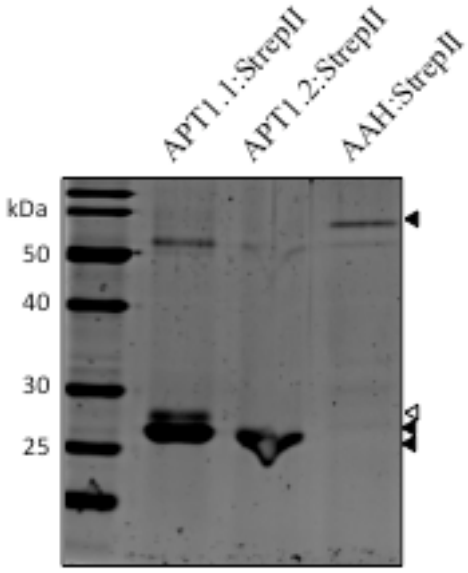

Figure 14. Affinity purification of APT1.1:StrepII and APT1.2:StrepII protein from 4-week-old Arabidopsis leaves. *APT1.1* and *APT1.2* ORFs were cloned into the pXCS-StrepII vector containing the constitutive 35S CaMV promoter and C-terminal StrepII tag (Witte *et al*., 2004). One gram of crude leaf protein was incubated with StrepTactin Macroprep resin (Novagen) to pull down StrepII tagged protein complexes as described in Witte *et al*., 2004. Purified extracts were electrophoresed on a 12.5% SDS polyacrylamide gel and stained using Sypro Ruby Protein Gel Stain (Invitrogen). Lane 1, APT1.1-StrepII purification; Lane 2, APT1.2-StrepII purification; Lane 3, AAH-StrepII purification used as a control for non-specific protein interactions. Black arrows represent StrepII tagged APT1.1, APT1.2 and AAH; white arrow represents unique polypeptide.

To identify the unknown protein, the polypeptide was excised from the polyacrylamide gel. Z. Cheng performed sample preparation, mass spectrometry, and analysis as described in Cheng *et al*., 2009. Briefly, sample preparation involved trypic digestion that cleaves proteins after every arginine residue resulting in a number of smaller peptide fragments. The mass of these fragments was analyzed by mass spectrometry using a Waters Micromass quadrupole time of flight (Q-TOF) Ultima. PEAKS software 3.1 was used to predict the amino acid sequence of these fragments based on their molecular weight and additionally used to search databases for the

identity of the unknown proteins. Using this approach, the unknown polypeptide recovered from SDS PAGE analysis was determined to be the APT1.1-StrepII fusion protein.

To understand the basis of recovering the 3 kDa larger APT1.1-StrepII fusion protein the molecular weights empirically determined by mass spectrometry were compared to the expected molecular weights; no differences were identified. This result signifies that no post-translational modifications occurred to the APT1.1-StrepII fusion protein to account for its 3 kDa shift in size.

Interestingly, the mass spectrometry analysis recovered peptide fragments that covered the entire sequence of APT1.1 except for those amino acids from Exon 1. This could be explained by the amino acid sequence of Exon 1, which is rich in arginine residues. As arginines are the target sites for trypsin digestion, Exon 1 is cleaved in multiple locations producing a number of smaller peptides that are not detected in the mass spectrometry analysis. However, a peptide fragment arising from Exon 2 was identified that contained the amino acid residues DSE at its N-terminus; Exon 1 codes for all three of these amino acids. Despite this unusual anomaly, the initial objective of this experiment was not obtained as no protein interacting partners were identified for APT1.1 and APT1.2 StrepII fusion proteins.

Complementation of the male sterile phenotype of *apt1-3*

Since the investigation of APT1.1 and APT1.2 protein interactors did not reveal any insights into the *in vivo* functional significance of the APT1 isoforms, another means was sought to test their metabolic potential. I tested whether the constitutive expression of either APT1.1 or APT1.2 could rescue the male sterility of *apt1-3*. Previous work by Gaillard *et al*. (1998) showed that expression of the APT1.2 ORF from the 35S promoter could complement the sterility of *apt1-3*. The plan was to do the same for the APT1.1 isoform. As *apt1-3* mutants are male sterile

and not easily transformed by the commonly used floral dip method (Clough & Bent, 1998) the APT1 transgene was introduced into the *apt1-3* background by genetic crossing.

The APT1.1 cDNA was cloned under the expression of the actin promoter in a vector expressing glufosinate ammonium resistance (which confers BASTA resistance). The construct was introduced into WT Arabidopsis by the floral dip method. Four stable transformants were recovered and immunoblot analysis was used to confirm APT1.1 over-expression in them (data not shown).

These plants, which were assumed to be carrying one copy of the APT1 transgene, were then crossed to *apt1-3* lines. The resulting progeny were all heterozygous for the *apt1-3* allele, however, only half were resistant to BASTA treatment. Four resistant F1 plants were allowed to self fertilize to ideally produce a F2 population segregating 9:3:3:1 (9 WT containing the transgene, 3 WT, 3 *apt1-3* containing the transgene, and 1 *apt1-3*). Approximately 50 F2 progeny were germinated on soil and sprayed with BASTA to eliminate all individuals not containing the transgene. The remaining plants were genotyped as described by Gaillard *et al* 1998 to identify the *apt1-3* plants containing a transgene (Figure 15). The *apt1-3* allele causes a mutation in a *Bst*NI restriction site associated with the 4th exon. Thus PCR amplification of this region of the *APT1* gene followed by digestion with *Bst*NI reveals whether plants carry the WT or *apt1-3* allele. PCR was also used to verify the presence of the transgene in the *apt1-3* plants.

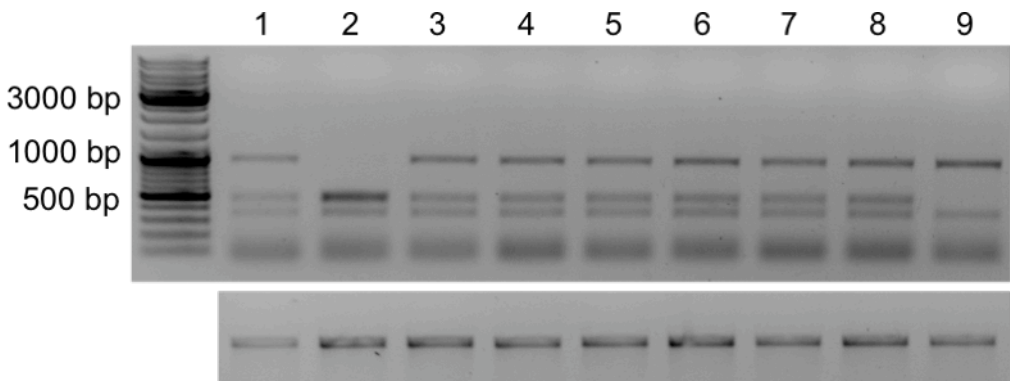

Figure 15. Restriction mapping of the *APT1* locus to identify homozygous *apt1-3* lines. *APT1* was PCR amplified from genomic DNA for each individual (bottom panel). The PCR product was digested with *Bst*NI (top panel) as the *apt1-3* allele has a single point mutation within this recognition site found endogenously within the *APT1* gene. The following is the restriction fragments expected for each allele: WT 479 bp, 461 bp, 344 bp, 144 bp (lane 2); heterozygotes 940 bp, 479 bp, 461 bp, 344 bp, 144 bp (lanes 1, 3, 4, 5, 6, 7, 8); *apt1-3* 940 bp, 344 bp, and 144 bp (lane 9).

Immunoblot analysis confirmed over-expression of the APT1.1 isoform in positively identified *apt1-3/actinp::APT1.1* plants (Figure 16). The degree of over-expression varied amongst these lines, where approximately 10-fold greater APT1.1 protein relative to WT was observed in the 6-4 line and 100-fold greater expression was observed in the 7-9 line. In all three independent lines the expression of APT1.1 from the actin promoter provided sufficient APT activity for normal development indicating it must function on all substrates that APT1.2 does. This was quite remarkable considering the plastid subcellular localization of APT1.1.

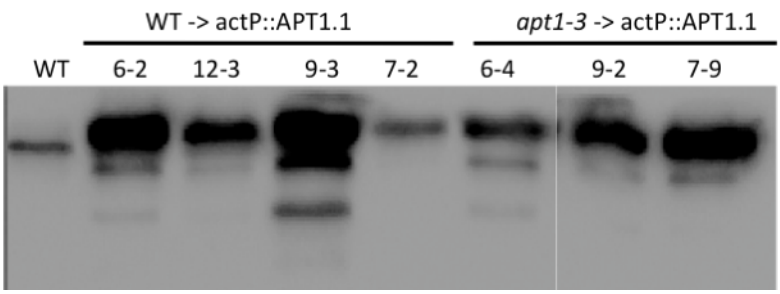

Figure 16. Immunoblot analysis of APT1.1 over-expression in WT and *apt1-3*. Leaf protein extracts (20µg) were probed with anti-APT1 antibody and bound antibody detected using an anti-rabbit antibody conjugated to HRP. Four independent lines were analyzed in the WT background (6-2, 12-3, 9-3, and 7-2), three independent lines were analyzed in the *apt1-3* background (6-4, 9-2, and 7-9).

Using an amiRNA-based approach for isoform specific gene silencing

Since constitutive expression of APT1.1 and APT1.2 both restore male fertility to *apt1-3* this provided evidence that these isoforms may act on similar substrates in their respective subcellular localizations. An alternative approach to evaluate differences in the functionality of APT1.1 and APT1.2 involved analyzing the phenotypes of mutants that lacked only one isoform. The method chosen to accomplish this was the design and construction of artificial microRNA (amiRNA) lines.

AmiRNAs have become a widely used tool for gene silencing in organisms with sequenced genomes and established transformation methods. In Arabidopsis, the mechanisms of gene silencing mediated by amiRNAs have been well elucidated. The empirical data obtained from these studies has lead to the development a bioinformatic tool that attempts to design amiRNAs with high silencing efficiency for specific transcripts (Schwab *et al*., 2005). In the case of *APT1.1* and *APT1.2*, amiRNAs were designed to target their respective 5′ UTRs (ami1.1 was designed to silence APT1.1 transcripts; ami1.2 to silence APT1.2).

The amiRNAs were designed and cloned as outlined in Schwab *et al*, 2005. Briefly, the region of interest for targeting was inputted into the online tool *WMD2 Web MicroRNA Designer* (http://wmd2.weigelworld.org). The output consisted of a list of amiRNAs that would potentially be effective in silencing the region of interest. This list was ranked according to a number of criteria that have been experimentally confirmed as being the most important in endogenous amiRNAs. There is no guarantee that any of the amiRNAs chosen will be effective, nor is there a guarantee that the amiRNA at the top of the list will be more effective than the one at the bottom. However, the creators of this tool recommend to choose the top-listed amiRNAs categorized in the green section as opposed to those in the yellow and red sections. Once the amiRNA of interest has been selected, it is synthesized in a series of three PCRs using four oligonucleotides, the sequences of which are provided by *WMD2*. The PCR product is designed to be cloned into pRS300, replacing an amiRNA-encoding sequence resident in this plasmid. This sequence will be transcribed from the constitutive 35S promoter when introduced into plants. Five T1 lines for ami1.1 and five T1 lines for ami1.2 were recovered. These lines were followed through to the T3 generation when homozygous lines for all lines were identified.

Immunoblot analysis of ami1.1 lines showed about a 50% reduction in APT1.1, as compared to the WT, in leaves of 4-week-old plants in the most efficient lines (Figure 17B, lines 3, 4, and 5). In line 2, APT1.1 protein levels were slightly higher than that observed in lines 3, 4, and 5. Line 1 showed APT1.1 protein levels similar to WT.

Interestingly, the amount of APT1.2 protein was also affected in the ami1.1-expressing lines. This reduction seemed to correlate with of the degree to which APT1.1 was reduced. Lines 3, 4, and 5 showed half the APT1.2 protein observed in WT, while line 2 had one-quarter the

amount of APT1.2. Phenotypically, all the ami1.1 lines showed normal vegetative and reproductive growth despite these differences in APT1.1 and APT1.2 protein levels.

Of the lines expressing the ami1.2, lines 8 and 9 had the greatest reduction in APT1.2 (approximately 75%), in leaves of 4-week-old plants. A reduction of approximately 50% was observed in lines 6, 7 and 10. Unlike the ami1.1 lines where reduction of APT1.1 was associated with decreases in APT1.2, ami1.2-expressing lines did not show reduced APT1.1 protein levels (Figure 17A). Phenotypically, the growth of the ami1.2 lines was indistinguishable from that of WT and ami1.1 lines.

Immunoblot analysis was also used to examine the extent of amiRNA-induced silencing of APT1 in inflorescences. In both ami1.1 and ami1.2 lines, APT1 protein levels were similar to those in WT (Figure 17C). This may explain why all amiRNA containing plants observed were normal in their reproductive growth and as fertile as WT. Thus, these particular amiRNA constructs were partially successful in reducing APT1 protein in leaves, but unsuccessful in silencing either isoform in inflorescences.

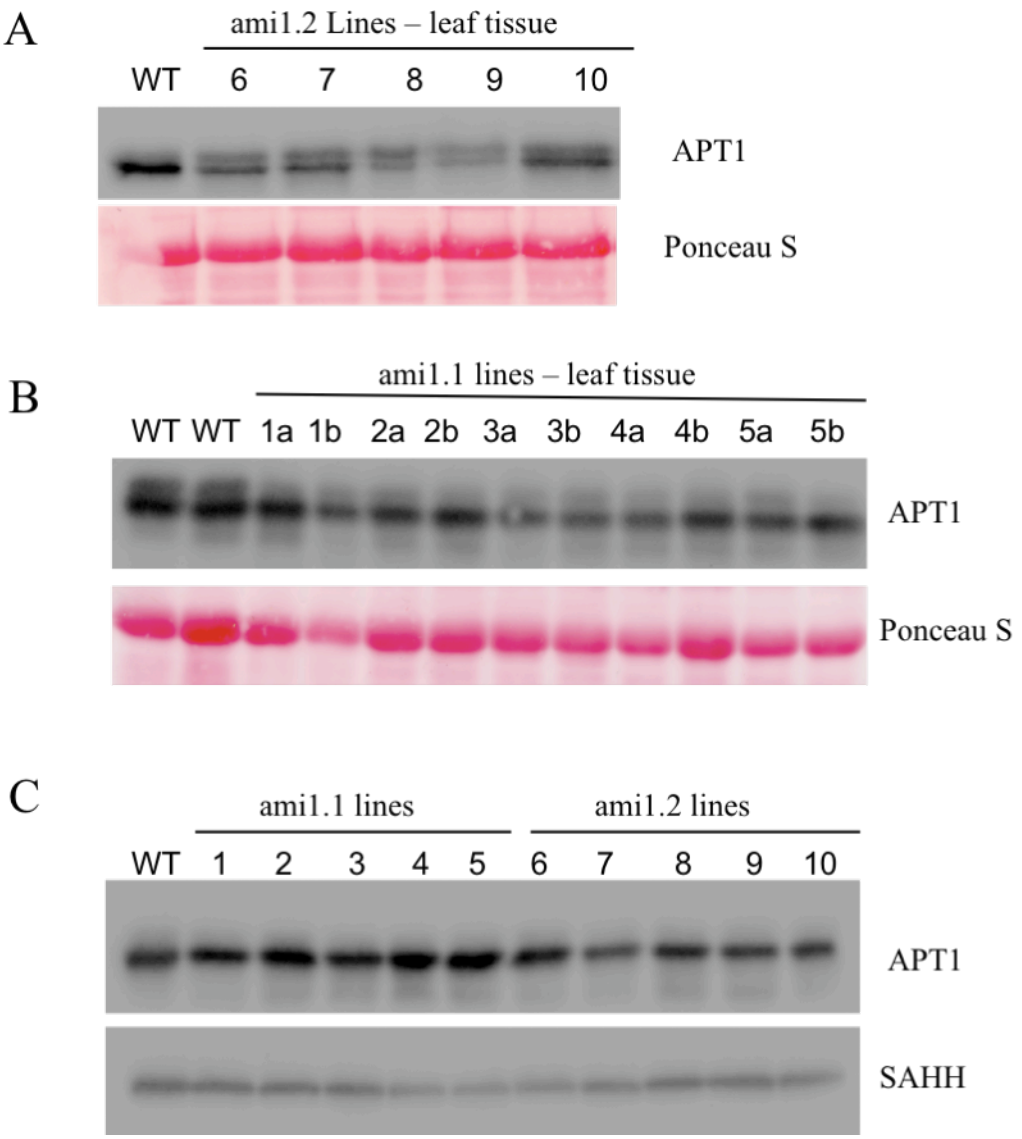

Figure 17. Immunoblot analysis of APT1 protein in ami1.1 and ami1.2 lines. Artificial microRNA (amiRNA) transgenes were designed using *WMD2 Web MicroRNA Designer* (Schwab *et al*., 2006). Five independent homozygous lines for ami1.1 and ami1.2 were studied. Leaf protein extracts (20µg) for ami1.1 (B) and ami1.2 (A) as well as inflorescences (C) were probed with anti-APT1 antibody (top panel). Ponceau S staining of Rubsico was used to test for equal loading in A and B; anti-SAHH antibody was used in C to test for equal loading.

Chapter 2 - Results

Recently, a novel APT1-deficient mutant carrying a T-DNA insertion between Exon 1 and Exon 2 was identified during a screen for mutants with increased tolerance to chemically induced oxidative stress (D. Falcone, personal communication). This mutant is called *oxt1* (oxidative stress-tolerant 1). Unlike previously described APT mutants, such as *apt1-3*, which have a male sterile phenotype, *oxt1* is completely fertile. APT activity in leaves of oxt1 plants was undetectable using a spectrophotometric assay (D. Falcone, unpublished data).

The objective of this part of my research was to determine the basis of the *oxt1* fertility. The following questions were addressed in this study: 1) To what degree is *oxt1* APT1-deficient? 2) Does *apt1-3* have similar stress tolerance to that of *oxt1*? 3) Is there a correlation between APT activity and fertility? 4) Does the expression of other APT genes change in these APT1-deficient mutants? 5) Does the activity of the two-step adenine salvage pathway change in APT1-deficient mutants?

Is *oxt1* APT-deficient?

Moffatt and Somerville isolated the first APT-deficient mutants based on their resistance to 2,6-diaminopurine and found that they all carried mutations in the *APT1* gene; all were male sterile to some extent. The degree of APT deficiency in these plants correlated with the severity of the fertility defect. *apt1-1* has 10-15% residual APT activity and produces about 2% of the seed that WT plants do. *apt1-3* has 1-2% residual APT activity and is completely sterile (Moffatt and Somerville 1988).

oxt1 was DAP resistant suggesting it was also APT deficient (D. Falcone, unpublished data). Although the spectrophotometric assay data indicated a lack of APT activity in leaf extracts, a more quantitative measurement was needed. Thus, the first step in this research was to measure APT activity in *oxt1* extracts using the more sensitive radiochemical assay that detects the conversion ^{3}H-adenine to ^{3}H-AMP. In *oxt1*, the residual WT activity averaged 3.1% (0.21 ± 0.03 nmol AMP mg protein^{-1} min^{-1}) (Figure 18). This is slightly higher than *apt1-3* as the average was 2.1% (0.15 ± 0.04 nmol AMP mg protein^{-1} min^{-1}), but not statistically significant ($p=0.137$, $n=13$, T-Test). The value for *apt1-3* matches previously reported values (Allen *et al*., 2002).

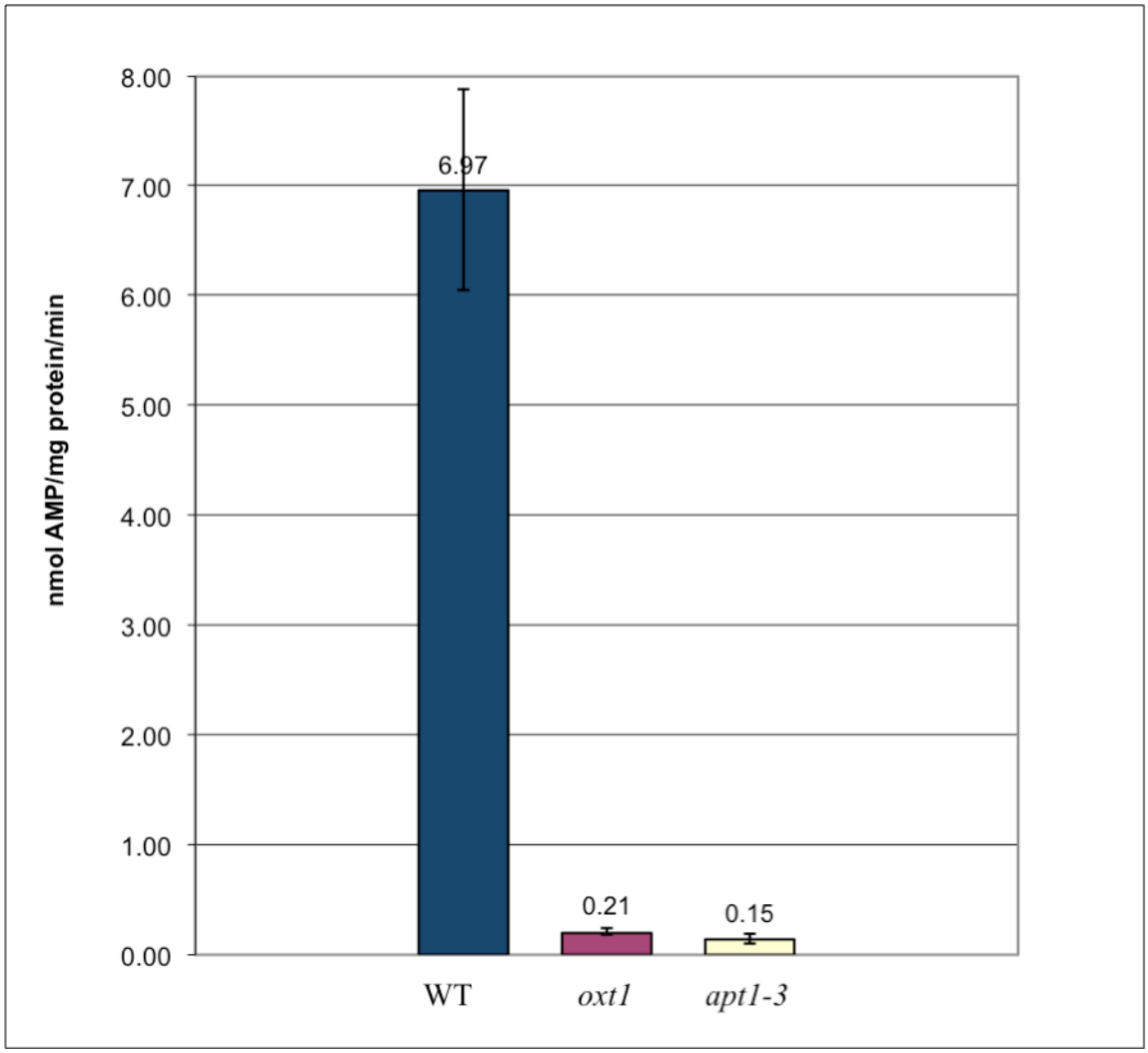

Figure 18. APT enzymatic activity in WT, *oxt1,* and *apt1-3* leaves of 4 week-old plants. APT activity was measured in crude protein extracts using a radiochemical assay that measures the amount of ^{3}H-adenine converted to ^{3}H-AMP. *oxt1* activity was 3.1%, *apt1-3* was 2.1%. Error bars represent standard error of the mean where n=4 for WT, n=13 for *oxt1*, and n=3 for *apt1-3*. The difference in APT activity between *oxt1* and *apt1-3* is not statistically significant (p=0.137, T-Test).

A qualitative means to evaluate APT deficiency involves measuring the length of the primary root of seedlings grown on solid media supplemented with DAP. WT, *oxt1*, and *apt1-3* seeds were germinated on ½ MS media supplemented with 0.1 mM DAP and root length was

measured after 11 days (Figure 19). Root length measurements were lowest for WT (0.15 ± 0.01 cm, n=12) followed by *oxt1* (0.50 ± 0.02 cm, n=12) and *apt1-3* (3.16 cm ± 0.2, n=8). These results also indicated that *oxt1* is APT-deficient, consistent with the results of the radiochemical assay. However, the APT1 deficiency in the *oxt1* mutant as predicted by the DAP growth test is less profound as its tolerance to DAP resembles WT more than it does *apt1-3*.

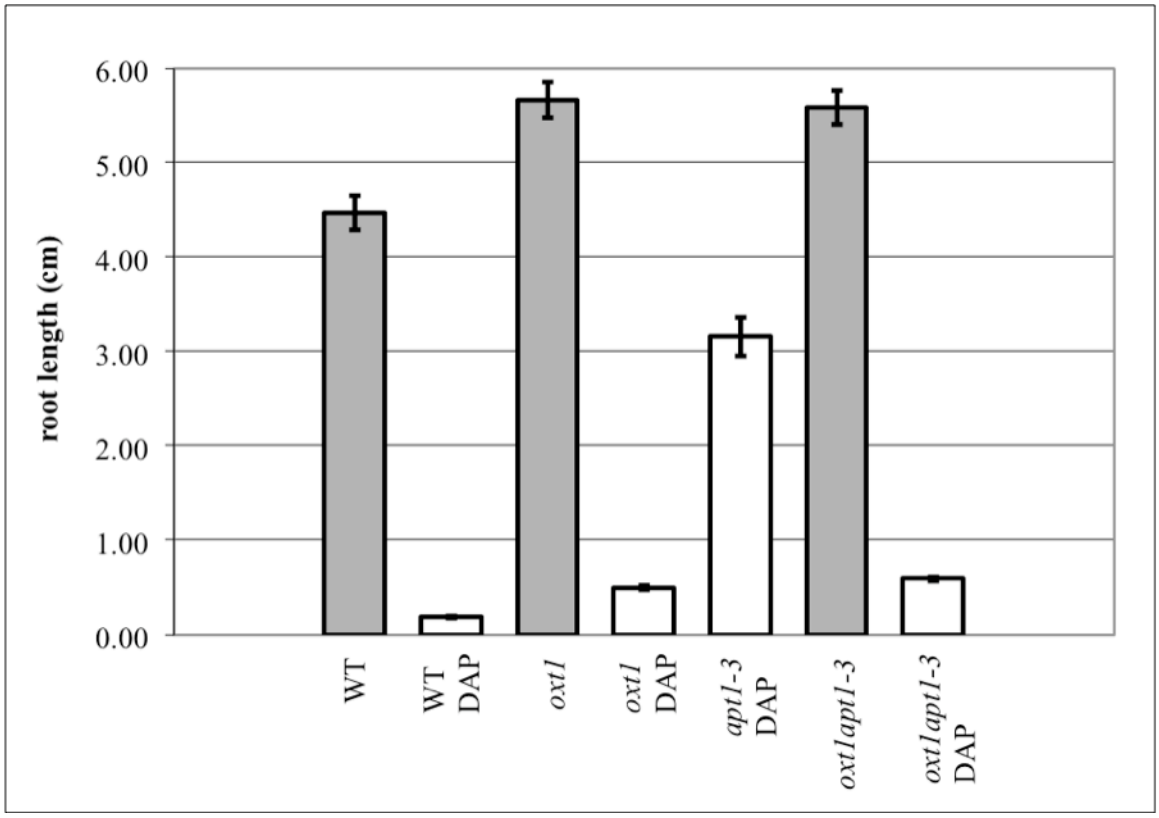

Figure 19. Primary root growth analysis of WT and APT1-deficient mutants on 2,6-DAP media. Seeds were germinated on ½ MS media alone (grey bars) or ½ MS media supplemented with 0.1 mM DAP (white bars). At 11 days, the primary root length was measured. The average root length is shown along with the standard error of the mean; n=12 for WT and *oxt1*, n=8 for *apt1-3* and *oxt1apt1-3*.

Is *apt1-3* stress tolerant since it is also APT1-deficient?

The similarity in the APT-deficiency of *oxt1* and *apt1-3* led to the obvious question of whether *apt1-3* was also stress tolerant. This was examined using the same growth test used for

the isolation of the *oxt1* mutant. Seedlings are grown on media supplemented with AT and BSO, which lead to the production of H_2O_2 and reduced glutathione biosynthesis, resulting in oxidative stress in seedlings (D. Falcone, personal communication). The test was slightly modified to include an initial germination on ½ MS media (WT and *oxt1*) or ½ MS + DAP (*apt1-3*) to identify the homozygous *apt1-3* seedlings within the segregating F2 population.

WT, *oxt1* and *apt1-3* seedlings were transferred to ½ MS media supplemented with 2 μM AT and 0.4 mM BSO and their growth was evaluated after two weeks (Figure 20). The WT seedlings were stunted and had chlorotic leaves; *oxt1* seedlings showed no growth inhibition or chlorosis. *apt1-3* seedlings had evident chlorosis, and their growth was reduced.

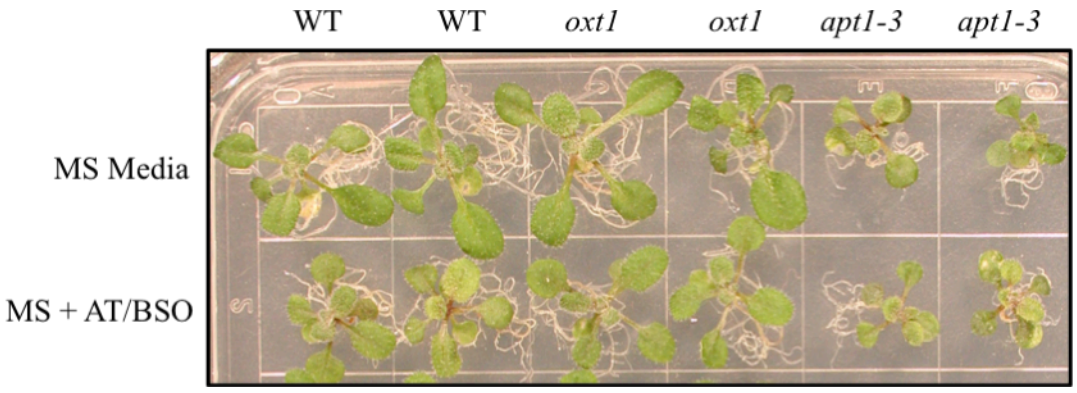

Figure 20. Growth of WT and APT1-deficient mutants on oxidative stress inducing media. WT and *oxt1* seeds were initially germinated on ½ MS media; *apt1-3* was germinated on ½ MS media supplemented with 0.1 mM DAP to select for homozygous *apt1-3* seedlings. At 2 weeks seedlings were transferred to ½ MS media containing 2 uM AT and 0.4 mM BSO. Top panel shows representative seedlings after 4 weeks on ½ MS media alone, bottom panel shows representative seedlings grown on AT+BSO media for 2 weeks.

The inhibitory effects of the AT/BSO media on seedling growth are quantified by measuring the lengths of their primary roots (D. Falcone, personal communication). This was not done for this analysis of *apt1-3* because of the confounding growth effects of the initial DAP

selection. Although, *apt1-3* mutants are more resistant than WT to the effects of DAP, these mutants are not completely APT1-deficient and as a result their growth is affected by the DAP; this results in stunted growth in comparison to their growth on ½ MS media alone. However, even visual observation of the seedlings showed that *apt1-3* seedlings did not thrive on the AT/BSO media as well as *oxt1*. Thus there is no correlation between APT-deficiency and stress tolerance. Instead there is something distinct about the APT deficiency of *oxt1* that leads to its tolerance.

What is the correlation between APT activity and fertility?

Although the difference in APT activity is quite marginal between *oxt1* and *apt1-3* it is quite extraordinary that one genotype is completely fertile and the other is sterile. One could postulate that there is a threshold of APT activity whereby activity above this threshold is sufficient to sustain male fertility and any lower APT level results in male sterility. If there is a fertility threshold then the APT activity of *oxt1* must lie above this level and a decrease in APT activity would diminish fertility. To test this hypothesis, *oxt1* and *apt1-3* plants were crossed to generate *oxt1apt1-3* F1 hybrids which express only one APT 1.2 allele. It was postulated that these plants would have an intermediate APT activity and perhaps be sterile.

In order to interpret the phenotype of *oxt1apt1-3* plants the level of APT activity in different organs needed to be established. A qualitative measure of APT activity was estimated by germinating *oxt1apt1-3* seedlings on ½ MS media supplemented with 0.1 mM DAP. After 11 days of growth, root length measurements were taken to establish residual APT activity (Figure 19). *oxt1apt1-3* roots were slightly longer than those of *oxt1* (0.59 cm ± 0.02 cm, n=8 versus 0.50

cm, respectively) This difference in root length between *oxt1* and *oxt1apt1-3* is statistically significant (p=0.002, T-Test).

Next, the DAP-resistant seedlings were transferred to soil and their growth observed for up to 7 weeks. After about 4.5 to 5.5 weeks mature siliques had developed on *oxt1* and *oxt1apt1-3* plants, similar to those that developed on the WT. However, after about 5.5 weeks of growth the subsequent siliques that formed on the *oxt1apt1-3* plants were sterile, similar to those on *apt1-3* (Figure 21). This "shift" from fertile to sterile was indeed a phenomenon of the F1 heterozygous mutant line and not a result of pest infestation or growth chamber conditions as this shift was apparent each time these plants were grown.

Figure 21. A seven-week-old *oxt1apt1-3* plant. Photographed is the primary shoot of a representative *oxt1-apt1-3* plant. The initial siliques have dried out at this time and are all fertile; the later siliques are all sterile.

To determine how consistent this fertility shift was in *oxt1apt1-3* line thirteen individuals were analyzed; these individuals were derived from multiple crosses between at least three *oxt1* plants onto at least three different *apt1-3* female recipient plants. The siliques on the primary shoot of thirteen 7-week-old plants were counted and recorded as to whether each was fertile or

sterile. On the primary shoot, upwards of the first 10 siliques were fertile, or approximately 20-40% of the total number of siliques (Figure 22A). All subsequent siliques were sterile. Interestingly, these plants would produce many more sterile siliques than fertile siliques, at times numbering upwards of 60.

This fertility shift was also observed on the secondary branches. However, the timing of the shift was more variable on the secondary branches than it was on the primary shoot. For any given secondary branch, 10-60% of the siliques were sterile. Moreover, it was not uncommon to see fertile siliques intermixed amongst the sterile siliques along these branches (Figure 22B).

Together these observations are consistent with the model that there is a threshold of APT activity that is necessary for fertility in Arabidopsis and the reduction in APT activity in *oxt1apt1-3* plants relative to the *oxt1* homozygote mutants leads to sterility. During vegetative growth on ½ MS media supplemented with DAP the *oxt1apt1-3* seedlings had root lengths that were more comparable to *oxt1* than they were to *apt1-3*. During the early stages of reproductive growth fertile siliques were observed on *oxt1apt1-3* plants like that seen on *oxt1*, and later a shift to sterility occurred, similar to the phenotype of the *apt1-3* mutant.

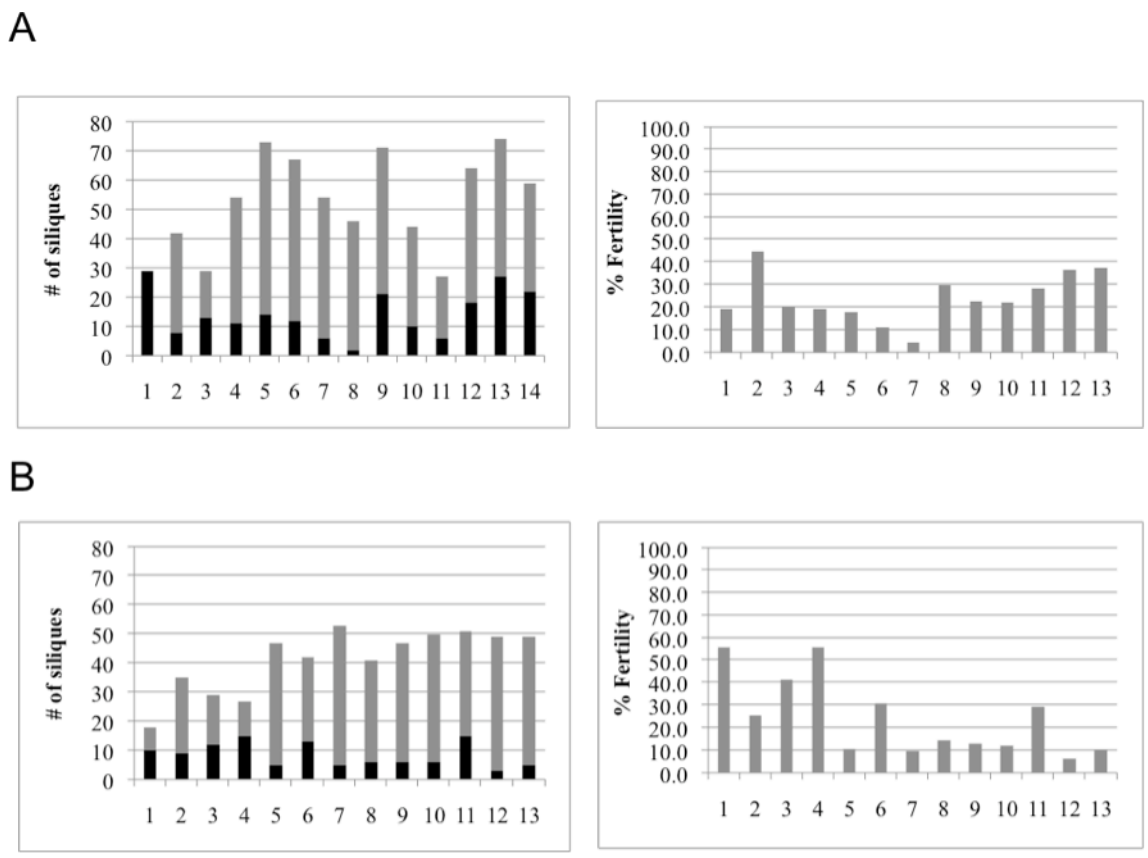

Figure 22. Analysis of fertile and sterile siliques on primary and secondary shoots of *oxt1apt1-3* plants. Thirteen *oxt1apt1-3* individuals were used to determine the extent of fertility and sterility displayed on the primary shoot (A) and secondary shoot (B).Left panels: fertile siliques are represented as black bars, grey bars represent number of sterile siliques for each individual. Right panels: percent of fertile siliques.

The next question addressed was whether the shift to sterility seen in *oxt1apt1-3* plants was accompanied by a decrease in APT activity. To test this APT activity was measured by the radiochemical assay in protein extracts of inflorescences of WT, *oxt1*, *apt1-3* and *oxt1apt1-3* plants. Extracts were prepared from the first inflorescences (those that gave rise to the early fertile siliques) and from later inflorescences (those that gave rise to sterile siliques). The early buds and late buds of WT, *oxt1*, and *apt1-3* plants had consistent APT activities, in each case (Figure 23). Surprisingly, the late, sterile buds of the *oxt1apt1-3* plants had a significant increase in APT activity as compared to the early buds ($p < 0.05$, T-Test). Across the two individual

experiments there was a consistent increase of 4.6% in APT activity in sterile buds over fertile buds. The APT activity in the early, fertile buds of *oxt1apt1-3* is equivalent to that of *oxt1*, but in late, sterile buds the APT activity increases. This observation provides evidence that in the case of *oxt1* and *oxt1apt1-3*, APT activity is not clearly correlated with sterility. Thus, the hypothesis concerning a threshold of APT1 activity can be rejected.

A

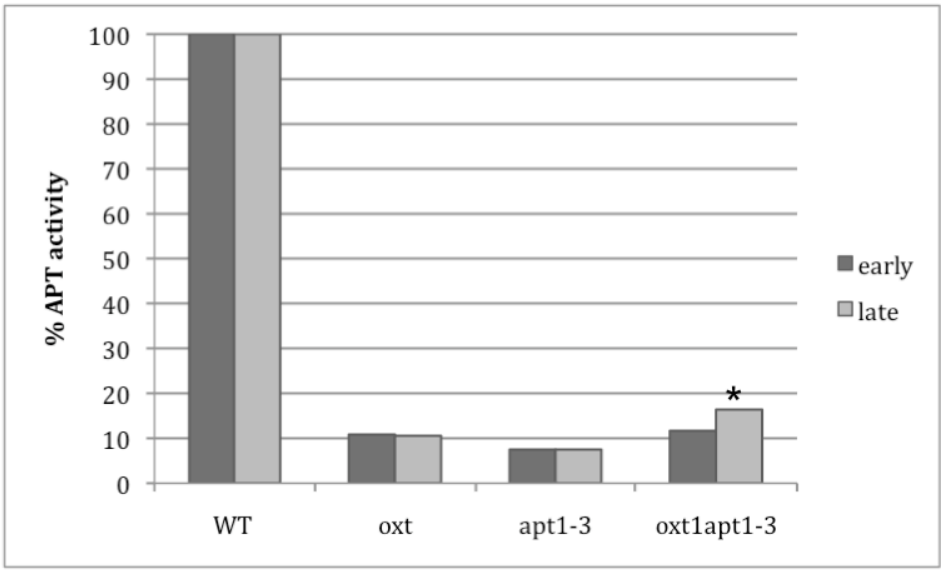

B

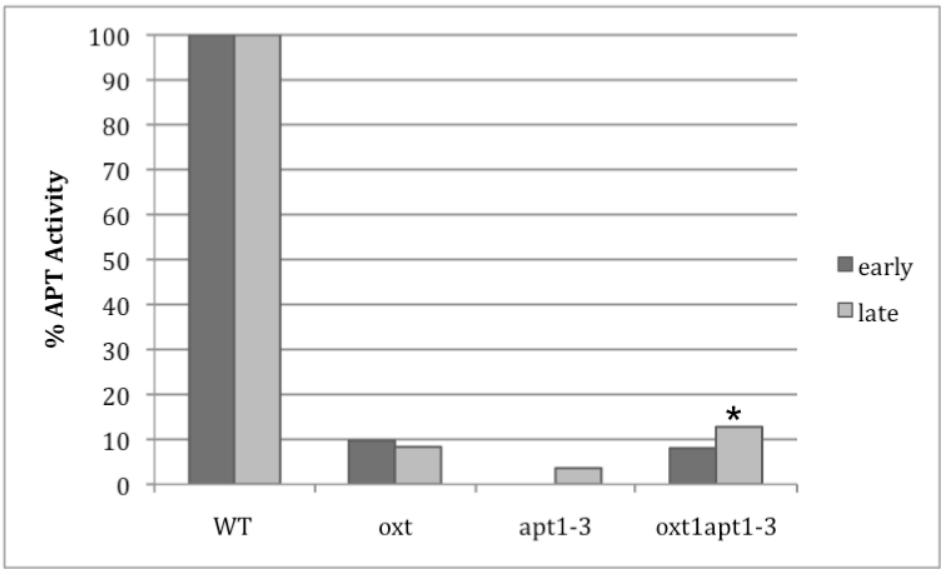

Figure 23. APT enzymatic activity in early and late buds of *oxt1apt1-3* plants. Crude protein extracts for WT, *oxt1*, *apt1-3*, and *oxt1apt1-3* buds were assayed for APT activity at two stages of development. The early stage involved collecting the first initial buds produced by the plant, the late stage defines buds collected after the first observation of sterile siliques. The two sets of data for each experiment is shown where the WT activity was 12.39 and 12.75 nmol of AMP/mg of protein/min (A); and 28.71 and 16.76 nmol of AMP/mg of protein/min (B). The asterisk marks significant changes between early and late buds where p=0.004 (A) and p=0.02 (B) using Student's T-Test.

Does the expression of other APT genes change in APT1-deficient mutants

The unexpected increase in APT activity in the sterile buds of *oxt1apt1-3* plants led to the consideration that the fertility differences in *oxt1* and *apt1-3* plants might be a result of how these two APT1 alleles signal another component of cellular metabolism. Perhaps *oxt1* mutants activate a compensatory activity to alleviate male sterility associated with APT1-deficiency? One possibility was that *oxt1* was able to activate another APT gene. Allen *et al* (2002) showed that APT1, APT2 and APT3 have similar apparent K_m values for adenine. However APT1 has the highest V_{max} of the three isoforms (APT1 V_{max} = 9.6; APT2 V_{max} 0.31; APT3 V_{max} 0.18; units are expressed in nmol of AMP mg of protein^{-1} min^{-1}). So the other APTs that are naturally expressed only in flowers (Zhang, 2000) might contribute to the increase in APT that is observed in the *oxt1apt1-3* flowers.

Thus, I investigated whether the *oxt1* APT1-deficiency might signal a transcriptional response from APT2 or APT3. RNA was extracted from the late buds of WT, *oxt1*, *apt1-3,* and *oxt1apt1-3* and APT2 and APT3 transcript abundance analyzed by semi-quantitative RT-PCR. Each primer's linear range was determined using WT cDNA as a template. For the APT2 primer set the linear range was between 32 and 36 cycles; for the APT3 primer set it was between 28 and 36 cycles. Initially, 34 cycles was chosen for RT-PCR, however, there was concern that the signal strength of each DNA fragment may have been saturated and closing in on the higher end of the linear range (Figure 24). The cycle number was than lowered to 30 cycles for further analyses.

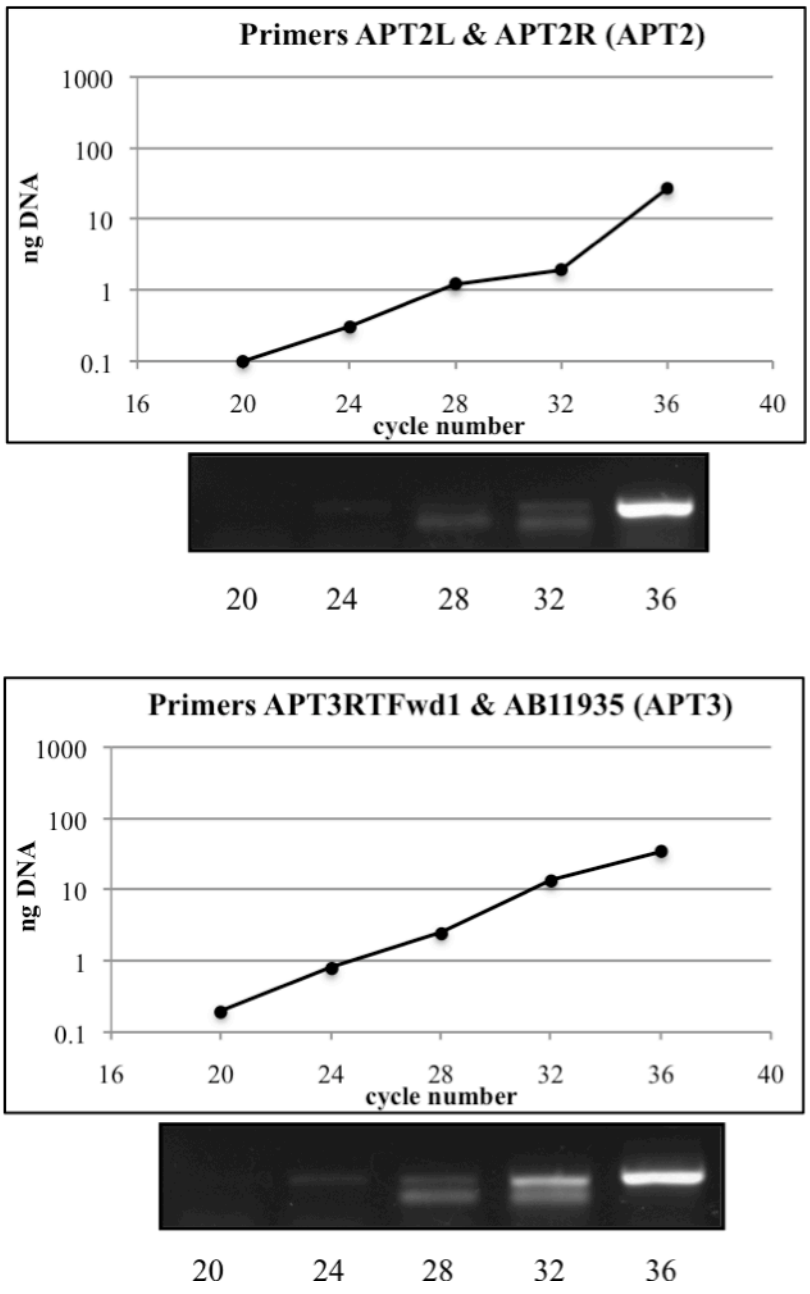

Figure 24. Linear range testing of APT2 and APT3 primer sets for RT-PCR analysis. WT cDNA template was PCR amplified for 20 through 36 cycles and electrophoresed on a 1% TAE agarose gel. The gel image was digitized and each DNA fragment quantified, in nanograms, using spot density analysis. The nanograms of cDNA synthesized was plotted against the cycle number on a semi-log graph. 34 cycles was chosen as the linear range for APT2; 30 cycles was chosen for APT3.

At 30 cycles, the RT-PCR results showed a modest decrease in *APT2* transcript abundance for *oxt1*, *apt1-3*, and *oxt1apt1-3* relative to WT, but this was not substantially different (Figure 25). APT3 transcript abundance was equal across all the samples (Figure 25). These observations suggest that APT2 and APT3 are not transcriptionally responsive to APT1-deficiency, and are not likely contributing to the diverse phenotypes seen among *oxt1*, *apt1-3*, and *oxt1apt1-3* mutants. However, a translational activation of some sort cannot be ruled out.

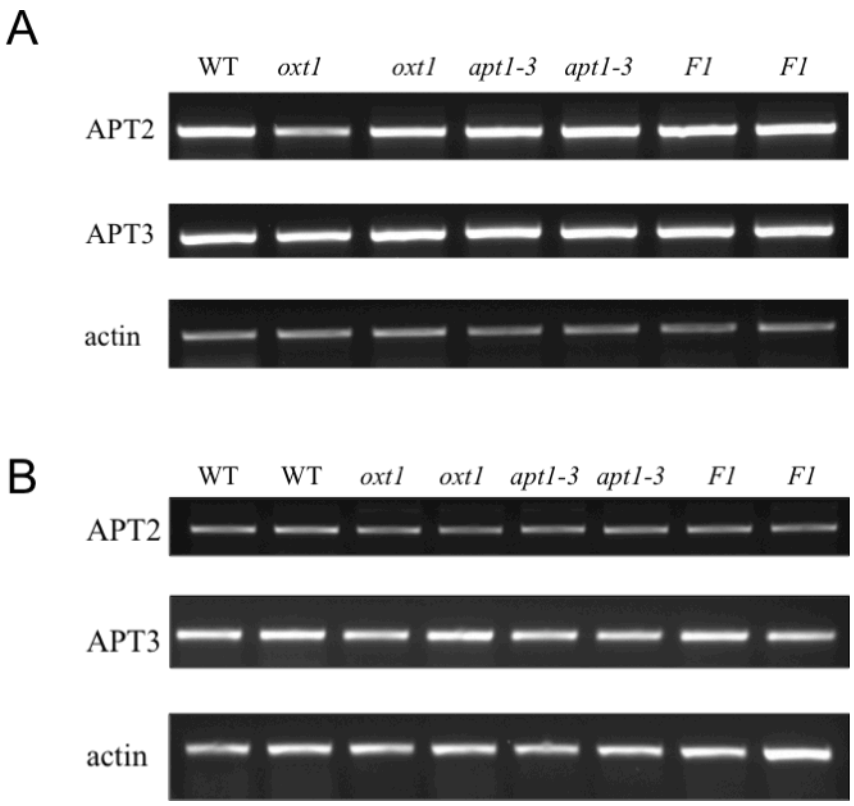

Figure 25. RT-PCR analysis of *APT2* and *APT3* in WT and APT1-deficient mutants. RNA was extracted and cDNA synthesized from late buds of two individuals per line. F1 represents *oxt1apt1*-3 line. RT-PCR was performed at 34 cycles (A) and 30 cycles (B). Actin was used to test for equal loading of cDNA.

Does the activity of the two-step adenine salvage pathway change in APT1-deficient mutants

Given that the other APT genes of the primary salvage pathway do not appear to account for the fertility differences of *oxt1* and *apt1-3* mutants, I next considered the possibility that the secondary salvage pathway was more active in *oxt1*. This pathway involves the sequential action of adenine phosphorylase and ADK. Adenine phosphorylase converts adenine to adenosine, which is subsequently phosphorylated to AMP.

ADK activity was assayed in leaf extracts to determine if the two-step pathway is differentially active in *oxt1* versus *apt1-3* plants. The radiochemical ADK assay monitors the rate

of conversion of ^{3}H-adenosine to ^{3}H-AMP in protein extracts. Extracts were prepared from leaves of 4-week-old plants. In *oxt1* the ADK activity was 2.07-fold greater than that in WT; in *apt1-3* ADK activity was 1.67-fold greater (Figure 26). However, neither increase was statistically significant (*oxt1* p=0.07, *apt1-3* p=0.05). These data showed that ADK activity might be slightly higher in *oxt1* and *apt1-3* relative to WT, but was not significantly different in *oxt1* and *apt1-3* (p=0.30, T-Test). However, since ADK activity was similar in *oxt1* and *apt1-3* the two-step adenine salvage pathway cannot account for the phenotypic differences observed in these mutants.

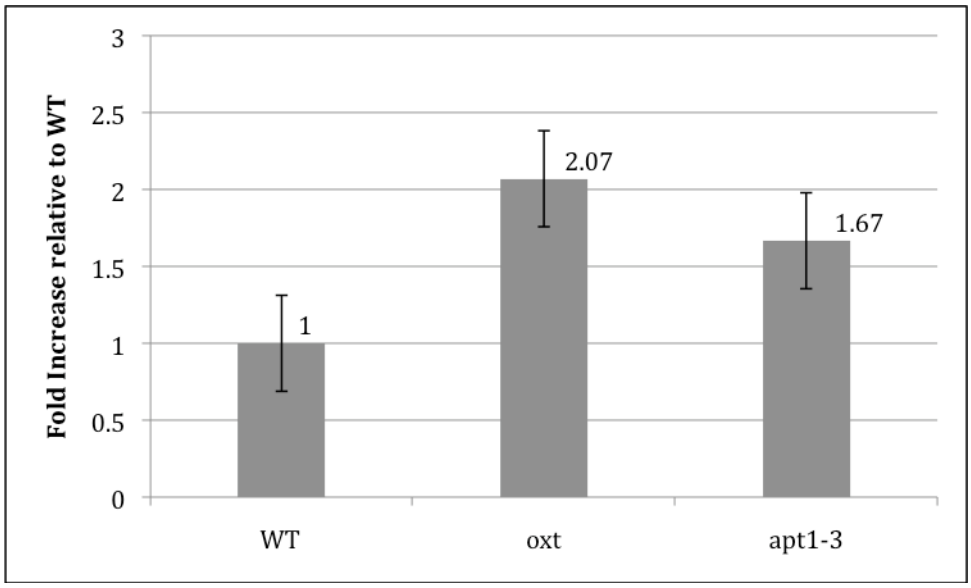

Figure 26. ADK enzyme activity in leaves of WT and APT1-deficient mutants. ADK activity was measured in crude protein extracts using a radiochemical assay that measured the amount of ^{3}H-adenosine to ^{3}H-AMP. Error bars represent standard error of the mean, where n=3 for WT, *oxt1*, and *apt1-3*. The difference between *oxt1* and *apt1-3* is not statistically significant (p=0.30, T-Test).

Discussion

At present, Arabidopsis APT1 is unique in comparison to the APT genes of other species as it is the only APT locus for which there is experimental evidence for two gene models: one with 7 exons (APT1.1) and another with 6 (APT1.2). To date, all other annotated APTs encode only one polypeptide that has a high amino acid sequence similarity to APT1.2; the sizes and locations of the introns and exons are also conserved amongst these genes. It is possible that all organisms express an APT1.1 but the genetic resources are not yet available to detect this expression. Thus although Arabidopsis may be the only plant documented to have a dual isoform APT1 locus to date, the study of these dual gene products will further our understanding of the role of this enzyme activity in all plants.

The NCBI EST database has 18 entries for *APT1.1* transcripts and 53 records for *APT1.2*. The *APT1.2* ESTs were recovered from all tissue types whereas the *APT1.1* ESTs have only been isolated from either leaves of young seedlings or floral organs. The predicted gene models derived from these ESTs suggest that the *APT1.1* and *APT1.2* transcripts arise from distinct promoters. This conclusion is based on two observations: both transcripts are capped and they have unique transcriptional start sites and 5′ UTR sequences. Their specific promoter regions have yet to be delineated.

Earlier studies of APT1 expression (which is now designated APT1.2) located a promoter activity in the 950 bp upstream of the first methionine in Exon2. This stretch of nucleotides directed constitutive expression of a downstream β-glucuronidase reporter gene similar to the pattern of APT1.2 (Smith, 1997). The "native APT promoter" used in the transcriptional studies outlined in this thesis are the 800 bp upstream of the initiating methionine of Exon 1.

The first objective was to address the expression of *APT1.1* and *APT1.2* transcripts. Semi-quantitative RT-PCR was used to measure transcript abundance in leaves from 4-week-old plants and older inflorescences. These data showed that *APT1.1* and *APT1.2* transcript levels are similar in both tissues. This result is quite extraordinary considering that only a few ESTs are reported for *APT1.1*, while *APT1.2* has over double the number of ESTs.

The basis for this discrepancy may be related to the difficulty to recover ESTs that include the 5′ end of this transcript. In the course of my research, I attempted to recover the full-length cDNA for *APT1.1* using RLM-RACE and high-temperature cDNA synthesis. I was successful in isolating a full-length cDNA for *APT1.2*, but not for *APT1.1* using RLM-RACE. As this method is dependent on the availability of a 5′-capped end to mediate RNA ligation of an adaptor sequence, any significant secondary structure could inhibit this reaction. I attempted to reduce potential secondary structure using high temperature cDNA synthesis at 55°C, and three primers were designed to cover the entire 5′ UTR region of *APT1.1* (Appendix 3) The only primer that did not lead to synthesis of a RT-PCR product was the one that anneals at the 5′ terminus of the UTR.

To further investigate any significant secondary structure in the 5′ UTR, computational modeling of the mRNA structure was performed. This modeling revealed a possible RNA secondary structure at the 5′ UTR of *APT1.1* that contains a region with a substantial stem-loop located at the terminal 5′ end (Appendix 2; Y.Li, personal communication).

Concurrently, a comparative analysis of the *APT1.1* 5′ UTR with characterized metabolite-binding regions was also carried out. These metabolite-binding regions are more commonly known as riboswitches and have been elucidated in prokaryotes with two cases

reported in eukaryotes (Breaker *et al*., 2008). Interestingly, a thiamine pyrophosphate (TPP)-sensing riboswitch has been found in bacteria, fungi, and plants yet the mechanism of gene repression is different in these species. In bacteria, TPP binds the mRNA inducing a conformational change in the mRNA that blocks the ribosome binding site, leading to reduced expression (Winkler *et al*., 2002). In fungi, TPP binds the mRNA in the 5′ UTR inducing an alternative splicing event that leads to an upstream open reading that acts as a decoy for translation and reduces expression of this mRNA (Cheah *et al*., 2007). In plants, TPP binds within the 3′ UTR of the mRNA inducing an alternative splicing event that leads to changes in the 3′ UTR length and sequence whereby mRNA stability is affected leading to reduced expression (Wachter *et al*., 2007).

The comparative analysis of the secondary structure in *APT1.1* was performed against known riboswitches. This analysis showed no similarity between known riboswitches and the RNA structure predicted in the APT1.1 5′ UTR (Y. Li, personal communication). However, this analysis does not rule out the possibility of a riboswitch or a metabolite-binding region within the 5′ UTR. As this analysis was performed using prokaryotic sequences, and only a few riboswitches have been elucidated in eukaryotes, it could be possible that these regulators of gene expression have evolved differently in eukaryotes. Future experiments such as in-line probing assays to test conformational changes in RNA secondary structure upon binding of metabolites may provide valuable insight into whether for example, adenine or cytokinins can provoke this event (Li and Breaker, 1999).

With the evidence that both *APT1.1* and *APT1.2* mRNAs are synthesized *in vivo*, the next question addressed whether both transcripts were translated *in vivo*. Immunoblot analysis of leaves and inflorescences showed that APT1.2 is abundant in both tissues. In leaves, the APT1.1

level was approximately one-tenth that of APT1.2, and below the level of detection in inflorescences. Thus, the protein levels do not match transcript abundances estimated by the RT-PCR analysis suggesting that *APT1.1* may be subject to post-transcriptional regulation, while *APT1.2* is constitutively expressed. Interestingly, these expression patterns are in agreement with the analysis of alternative first exons by Chen *et al* (2007). This group showed that most alternative first exon events in rice and Arabidopsis involve a short isoform that is constitutively expressed, and a longer isoform that is spatially/temporally/developmental expressed. Although, it is unknown what induces expression of APT1.1 this model is consistent with the APT1 isoforms as APT1.2 is expressed in all tissues.

What is the possible basis for the post-transcriptional regulation of APT1.1?

In WT, it was found that the equal transcript abundance of *APT1.1* and *APT1.2* did not correlate with the amount of protein detected on immunoblots as APT1.2 was much more abundant than APT1.1. As the only difference between these mRNAs is their 5′ UTR regions, it was hypothesized that the 5′ UTR of *APT1.1* must be the target of post-transcriptional regulation resulting in its lower expression. The secondary structure of *APT1.1* alluded to earlier in this discussion may be involved in this regulation. While this may be true, a second target of post-transcriptional regulation was elucidated by two GFP fusion constructs.

Two constructs were initially designed to test the expression of Exon 1 *in vivo*. The first construct consisted of the first 800 base pairs of the APT1.1 promoter including the 5′ UTR and Exon 1 fused in-frame with GFP (*APT1*::Ex1:GFP). The second construct was identical to *APT1*::Ex1:GFP but included Intron 1 and Exon 2, fused in-frame with GFP (*APT1*::Ex1-i-Ex2:GFP).

Immunoblot analysis of *APT1*::Ex1:GFP detected an abundant 28 kDa Ex1-GFP fusion protein. This was not expected, as *in vivo* APT1.1 expression from this promoter and 5′ UTR produces a low level of APT1.1. These results suggested that perhaps the 5′ UTR alone was insufficient in regulating translation of the Ex1-GFP fusion protein; the same may be true for the WT gene *in vivo.*

Two polypeptides were expected to arise from the *APT1*::Ex1-i-Ex2:GFP transgene: the 36 kDa Exon1-Exon2-GFP fusion protein and the 29 kDa Exon2-GFP fusion protein. Surprisingly only the 29 kDa polypeptide was detected. Although the abundance of Exon1-Exon2-GFP and Exon2-GFP fusion proteins did not reflect that found in the corresponding proteins arising from the native gene, it can be said with some confidence that only Exon2-GFP is synthesized and Exon1-Exon2-GFP is once again subject to regulation. Both transcripts that code for these proteins were detected by RT-PCR. Preliminary semi-quantitative RT-PCR analysis indicated that the two transcripts were equally abundant, consistent with transcription from the native gene (Y. Li, personal communication). Thus, APT1.1 is subject to post-transcriptional regulation and the cis elements required for this regulation are present in the *APT1*::Ex1-i-Ex2:GFP transgene.

These results suggest that Exon 1 must be upstream and colinear with Intron 1 and Exon 2 for the post-transcriptional regulation of APT1.1 (i.e. this regulation affected transcripts arising from *APT1*::Ex1-i-Ex2:GFP and WT *APT1* genes but not from the *APT1*::Ex1:GFP transgene). The commonality between *APT1*::Ex1-i-Ex2:GFP plants and WT is the co-linearity of Exon1, Intron 1, and Exon 2. The cis nature of the factors controlling this regulation is further supported by the fact that the *APT1*::Ex1:GFP construct was expressed in a WT background that contains two functional copies of the APT1 gene, yet no effect on translation of the WT alleles from Exon

1 was detected in these plant lines. If this is the case, then the target of post-transcriptional regulation could be the primary mRNA. Future work will address the effect of removing Intron 1, to further distinguish the contribution of this intron and the 5′ UTR of APT1.1 in its post-transcriptional regulation. As such, work has begun to clone the genomic fragment of *APT1* beginning with the 800 base pair promoter region and ending with the terminal exon fused to GFP (*APT1*::Ex1-Ex7:GFP). The expression of the APT1.1 and APT1.2 polypeptides arising from this transgene will be monitored by immunoblotting with an anti-GFP antibody. These *APT1*::Ex1-Ex7:GFP transgenic plants will be a control for another set of transgenic plants that do not contain the first intron (*APT1*::Ex1-ΔIntron1-Ex7-GFP).

APT1.1 is an active enzyme localized to chloroplasts

It was next addressed whether the APT1.1 polypeptide is an active enzyme. Recombinant APT1.1 and APT1.2 fused with a 6xHIS tag were over-expressed in *E.coli*, purified, and dialyzed into Tris-HCl buffer. Using a radiochemical assay their activities on adenine substrates were tested relative to the APT activity in WT crude extracts (expressed as nmol AMP mg^{-1} min^{-1}). In a preliminary kinetic analysis APT1.1 had 805-fold greater APT activity; APT1.2 showed 41-fold greater activity. As these data are preliminary, it can only be concluded that APT1.1 is an active enzyme. Future work will determine the apparent binding affinities of each isoform to adenine and cytokinins, in order to provide a meaningful idea of what substrate each prefers and its efficiency in metabolizing each of these.

The subcellular localization of each APT1 isoform was investigated to discern if Exon 1 functions as a transit peptide as predicted by multiple subcellular localization programs. To test this two different transgenic plant lines were studied: those expressing the *APT1*::Ex1:GFP transgene and those expressing *actP*::APT1.1:2xGFP. The GFP signal from *APT1*::Ex1:GFP

transformants was observed in the cytosol of leaf epidermal cells, as well as in punctate bodies and nuclei of mesophyll cells.

Two issues arose from these results. First, the nuclear GFP signal is likely due to diffusion since the size of the GPF fusion protein is below the exclusion limit of the nuclear pore (28 kDa versus 70 kDa; D'Angelo *et al*., 2009). The second issue was the overall low expression of GFP in these lines, which made it difficult to tell if it co-localized with the chlorophyll autofluoresence of the chloroplast. To overcome this problem, the native *APT1* promoter was substituted with the constitutive actin promoter to drive the expression of an APT1.1 ORF with two tandem GFP ORFs (*actP*::APT1.1:2xGFP). These lines eliminated the nuclear localization, as this fusion protein was larger than the size exclusion limit (78 kDa versus 70 kDa). The stronger expression from the actin promoter clearly showed co-localization of GFP with chlorophyll autofluorescence. Additionally, the localization of APT1.1 to punctate-bodies was observed again. Taken together these observations implicated Exon 1 as a transit peptide. However, it remained unclear as to whether Exon 1 was proteolytically cleaved in this process.

Immunoblots of leaf extracts of *APT1*::Ex1:GFP transformants showed that Exon1 was cleaved from GFP. This construct was amplified from genomic DNA and only the genomic fragment of Exon 1 upstream of Intron 1 was used; the portion of "Intron 1" that contains the first six amino acids of APT1.2 were not included. This transgene was constructed to determine whether translation initiation occurred at Exon 1 *in vivo* and the localization of the resulting polypeptide. It remains unclear as to whether the fusion of Exon 1 splice site with GFP resulted in a false cleavage site. The subcellular prediction tool, MitoProtII, suggests that APT1.1 has a transit peptide the end of which lies within the 6 amino acid region left out of this construct. To restore the native amino acid sequence the full-length APT1.1 ORF was used in the

actP::APT1.1:2xGFP plant lines. Immunoblots of leaf extracts from these transgenic lines showed that in the absence of Intron 1 splicing, Exon 1 was not cleaved from APT1.1. The discrepancy as to whether APT1.1 is proteolytically cleaved or not, is important since it impacts two other questions: the method by which an un-cleaved protein is imported into chloroplasts, and second, the degree of post-transcriptional regulation on APT1.1.

With respect to the chloroplast import issue, it was recently estimated that 86% of 1325 nuclear-encoded plastid proteins are translocated across the chloroplast envelope via the TOC-TIC machinery (Zybailov *et al*., 2008). All these proteins possess an N-terminal cleavable transit peptide that is released from the preprotein after translocation across the chloroplast envelope (Oblong and Lamppa, 1992). However there is growing evidence that some nuclear-encoded chloroplast proteins do not have cleavable transit peptides. One example is Tic32 that contains a small, N-terminal transit peptide sufficient for chloroplast targeting to the inner-membrane yet is not cleaved (Nada and Soll, 2004). The import method for Tic32 has yet to be elucidated, however it has been determined that inhibition of Toc159, Toc34, and Toc75 receptors does not inhibit the translocation of Tic32 into chloroplasts. Inaba and Schnell (2008) postulate in a recent review that although the import of a few proteins have been shown to be independent of the most characterized TOC-TIC proteins (i.e. Toc159), an alternative pathway may use other characterized TOC translocons. The results of a recent Arabidopsis plastid proteome analysis supports the existence of an alternative import method. Using mass spectrometry 3800 proteins were identified as part of the plastid proteome, but only 67% of these proteins were predicted by TargetP to have cleavable transit peptides (Kleffmann *et al*., 2004). *In vitro* chloroplast import assays could be used to determine whether APT1.1 is dependent or independent of Toc159, Toc34 and Toc75 machinery for import.

If APT1.1 is proteolytically cleaved when it is imported into plastids then the issue of its post-transcriptional regulation will need to be reviewed. The cleavage of APT1.1 would result in a peptide of 24 kDa, equal to that of APT1.2. Thus the intensity of 24 kDa polypeptide band visualized on immunoblots of crude leaf extracts would reflect the sum of APT1.2 and the processed APT1.1. To date, immunoblot analysis of over-expressed APT1.1 ORF and APT1.1 fusion proteins has always detected the full-length un-cleaved protein. This evidence supports the notion that APT1.1 is post-transcriptionally regulated and not subject to proteolytic cleavage. However these proteins are being expressed from transgenes residing outside the native genomic context of APT1 and it could be argued that this may affect their expression. Moreover, their expression from a cDNA removes numerous potential regulatory steps that may be a component of the processing. Future tests could involve constructing transgenes harbouring mutations at the predicted cleavage sites by TargetP and MitoProtII. If these predicted sits are indeed necessary for proteolytic processing of APT1.1 than an increase of APT1.1 protein abundance should be detected by immunoblotting.

Punctate localization of APT1.1 may be related to Chloroplasts

The localization of APT1.1 in punctate-bodies led me to consider its possible localization in mitochondria or peroxisomes because of their similarity in size and shape. However, these organelles are well known for their dynamic movement (Logan and Leaver, 2000; Titorenko and Mullen, 2006) and this movement was not observed for any of the punctate bodies in *actP*::APT1.1:2GFP plants. Additionally, the estimated size of the GFP punctate bodies was 2μm in diameter, whereas mitochondria and peroxisomes are normally 0.5 to 1μm in diameter.

The question arose as to whether these punctate bodies could reside in the chloroplast or perhaps be proplastids. This was considered because the majority of the punctate-bodies were localized adjacent to chloroplasts and detected only in optical sections where mesophyll cells were in focus. A literature search has identified two distinct proteins that are localized to chloroplasts and report similar confocal images of GFP-fusion proteins to those obtained in this study.

Plastid Envelope DNA binding protein (PEND) is a chloroplast-localized protein that is specifically targeted to the plastid nucleus, which is also known as the plastid nucleoid (Terasawa and Sato, 2005). Plastid nucleoids harbour chloroplast DNA that codes for proteins involved in photosynthesis, gene expression, or essential to plastid metabolism. PEND aids in anchoring the plastid nucleoid to the stromal side of the inner envelope. Interestingly, Myouga *et al*., 2008 showed that Iron Superoxide Dismutase 3 (FSD3) co-localizes with PEND in plastid nucleoids. Both PEND-GFP and FSD3-GFP confocal images show punctate-like structures, similar to those seen in the plants expressing *APT1.1-GFP*. In all three cases, there was no clear overlap of the punctate bodies with chlorophyll autoflorescence. Thus, it is possible that APT1.1 is being localized to non-chlorophyll containing regions of the chloroplast, similar to PEND and FSD3.

Immunogold labeling was performed on leaves of 3-week-old *apt1-3* plants containing an *actp::APT1.1* transgene to further clarify the localization of APT1.1 (Figure 27). The epitope was detected using a secondary antibody conjugated to 10 nm gold balls, via transmission electron microscopy. The results have yet to be analyzed quantitatively but it was quite evident that the gold balls were concentrated in bodies located within chloroplasts (B. Moffatt, personal

communication). Interestingly, these bodies appeared to be located near the edges of the plastids in regions with few thylakoids. To date these bodies have only been observed in the APT1.1 overexpressing line and not in the WT, but further analysis is needed confirm this conclusion. The localization of these bodies may well correspond to the punctate GFP signals observed using confocal microscopy as they both reside in regions of the chloroplast with little or no chlorophyll.

However, one discrepancy between the two detection methods is the predicted size of the punctate-bodies. Using confocal microscopy the GFP-tagged punctate-bodies were estimated to be 2 μm in diameter, whereas those imaged using the TEM were under 1 μm in diameter. One possible explanation for this could be that the intensity of the GFP fluorescence is contributing to its larger appearance by confocal microscopy.

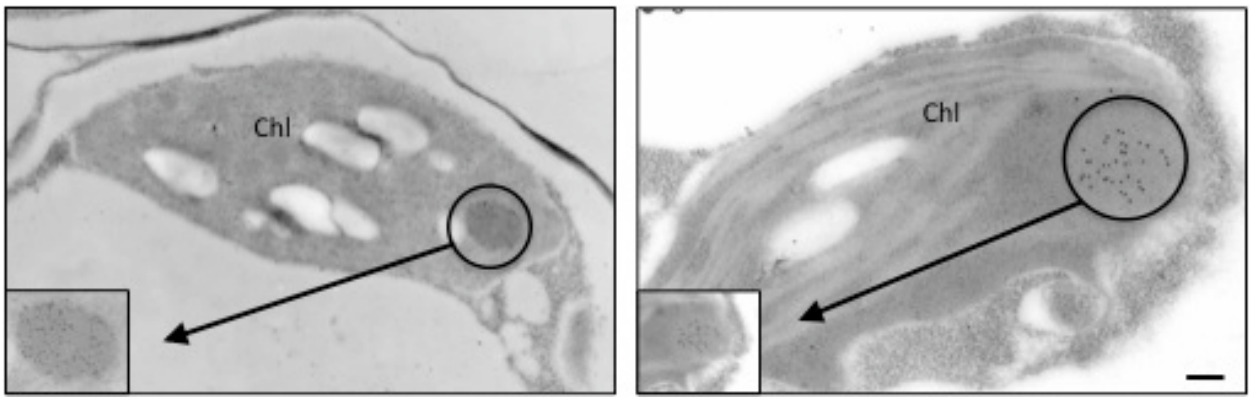

Figure 27. TEM images of *apt1-3 actP*::APT1.1 containing plant lines. Immunogold labeling of APT1.1 resulted in 10 nm gold beads localized to chloroplasts within peripheral located bodies. Chl (Chloroplast). Inset is a magnified image of the marked area. Tissue preparation and imaging performed by B. Moffatt. Scale bar represents 0.2μm.

The punctate localization of APT1.1 is perhaps of greater interest than its identified chloroplast localization. As observed in both GFP lines, expression of Exon 1-GFP fusion from

the native *APT1* promoter and over-expression of the full-length APT1.1 consistently showed this punctate signal. If these punctate bodies are representative of a specific region within chloroplasts then the *APT1*::Ex1:GFP plant lines give an accurate representation of of APT1.1's predominant localization in WT plants. Thus, the co-localization with chlorophyll auto fluorescence seen in *actP*::APT1.1:2GFP may be a result of over-expressed protein and not be representative of localization under native conditions.

Communication between *de novo* synthesis and purine salvage activities

With the localization of APT1.1 determined, future studies will need to investigate the purpose behind compartmentalizing APT1.1 within plastids. In non-plant cells *de novo* synthesis and purine salvage are both localized in the cytosol (An *et al*., 2008). This is contrary to plant cells that situate *de novo* synthesis within chloroplasts, and the purine salvage pathway in the cytosol. As a result, non-plant cells have the majority of their adenylate pool in the cytosol, whereas in plant cells the adenylate pool is equally divided between the chloroplast and cytosol. This was shown in leaf protoplasts of wheat where 47% of adenylates were found in the chloroplasts, 44% in the cytosol, and 9% in the mitochondria (Stitt *et al*., 1982). It could be argued that localizing APT1.1 to chloroplasts may mediate some kind of metabolic cross talk or coordination between the two purine biosynthesis pathways. Alternatively, the purine salvage pathways may have evolved to be targeted to chloroplasts to assist in sustaining its nucleotide pool in an energy efficient manner, as it does in the cytosol of both plant and non-plant cells.

Coordinating *de novo* synthesis and purine salvage could result in regulation of *de* novo synthesis by purine salvage. For example, in yeast, fusions of *de novo* purine gene promoters to lacZ have a 3-18 fold lower expression in the presence of adenine (Daignan-Fornier and Fink,

1992). A potential role for APT in this system was suggested to involve metabolism of adenine via APT activity, thereby removing repression from the *de novo* synthesis pathway. This mechanism would further contribute to the salvage of adenine to AMP. However, the repression of adenine on *de novo* synthesis has yet to be demonstrated outside of yeast. Rather, in plants it was shown that adenylates arising from either *de novo* synthesis or purine salvage act as negative regulators that feedback to the first enzyme (amidophosphoribosyltransferase; ATase) in *de novo* synthesis (Reynolds *et al*., 1984). Thus, in both yeast and plants purine metabolites may affect the regulation of *de novo* synthesis. The salvage pathway may supplement the adenlyate pool more in these situations, in a less energetically demanding manner. As the synthesis of purine nucleotides via the *de novo* route is energetically expensive, acknowledging the output of a less energy-demanding pathway would assist the cell in synthesizing purine nucleotides in the most energy efficient manner.

Apart from regulation, the *de novo* purine biosynthesis enzymes may be co-localized with purine salvage enzymes to coordinate metabolism during development. This would be beneficial, as nucleotide pools need to be sustained during times of cell growth and differentiation. Two studies have followed the metabolic fate of labeled purine precursors during developmental processes in plants. Both studies highlight the importance of the purine salvage pathway in growing and sustaining nucleotide pools early in development.

Brassica embryos early in development incorporate up to 75% of [8-^{14}C] adenine into adenine nucleotides with a gradual decrease to 46% incorporation during later developmental stages (Ashihara *et al*., 2008). The next largest portion of adenine was recovered in RNA, with 15-20% being incorporated throughout the four developmental stages observed. In white spruce,

a similar pattern of high purine salvage activity occurs during shoot organogenesis (Stasolla *et al*., 2006). These authors found that under shoot inducing conditions (i.e. in the presence of an exogenous supply of cytokinins) the uptake of [8-^{14}C] adenine increased up to 2.5-fold over non-shoot inducing conditions, at the peak period (day 20) when shoots began to form. Furthermore, APT activity increased 1.5-fold under shoot-inducing conditions over non-shoot-inducing conditions, throughout the 30-day observation period. Additionally, APT activity was consistently higher than that of the secondary salvage pathway. Thus, these studies show that purine salvage activity contributes largely to nucleotide pools and are most active during early stages of growth and development. However, none of these studies followed the metabolic fate of *de novo* synthesis precursors in comparison to the salvage activites.

One study followed both *de novo* and salvage purine metabolic pathways in tobacco cells undergoing programmed cell death (PCD) (Stasolla *et al*., 2005). NO and H_2O_2 production were induced in tobacco cell culture to initiate PCD. After PCD induction the metabolic fates of [8-^{14}C] adenine (purine salvage precursor) and [8-^{14}C] AICAR (*de novo* synthesis precursor) were monitored for 8 hours (Stasolla *et al*., 2005). After 2 h, APT enzymatic activity reached its maximum and the incorporation of adenine into the nucleotide fraction was higher (40% incorporation) than AICAR (12% incorporation). After 4 h, the incorporation of adenine declined to 13%, while the incorporation of AICAR increased to 18%. In addition, at 4 h a large fraction of [8-^{14}C] AICAR was shifted from degradation products to the nucleotide fraction, representing the time at which *de novo* synthesis initiates. At no point throughout the time course was there a significant incorporation of either adenine or AICAR into the nucleic acid fraction. This study was one of the first to demonstrate the early activation of purine salvage and later initiation of *de novo* synthesis. This showed the importance of coordinating purine nucleotide biosynthesis

pathways to provide quick and constant growth of nucleotide pools helping to sustain them through periods of high demand.

Based on the literature, a metabolic role for APT1.1 within chloroplasts could be proposed. The previous studies all highlight the importance of adenine salvage during intense growth periods as the majority of adenine was recovered in nucleotide fractions. It is possible that APT1.2 is insufficient to maintain nucleotide pools in the cytosol and the chloroplasts. If *de novo* synthesis initiates later than the purine salvage pathway, as reported in tobacco cells, APT1.1 may function in sustaining nucleotide pools in the chloroplast prior to start of *de novo* synthesis. Thus, one possibility is that APT1.1 and APT1.2 might be functionally similar enzymes involved in sustaining nucleotide pools.

Purine Salvage and CK metabolism in chloroplasts

A second possible role for APT1.1 in chloroplasts could relate to cytokinin metabolism. In plants, plastids are the predominant site of cytokinin biosynthesis (Sakakibara *et al*., 2006). Localization of the adenosine phosphate-isopentenyltransferase (IPT) genes that catalyze the synthesis of cytokinins has been studied in Arabidopsis using GFP protein fusions. It was shown that half of the IPT gene family (IPT1, 3, 5, 8) are localized to plastids (Kasahara *et al*., 2004). The IPT genes catalyze the synthesis of cytokinins by transferring the isoprenoid side chain to either ADP or ATP. The isoprenoid side chain can arise from two pathways: the plastid-localized methylerythriol phosphate (MEP) pathway or the cytosolic mevalonate (MVP) pathway (Rohmer, 1999). Kasahara *et al* (2004) showed that only 20% of the labeled ^{13}C precursors for the MVP pathway were incorporated into tZ and iP cytokinins; in the MEP pathway 90% of the ^{13}C precursor was recovered for the same cytokinins. These results show that MEP is the

predominant pathway for the synthesis of isoprenoid side chains as well as demonstrate that plastids are a major site of CK biosynthesis in plants.

As ADP/ATP are essential precursors for the biosynthesis of cytokinins, APT1.1 may be localized to the plastids to support the synthesis of these molecules. Cytokinins are important hormones in plant growth and development, thus the synthesis of this precursor by a rapid and efficient pathway is essential. Alternatively, APT1.1 may function in CK homeostasis by interconverting cytokinin bases to their corresponding less active nucleotide forms. These molecules can be converted back to their active base form, reducing the need for their constant *de novo* biosynthesis (Kurakawa *et al*., 2007).

To gain insight into the function of APT1.1 and APT1.2, I sought to identify their protein interactors. The objective was to find potential protein-protein interactors that would provide insight into the function or metabolic pathway in which each isoform participates. Furthermore, it was anticipated that this approach might confirm the subcellular localization of each isoform depending on the identity of the protein(s) it interacted with. The method chosen involved over-expressing each APT1 isoform fused to the eight-amino acid StrepII epitope tag, in WT plants. The hope was that this would allow for each APT1 to form its natural protein complexes *in planta* and these complexes could be recovered by affinity chromatography. Unfortunately, this method did not reveal any protein interacting partners for either isoform. However this is not a definitive result; other methods should be followed up to capture protein interacting partners since some interactions are quite dynamic and weak, although yet still functionally important. In addition, there are a number of other factors that may have contributed to a negative result. One factor could be the buffers and conditions used to purify protein complexes using the StrepII tag that may be incompatible with the APT1 proteins. This even includes the addition of other

metabolites necessary for mediating interacting partners as demonstrated by Katsir *et al* (2008). These authors showed that the presence of the hormone-conjugated amino acid (JA-Ile) was necessary to pull down tomato COI1 protein from leaf extracts using the his-tagged JAZ1 protein. For APT1.1, this may implicate the need to add adenine or cytokinins into the purification mix. A second cause of this negative result could apply to the timing at which APT1.1 is expressed. If APT1.1 and its potential protein interacting partners are co-expressed then over-expression of APT1.1 will not yield any protein interacting partners until the others are expressed.

Functional complementation of *apt1-3*

Previous work suggested that changes in both adenylate and/or cytokinin metabolism via APT1 contribute to the male sterility phenotype in *apt1-3* mutants (Zhang *et al*, 2002). To test whether APT1.1 alone could rescue male fertility the APT1.1 ORF was introduced into *apt1-3* by genetic crossing. Fertility was completely restored in all three lines of *apt1-3* mutants that over-expressed APT1.1. No abnormal phenotypes were observed in these transgenic lines with regards to their vegetative or reproductive growth.

There are several interpretations of this result. One, over-expression of APT1.1 may provide sufficient cytosolic expression for complementation of fertility. Support for this argument can be clearly seen in the *oxt1* mutant where a small fraction of cytosolic APT activity (4-6%) is able to sustain fertility. The second interpretation is that restoring one adenylate pool, that within the plastids, was sufficient to provide needed adenylates required for pollen development. Alternatively, if altered cytokinin metabolism is contributing to the male sterile phenotype then maybe over-expressed APT1.1 can restore this imbalance either in chloroplasts

or in the cytosol. Use of the native *APT1.1* promoter might reveal if the natural level of APT1.1 expression is sufficient to restore male sterility. Nonetheless, previous complementation using the APT1.2 isoform by Gaillard *et al* (1998) and in this thesis using APT1.1 provides strong evidence that both isoforms are functionally similar. However, these data do not imply that these enzymes have similar enzymatic activities. In both cases male sterility was restored in *apt1-3* plants. However, these results do not distinguish whether adenine or cytokinin metabolism is responsible for this effect.

Using amiRNAs in isoform specific gene silencing

AmiRNA lines were constructed to learn the effect of having only one APT1 isoform in WT and gain insight into the functional contribution of each enzyme in its native context., These constructs were designed to specifically target the 5′ UTR of either *APT1.1* (ami1.1) or *APT1.2* (ami1.2). The ami1.1 lines had approximately 50% reduced APT1.1 in leaves relative to WT. Surprisingly, APT1.2 protein levels were also affected in these lines by up to 50%. In the ami1.2 lines, a 50-75% reduction in APT1.2 protein in leaves was observed in some lines; APT1.1 protein levels were unaffected. For both ami1.1 and ami1.2 plants, APT1 protein abundance in inflorescences was the same as WT.

No phenotypes were observed with respect to vegetative or reproductive growth in any of the five independent plant lines of each amiRNA construct analyzed. As a result, these lines were not assayed for APT enzymatic activity, as the reduced level of expression was not enough to induce any phenotypes. However this approach should not be neglected as improvements have been made to amiRNA design software. Clearly demonstrated in these lines is the need for amiRNAs with higher efficiencies to reduce protein levels much lower than observed in the

present lines. As of now, these lines could be analyzed by mass spectrometry for insights into small perturbations in purine, nucleotide, and cytokinin pools.

Annotating APT1.1 isoforms in other plant species

Currently, the only plant genome annotated to contain a second *APT1* transcript variant (APT1.1) is Arabidopsis. APTs from other plant and non-plant species are annotated as having one transcript variant with high sequence similarity to that of APT1.2. This allows one to question whether any other species, aside from Arabidopsis, has an APT transcript containing an additional N-terminal Exon that functions as a transit peptide. As Exon 1 was shown to function as a transit peptide and there is low sequence conservation among transit peptides it is inefficient to find homologous sequences using BlastP, tBLASTn, or PSI-BLAST. However, transit peptides from closely related species are less divergent making these algorithms useful in identifying putative Exon 1 sequences within a family.

The approach I took involved searching through APT EST collections and identifying the highly conserved Exon 2 start site found in all APTs. Once identified, the EST was virtually translated and then I manually searched for upstream methionines. Putative Exon 1 sequences were defined as sequences fulfilling two criteria. First, it must have only one upstream methionine in-frame with the methionine of Exon 2. The presence of additional methionines could confuse which one provides the start site of translation. In addition, setting the criterion for only one methionine adds greater confidence that this event is real. Second, the putative Exon 1 must contain at least 30 amino acid residues. Arabidopsis Exon 1 contains 60 amino acids residues, but as transit peptides are quite variable in length a more open-size limit was selected for this criterion.

This screen has lead to two interesting observations. The first observation was that putative Exon 1 sequences were only identified in plants; none were found in yeast, mammalian, or prokaryotic transcriptomes (Figure 28). Secondly, all of these putative Exon 1 sequences contained only one upstream methionine, and as anticipated, the sequence lengths and compositions are variable, consistent with their roles as transit peptides.

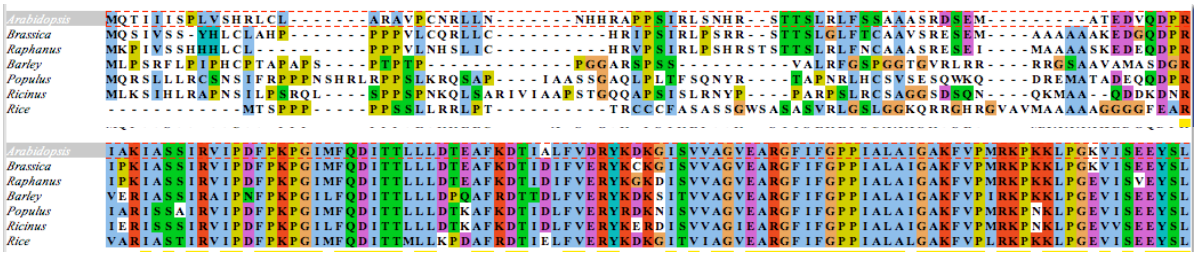

Figure 28. Multiple sequence alignment of Arabidopsis APT1.1 with APTs from other plants species. Putative Exon 1 sequences were identified by aligning the highly conserved amino acid sequence of APT1.2 with APT ESTs from other species. A manual search for an upstream open reading was carried out and sequences aligned using ClustalW.

To identify if these putative Exon 1-containing species follow speciation events, other APT sequences were analyzed. A radial tree of all APTs found in the NCBI database shows that APT evolution follows speciation (Figure 29). This is evident as plant, fungi, animal, and bacterial APT sequences all cluster together. Additionally, the phylogeny correctly shows that fungi and animal APTs are more similar than plant APTs consistent with speciation. Thus, this radial tree predicts that plant APTs evolved from a single plant APT ancestral gene.

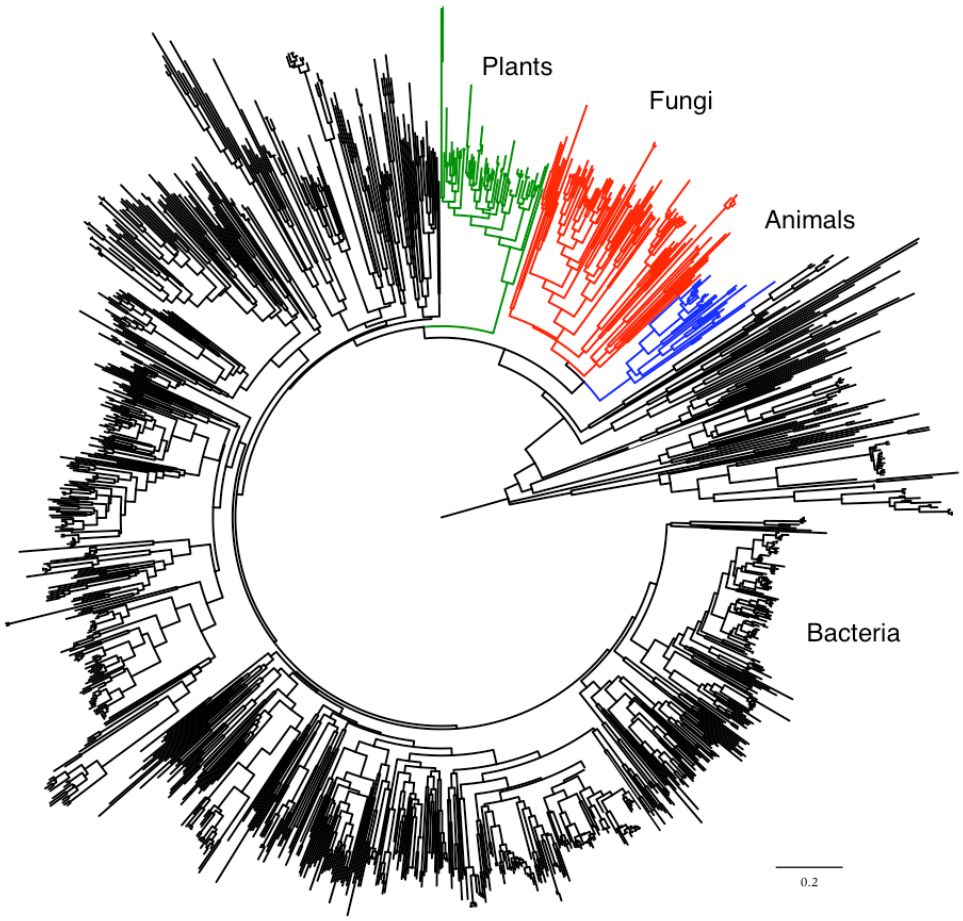

Figure 29. Radial phylogenetic tree of APT amino acid sequences from bacteria, animals, fungi and plants. All APT amino acid sequences in the NCBI database (1231 total sequences) were used to construct this phylogenetic tree. This tree shows that APT evolution is consistent with speciation as the bacterial sequences are the most ancestral, and due to the fact that and fungi and animal APTs cluster more closely together than plant sequences. Additionally, this tree predicts that all plant APTs arose from one ancestral APT gene. Bioinformatic analysis performed by Andrew Doxey.

Using this information the plant APTs containing a putative Exon 1 sequence were located on a phylogenetic tree (Figure 30). The most obvious observation from this tree is that APT isoforms from the same species exist within different clusters. This is likely due to genome duplication events. Assuming all species start off with one copy of an APT gene, genome

duplication events lead to the formation of gene families and sequence divergence throughout evolution. This explains why APT gene families are dispersed in different clusters.

Interestingly, the identified putative Exon 1-containing APT genes all cluster together. This preliminary analysis predicts that this Exon 1 arose from one common ancestor and is thus a monophyletic trait. Further investigations, will have to explore APT genes within this cluster to confirm they contain a putative Exon 1. The same analysis needs to be performed on those species outside the cluster to correctly identify the absence of Exon 1, and the time in evolution in which this monophyletic trait arose.

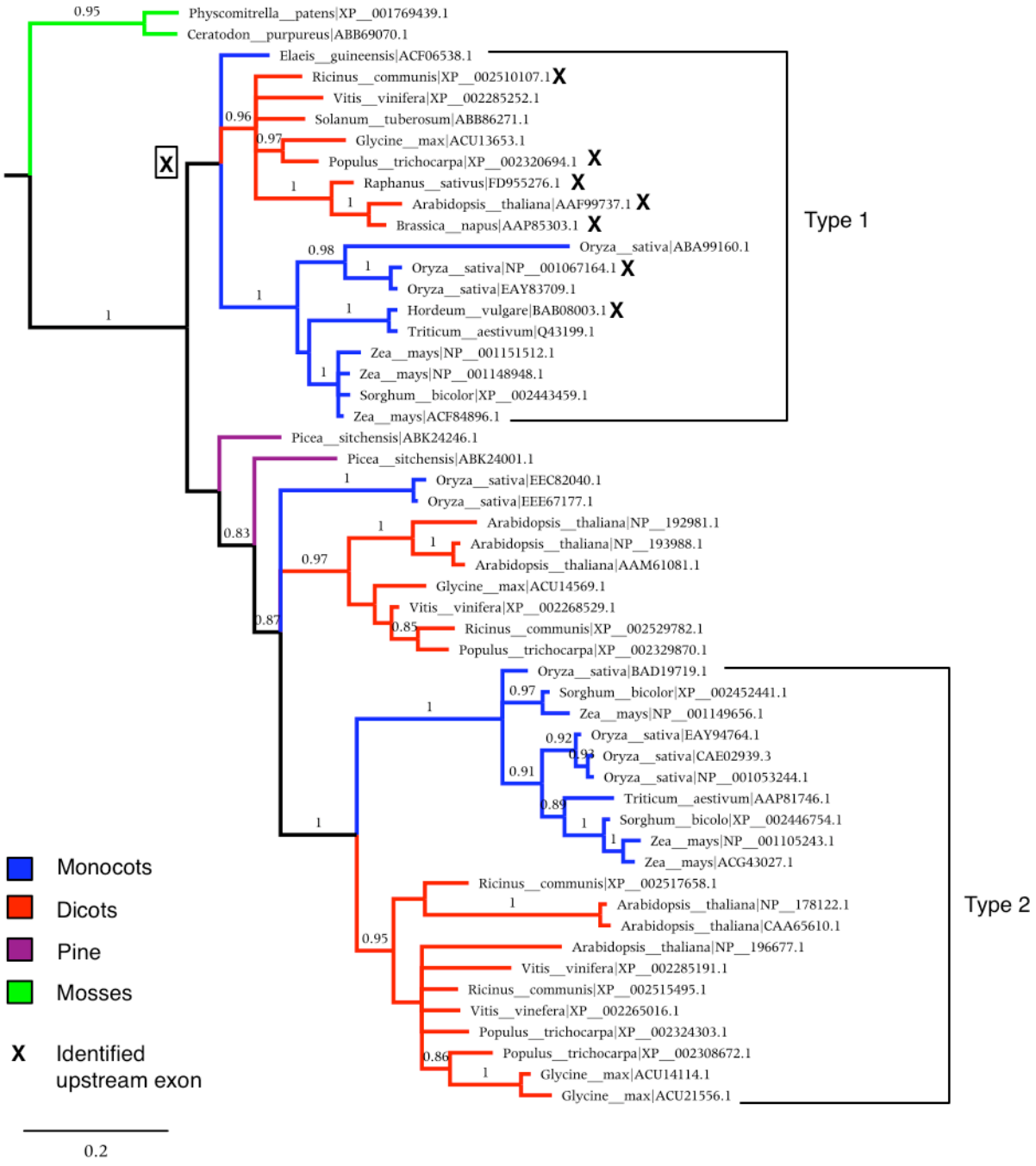

Figure 30. Bayesian phylogeny of plant APTs. All plant APT amino acid sequences from the NCBI database were used to construct this phlogeny rooted using a bacterial sequence. Consistent with speciation, this tree shows the most ancestral branches as moss (green) and pine (purple). Based on this phylogeny it is predicted that after moss the APTs diverged into three "types": the Type 1 and Type 2 sequences and a questionable third type found in-between. Interestingly, the monocot and dicot sequences form subclusters in both the Type 1 and Type 2 clusters. Putative Exon 1 sequences identified in an

earlier analysis (Figure 28) were identified on this phylogeny and remarkably these all group within one cluster. The boxed X in this image represents the ancestral APT protein in which the putative Exon 1 sequence arose. Support values for each cluster are shown on the branches; the scale bar signifies 2 amino acid mutations per 100 amino acids along this evolutionary distance. Analysis done by Andrew Doxey.

Although much remains to be learned, the results of this research indicate that the expression of this housekeeping enzyme is highly regulated and compartmentalized within the cytosol and chloroplasts of plant cells. Bioinformatic analyses support that these dual APT isoforms exist in many other plant species. This in turn will be useful in elucidating what event during plant evolution required this function to arise. The continued studies of the *APT1* locus will be of greater value in understanding the control of purine metabolism in plants.

The second part of this research focused on two APT1-deficient mutants, *apt1-3* and *oxt1*. The *apt1-3* mutant has a single nucleotide polymorphism at the splice junction of Exon 4. This mutant has about 1-2% of the APT activity of WT plants and is completely male sterile. The *oxt1* mutant contains a T-DNA insertion within Intron 1, which reduces its APT activity to about 3.1% of WT levels. However, unlike *apt1-3, oxt1* is as fertile as WT. The objective of this study was to investigate the basis of fertility in this APT-deficient mutant.

APT1 activity does not correlate with decreased fertility in *oxt1* and *oxt1apt1-3* mutants

Initial characterization of residual APT enzymatic activity showed that *apt1-3* leaves contained 2.1% residual WT APT activity while *oxt1* had 3.1% residual APT activity. These activity determinations were made using a radiochemical assay that measures the amount of ^{3}H-adenine converted to ^{3}H-AMP over time. The activities of different extracts are compared on a protein basis. Since these assays are done on crude extracts it is possible that the enzymes of the two-step adenine salvage pathway (adenine phosphorylase and ADK), which are presumably

also in the mixture, may contribute to the apparent APT activity. Since the crude extracts used for the APT assay are not desalted to remove small molecules, the ATP needed for the ADK reaction is available in small amounts (B. Moffatt, personal communication). I once tested the use of desalted extracts in the APT assay and noted a small decrease in ^{3}H-AMP production (data not shown). This decrease may be due to removal of ATP by the desalting step, thereby inhibiting ADK activity, and any contribution of the 2-step pathway. However this observation needs to be further investigated since adenine phosphorylase activity has been shown to be very low in plants and thus the contribution of the secondary pathway is likely very low as well (Ross, 1981). Thus it is doubtful that the use of desalted extracts would have changed my results or conclusions to any significant extent.

Previous phenotypic analysis of *oxt1* showed that it has 75% increased tolerance to chemically induced oxidative stress, when plated on ½ MS media supplemented with the catalase inhibitor, AT, and the glutathione biosynthesis repressor, BSO. In comparison, WT showed signs of chlorosis and root growth inhibition (D. Falcone, personal communication). Interestingly, *apt1-3* did not exhibit this stress tolerance as signs of chlorosis were observed. Root length measurements of *apt1-3* were not done due to the difficulty of growing these seedlings to be developmentally matched with WT and *oxt1*. These seedlings had to be initially germinated on ½ MS media supplemented with DAP to select for homozygous seedlings among the segregating F2 population. Although the apt1-3 seedlings are more resistant to this compound than WT plants, their residual APT activity does cause some DAP-associated toxicity and has marked effects by decreasing their growth rate relative to WT. Additionally, *apt1-3* plants are developmentally delayed relative to WT and *oxt1* throughout their life cycle in the absence of DAP selection.

To investigate whether the small difference in APT activity between *apt1-3* and *oxt1* was the basis for the difference in their fertility and stress tolerance, I created an F1 hybrid which would theoretically have an intermediate residual APT activity. The resulting F1 plant had a developmental chimeric phenotype in that the early flowers were fertile but later ones were sterile. To explain this effect, I hypothesized that the APT activity in the fertile buds was likely higher than that in the sterile buds. However, quite the contrary was observed: APT activity in the sterile buds was 4.6% higher than the fertile buds. Even more remarkable was that the APT activity in sterile buds of *oxt1apt1-3* plants was 2-4 % higher than in *oxt1* buds. The mechanism for how or why this occurs is unknown.

One possibility was that the other less predominant APTs, APT2 and APT3, might be contributing activity in the flowers. These APTs were previously shown to have a much lower affinity and V_{max} for adenine relative to APT1, but a higher affinity for cytokinins (Schnorr *et al*., 1996; Allen *et al*., 2002;). Semi-quantitative RT-PCR was used to detect any differences in the transcript abundances of APT2 and APT3 relative to WT. These data showed that there was no change in APT2 or APT3 transcript abundance in inflorescences of *oxt1*, *apt1-3*, and *oxt1apt1-3* relative to WT. While this may be true, these results are not consistent with those previously reported by Zhang (2000). Using *in situ* hybridization it was shown that APT2 and APT3 transcripts increase in *apt1-3* inflorescences relative to their abundance in WT inflorescences. The basis of this discrepancy may be attributed to the method used to detect transcript abundance in each case. The advantage of *in situ* hybridization is that changes in transcription can be detected in specific cells or tissues of an organ whereas for an RT-PCR an entire leaf or inflorescence is used as the source of RNA. In the case of these assays, I used entire inflorescences for all my assays (enzyme activity, RT-PCR and immunoblots). Thus my RT-PCR

analysis measures the total transcript abundance of all cells in the inflorescence and likely dilutes minor increases that occur in only a few cells, as was observed in the *in situ* hybridization data. A more accurate approach may involve measuring protein levels of APT2 and APT3 in *oxt1*, *apt1-3*, and *oxt1apt1-3* to confirm that changes in transcript abundance are resulting in changes in protein synthesis.

The contribution of the secondary salvage pathway was also assessed in *oxt1* and *apt1-3* for any differences that may account for their differing fertility. Radiochemical assays showed that while both had slightly higher ADK activity relative to WT (2-fold and 1.7-fold, respectively), the increases in the two mutants was not significantly different.

Although this result indicates that increased ADK activity does not account for the fertility of *oxt1,* the fact that ADK activity increases in both APT-deficient mutants is interesting. The increase in ADK activity may reflect a response to accumulating adenine. This would be accomplished by adenine phosphorlyase metabolizing adenine to adenosine, and ADK responding to this increased adenosine pool. Preliminary analysis of adenine levels in *oxt1* and *apt1-3* by HPLC and mass spectrometry analysis has shown that adenine levels are 1.5 to 3-fold greater in *oxt1* and *apt1-3* plants relative to WT (D. Falcone, personal communication). Thus it is possible that even modest increases in adenine are sensed by the cell and triggering a compensatory response in activity by the two-step adenine salvage pathway. It should be noted that these values are very preliminary and further work is underway to establish more reliable and consistent readings.

Altered cytokinin levels in *oxt1* and *apt1-3* plants

Kinetic analysis of recombinant APTs indicates that they are capable of accepting cytokinin bases as substrates. It was of interest to investigate whether cytokinin profiles of the APT-deficient mutants were altered. Leaf and bud tissue of *oxt1* and *apt1-3* plants was sent to the lab of Dr. Neil Emery (Trent University) to be analyzed by LC-tandem mass spectrometry for various cytokinin species. The data obtained to date from these measurements has not been consistent between different samplings so definitive conclusions cannot be made. However it is quite evident from these measurements that cytokinin bases are increased in both *oxt1* and *apt1-3* leaves and buds. Interestingly, the predominant cytokinin bases in Arabidopsis, tZ and iP, show the greatest fold change relative to WT (data not shown).

Interestingly, the cytokinin ribosides are not significantly altered for any of the cytokinin species measured. Thus, the cytokinin bases are accumulating but not being metabolized by adenine phosphorylase into cytokinin ribosides. This absence of adenine phosphorylase activity is consistent with previous reports that its activity is low in plants (Ross, 1981). Additionally, if cytokinin riboside levels are not affected it suggests that the higher ADK activity in these plants is not a result of increased cytokinin metabolism through the secondary salvage pathway.

As these measurements are preliminary and need further work to establish reliable values, it can be concluded at this time that the cytokinin pools are definitely altered by APT1-deficiency. Precautions have been taken to ensure consistent sampling methods each time. Such precautions include collecting tissue at a specific time in the photoperiod and collecting developmentally matched leaves and inflorescence buds.

Increased adenine is associated with stress tolerance in WT

The observations thus far have demonstrated that APT activity is not tightly associated with fertility. This is most evident in *oxt1apt1-3* plants where the APT activity is 4.6% higher in sterile buds as compared to the fertile buds. Equally as important is the approximate 1% difference in APT activity between *oxt1* and *apt1-3*. Furthermore, the secondary salvage pathway cannot account for differences in *oxt1* and *apt1-3* as the ADK activity measured is similarly increased in both mutants. These observations lead me to conclude that a third component outside of these purine salvage enzymes may be involved.

The identity of this third component might be a protein interactor, miRNA, or a metabolite. To test for a protein interacting partner StrepII epitope tagged APT1.1 and APT1.2 isoforms were introduced into Arabidopsis. As discussed in the previous section, no unique protein interacting partners were found using this particular approach; further research in this direction is necessary before the involvement of interacting partners can be ruled out. Alternatively, metabolite levels have also been investigated for differences that may attribute to the unique phenotypes observed in *oxt1* and *apt1-3* mutants.

Preliminary data suggests that adenine may contribute to the stress tolerance of *oxt1*. WT seedlings were grown on ½ MS + AT/BSO media supplemented with 2, 20, and 200 μM adenine (Figure 31). At 2 μM and 20 μM of adenine WT seedlings showed increased stress tolerance identical to *oxt1* on ½ MS + AT/BSO alone. However, *oxt1* seedlings on 20 μM adenine became stress sensitive as these seedlings grew to half the size of *oxt1* grown on lower concentrations of adenine. At 200 μM, *oxt1* showed marked defects in growth and chlorosis. Immediate signs of growth inhibition and chlorosis were observed in *apt1-3* mutants with any addition of adenine.

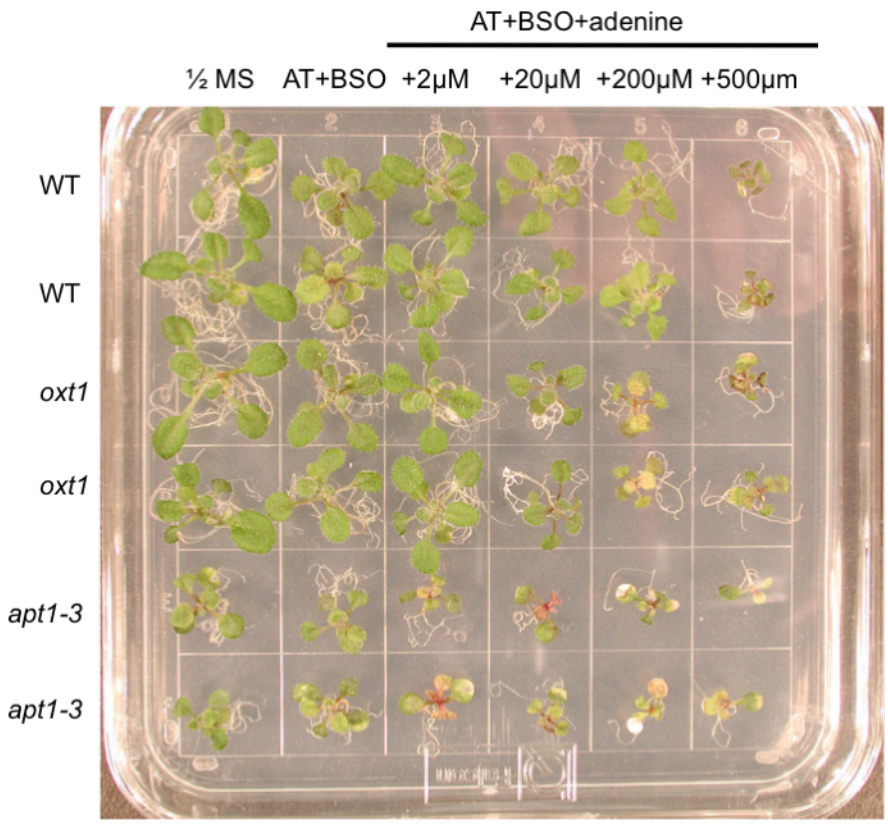

Figure 31. Effect of adenine on WT, *oxt1*, and *apt1-3* seedlings plated on stress inducing media. WT and *oxt1* seeds were first germinated and grown on ½ MS for 2 weeks; *apt1-3* seeds were germinated on ½ MS plus 0.1 mM DAP to select for homozygous seedlings. At 2 weeks, seedlings were transferred to ½ MS supplemented with 2 μM AT and 0.4 mM BSO alone or the same media with different concentrations of adenine. Seedlings were grown for an additional 2 weeks.

As mentioned earlier, HPLC analysis shows that adenine is modestly increased in *apt1-3* mutants (D. Falcone, personal communication) coinciding with the residual APT1 activity measured in each plant. Based on these observations, the earlier hypothesis of a threshold of APT activity can be revised. Instead of proposing protein activity perhaps metabolite levels are what distinguish the phenotypes observed in *oxt1* and *apt1-3*. Since metabolite measurements showed adenines levels increasing from *oxt1* to *apt1-3* then it is expected that further increases of adenine in *oxt1* would yield an *apt1-3* phenotype. This is consistent with the observation that

oxt1 mutants grown on 20 μM adenine are no longer tolerant to AT/BSO. Interestingly, adding adenine to WT seedlings resulted in an *oxt1*-like stress tolerant phenotype in these plants. Thus, *oxt1*'s APT1-deficiency may be enough to allow an accumulation of adenine that is advantageous to stress and additionally its residual APT activity is just sufficient to sustain adenylate synthesis, resulting in a fertile plant. In the case of *apt1-3*, its APT1-deficiency may be below a threshold that results in a cytotoxic accumulation of adenine and insufficient nucleotide biosynthesis to be fertile.

Although this metabolite difference is convincing of a threshold hypothesis for the *oxt1* stress tolerant phenotype, it is unknown whether adenine levels affect male fertility in the same dose-dependent manner. The current hypothesis is that a third component accounts for the phenotypic difference between *oxt1* and *apt1-3*. This third component may be a metabolite, protein, or non-coding RNA that *oxt1* uses to its advantage to compensate for APT-deficiency, in addition to conferring increased tolerance. This increase in stress tolerance may provide insight into the third component, as it could be the mechanism in which APT-deficiency is compensated for in *oxt1*. RT-PCR analysis of select antioxidant defense genes in *oxt1* indicates that three of these genes (stromal ascorbate peroxidase, thylakoid ascorbate peroxidase, and catalase 3) are up-regulated under non-stress conditions (Sukrong *et al*., manuscript in preparation). Thus, the next steps could involve investigating the transcriptional response of these genes in *apt1-3* in addition to expressing these genes in *apt1-3* as a means to test for the restoration of male fertility. Alternatively, one must consider that these genes may be indirectly involved in the observed fertility in *oxt1*. As such, the proteins with which these antioxidant defense proteins interact with and the collection of metabolites involved may also need to be elucidated. I hypothesize that these investigations may yield one of two conclusions. First, APT-deficiency is a source of stress

during pollen development and the increased response of antioxidant defense genes in *oxt1* is sufficient to rescue male sterility. Second, the increased stress response may be an indirect response to the true underlying pathway responsible for restoring male fertility in *oxt1*. I predict that the second conclusion is more plausible, as it is difficult to explain differences in adenine and cytokinin metabolism between *oxt1* and *apt1-3* based solely on a stress responsive pathway.

Thus, the basis of male fertility of *oxt1* and the sterility of *apt1-3* has yet to be learned. The data are clear that APT and ADK activities are not the only factors that determine fertility or sterility in *oxt1* and *oxt1apt1-3*. It is recognized that metabolites may be an important contributor to the fertility of these mutants. In *oxt1*, adenine may be key as this metabolite was able to confer the same degree of stress tolerance to WT seedlings as initially observed in *oxt1* plants. In both APT1-deficient mutants, the importance of cytokinin bases was clearly demonstrated by altered levels detected in both leaf and floral organs. Further resolution of the differences in cytokinin levels will no doubt provide valuable insight of these hormones in both stress tolerance and male fertility. The discovery and characterization of the unusual phenotype of *oxt1apt1-3* hybrids will lead the way in providing a model system to study changes in metabolite levels that contribute to the shift from fertility to sterility.

Appendices

Appendix 1

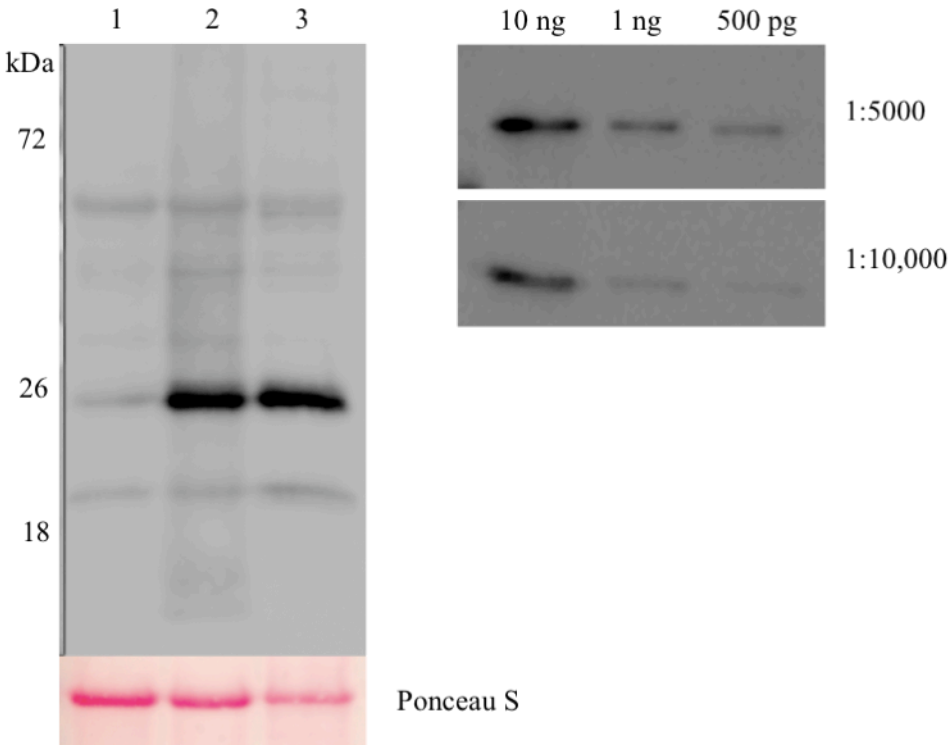

Figure 32. Testing the sensitivity and specificity of the anti-APT1 polyclonal antibody. WT (lanes 2 and 3) and *oxt1* (lane 1) leaf protein extracts were probed with the anti-APT1 polyclonal antibody at a dilution of 1:10,000 (Left panel). The anti-APT1 antibody proved to be specific as an abundant polypeptide at 24 kDa was detected in WT extracts, whereas very little polypeptide was detected for *oxt1*, consistent with this mutant being APT1-deficient. Ponceau S staining was used to test for equal loading. To test the sensitivity of the anti-APT1 antibody, 10 ng, 1 ng, and 500 pg of recombinant APT1.2-6xHIS protein was probed with the anti-APT1 antibody using two dilutions (Right panel).

Appendix 2

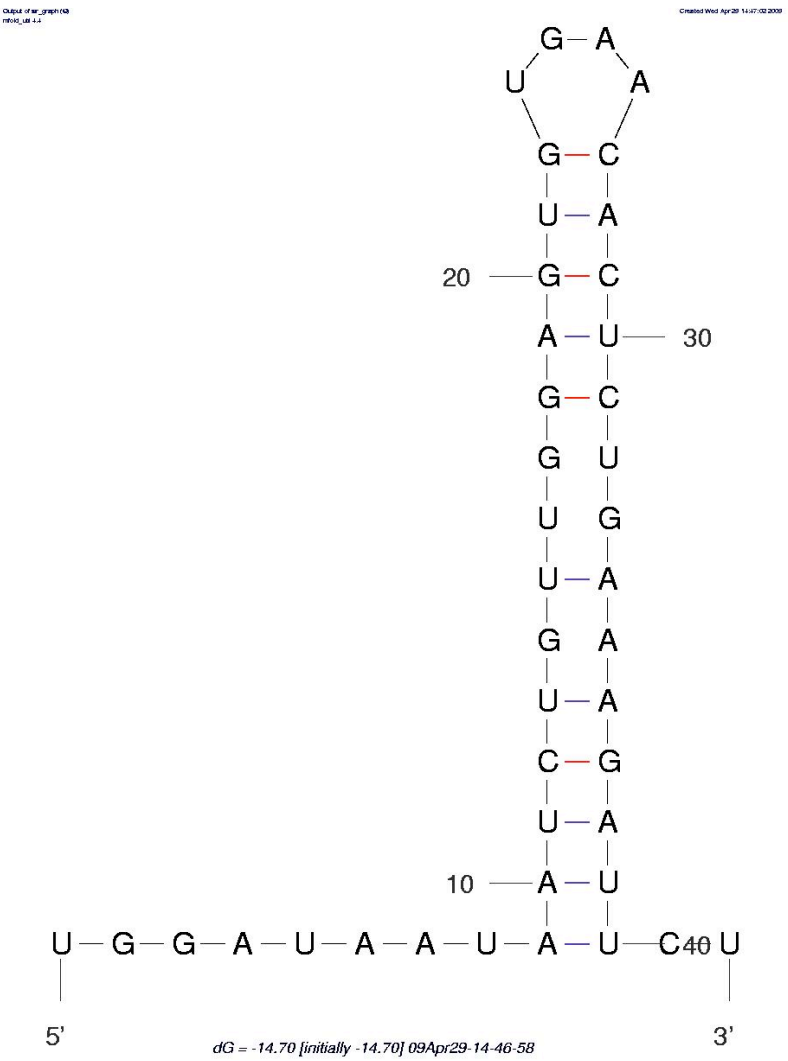

Figure 33. Computational modeling of the 5′ UTR of the *APT1.1* mRNA. The region depicted is the 5′ terminal end of the *APT1.1* mRNA consistent with that recovered in the RIKEN Arabidopsis full-length cDNA clone collection. RNA folding was performed by Yingfu Li, McMaster University.

Appendix 3

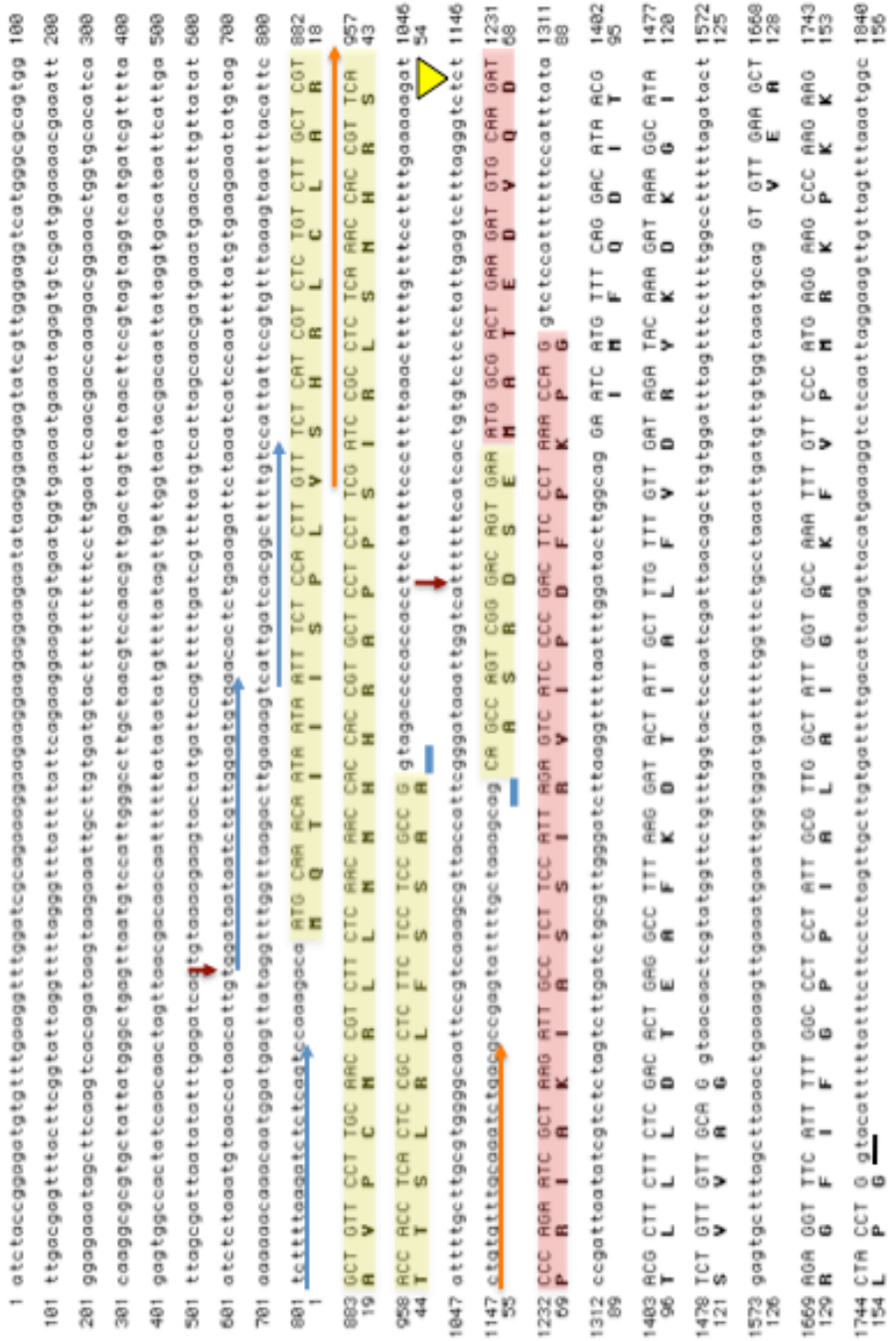

Figure 34. Partial genomic sequence of the APT1 gene. Two mRNAs arise from the *APT1* gene in Arabidopsis. The *APT1.1* primary transcript initiates at the first red arrow and is spliced at the splice acceptor and splice donor sites underlined in blue, to remove the first Exon. The translation of this mRNA begins at Exon 1 (highlighted in yellow) and the resulting polypeptide includes the 6 amino acids adjacent

to Exon 2 (highlighted in red). The *APT1.2* primary transcript initiates at the second red arrow with part of Intron 1 forming the 5′UTR. The translation of this mRNA initiates at Exon 2. Note that the APT1.2 polypeptide does not contain the 6 amino acids adjacent to Exon 2; these are only present in an APT1.1 polypeptide. Blue arrows represent forward primers AP183, AP184, and AP187 used to PCR fragments of the 5′ UTR in Figure 5. Primer AP183 (first blue arrow) is located in the same region as the predicted stem-loop structure shown in Figure 33. Orange arrows are forward primers AP186 and 187 using in semi-quantitative RT-PCR. Yellow triangle represents location of T-DNA insertion in *oxt1* allele; black line represents point mutation of apt1-3 (GT → AT).

Appendix 4

oxt1 transgenic lines expressing either the APT1.1 or APT1.2 ORF were constructed (*oxt1*/*actinP*::APT1.1 and *oxt1*/*actinP*::APT1.2, respectively). The APT1.1 and APT1.2 ORFs were cloned under the expression of the actin promoter in a vector expressing glufosinate ammonium resistance (which confers BASTA resistance). These constructs were introduced into *oxt1* mutants by the floral dip method. Three stable transformants were recovered for each line. Immunoblot analysis of *oxt1*/*actinP*::APT1.1 plant containing lines detected a 26 kDa APT1.1 polypeptide; a 24 kDa APT1.2 polypeptide was detected in *oxt1*/*actinP*::APT1.2 plants. For both plant lines no effects on vegetative and reproductive growth were observed relative to WT.

The detection of APT1.1 and APT1.2 polypeptides in the *oxt1* transgenic mutants is an interesting observation considering *oxt1* heterozygous plants (*oxt1*/WT *APT1)*. *oxt1* heterozygous plants grown on ½ MS media supplemented with AT + BSO exhibit increased stress tolerance and phenotypically resemble *oxt1* homozygous plants (Sukrong *et al*., manuscript in preparation). These data indicate that the *oxt1* allele is dominant to the WT *APT1* allele. However, this dominance is not exhibited over the *actinP*::APT1.1 or *actinP*::APT1.2 transgenes in *oxt1* as the respective APT1 polypeptides were detected by immunoblotting. In these transgenes only the APT1 ORFs were present, the *APT1* regulatory elements (promoter, UTR, intronic regions) were absent. Taken together, these results point towards the importance of the WT *APT1* regulatory elements as targets for *oxt1* to exhibit its dominance over this allele.

References

Allen, M., Qin, W., Moreau, F., & Moffatt, B. (2002). Adenine phosphoribosyltransferase isoforms of Arabidopsis and their potential contributions to adenine and cytokinin metabolism. *Physiologia Plantarum, 115*(1), 56-68

An, S., Kumar, R., Sheets, E. D., & Benkovic, S. J. (2008). Reversible compartmentalization of de novo purine biosynthetic complexes in living cells. *Science, 320*(5872), 103

Arabidopsis Genome Initiative. (2000). Analysis of the genome sequence of the flowering plant *Arabidopsis thaliana*. *Nature, 408*(6814), 796-815

Ashihara, H. (1983). Changes in activities of purine salvage and ureide synthesis during germination of black gram (*Phaseolus mungo*) seeds. *Zeitschrift Für Pflanzenphysiologie, 113*(1), 47-60

Ashihara, H., Luit, B., Belmonte, M., & Stasolla, C. (2008). Metabolism of nicotinamide, adenine and inosine in developing microspore-derived canola (*Brassica napus*) embryos. *Plant Physiology Et Biochemistry, 46*(8-9), 752-759

Ashihara, H., & Ukaji, T. (1985). Presence of adenine phosphoribosyltransferase and adenosine kinase in chloroplasts of spinach leaves. *The International Journal of Biochemistry, 17*(11), 1275-1277

Atkins, C. A., Smith, P. M. C., & Storer, P. J. (1997). Reexamination of the intracellular localization of de novo purine synthesis in cowpea nodules. *Plant Physiology, 113*(1), 127-135

Blanc, G., Barakat, A., Guyot, R., Cooke, R., & Delseny, M. (2000). Extensive duplication and reshuffling in the Arabidopsis genome. *The Plant Cell Online, 12*(7), 1093-1102

Boland, M. J., Hanks, J. F., Reynolds, P. H. S., Blevins, D. G., Tolbert, N. E., & Schubert, K. R. (1982). Subcellular organization of ureide biogenesis from glycolytic intermediates and ammonium in nitrogen-fixing soybean nodules. *Planta, 155*(1), 45-51

Boland, M. J., & Schubert, K. R. (1983). Biosynthesis of purines by a proplastid fraction from soybean nodules. *Archives of Biochemistry and Biophysics, 220*(1), 179-187

Breaker, R. R. (2008). Complex riboswitches. *Science Signaling, 319*(5871), 1795

Carninci, P., Nishiyama, Y., Westover, A., Itoh, M., Nagaoka, S., Sasaki, N., Okazaki, Y., Muramatsu, M., & Hayashizaki, Y. (1998). Thermostabilization and thermoactivation of thermolabile enzymes by trehalose and its application for the synthesis of full length cDNA. *Proceedings of the National Academy of Sciences, 95*(2), 520-524

Cheah, M. T., Wachter, A., Sudarsan, N., & Breaker, R. R. (2007). Control of alternative RNA splicing and gene expression by eukaryotic riboswitches. *Nature, 447*(7143), 497-500

Chen, W. H., Guanting, L., Congying, L., Changqing, Z., & Songnian, H. (2007). Systematic analysis of alternative first exons in plant genomes. *BMC Plant Biology, 7*(55)

Chen, C. M., Melitz, D. K., & Clough, F. W. (1982). Metabolism of cytokinin: Phosphoribosylation of cytokinin bases by adenine phosphoribosyltransferase from wheat germ. *Archives of Biochemistry and Biophysics, 214*(2), 634-641

Clough, S. J., & Bent, A. F. (1998). Floral dip: A simplified method for Agrobacterium-mediated transformation of *Arabidopsis thaliana*. *Plant Journal, 16*(6), 735

Daignan-Fornier, B., & Fink, G. R. (1992). Coregulation of purine and histidine biosynthesis by the transcriptional activators BAS1 and BAS2. *Proceedings of the National Academy of Sciences, 89*(15), 6746-6750

D'Angelo, M. A., Raices, M., Panowski, S. H., & Hetzer, M. W. (2009). Age-dependent deterioration of nuclear pore complexes causes a loss of nuclear integrity in postmitotic cells. *Cell, 136*(2), 284-295

Doree, M. (1973). Metabolism of exogenous adenine by *Acer pseudoplatanus* cells. *Phytochemistry, 12*, 2101-2108

Emanuelsson, O., Nielsen, H., Brunak, S., & von Heijne, G. (2000). Predicting subcellular localization of proteins based on their N-terminal amino acid sequence. *Journal of Molecular Biology, 300*(4), 1005-1016

Gaillard, C., Moffatt, B. A., Blacker, M., & Laloue, M. (1998). Male sterility associated with APRT deficiency in *Arabidopsis thaliana* results from a mutation in the gene *APT1*. *Molecular and General Genetics MGG, 257*(3), 348-353

Goggin, D. E., Lipscombe, R., Fedorova, E., Millar, A. H., Mann, A., Atkins, C. A., & Smith, P. M. C. (2003). Dual intracellular localization and targeting of aminoimidazole ribonucleotide synthetase in cowpea. *Plant Physiology, 131*(3), 1033-1041

Gooljarsingh, L. T., Ramcharan, J., Gilroy, S., & Benkovic, S. J. (2001). Localization of GAR transformylase in *Escherichia coli* and mammalian cells. *Proceedings of the National Academy of Sciences, 98*(12), 6565

Haan, C., & Behrmann, I. (2007). A cost effective non-commercial ECL-solution for western blot detections yielding strong signals and low background. *Journal of Immunological Methods, 318*(1-2), 11-19

Hirose, N., Takei, K., Kuroha, T., Kamada-Nobusada, T., Hayashi, H., & Sakakibara, H. (2007). Regulation of cytokinin biosynthesis, compartmentalization and translocation. *Journal of Experimental Botany, 59*(1), 75-83

Hung, W. F., Chen, L. J., Boldt, R., Sun, C. W., & Li, H. (2004). Characterization of Arabidopsis glutamine phosphoribosyl pyrophosphate amidotransferase-deficient mutants. *Plant Physiology, 135*(3), 1314-1323

Kakimoto, T. (2001). Identification of plant cytokinin biosynthetic enzymes as dimethylallyl diphosphate: ATP/ADP isopentenyltransferases. *Plant and Cell Physiology, 42*(7), 677-685

Kasahara, H., Takei, K., Ueda, N., Hishiyama, S., Yamaya, T., Kamiya, Y., Yamaguchi, S., & Sakakibara, H. (2004). Distinct isoprenoid origins of cis- and trans-zeatin biosyntheses in Arabidopsis. *The Journal of Biological Chemistry, 279*(14), 14049-14054

Katsir, L., Schilmiller, A. L., Staswick, P. E., He, S. Y., & Howe, G. A. (2008). COI1 is a critical component of a receptor for jasmonate and the bacterial virulence factor coronatine. *Proceedings of the National Academy of Sciences, 105*(19), 7100

Kimura, K., Wakamatsu, A., Suzuki, Y., Ota, T., Nishikawa, T., Yamashita, R., Yamamoto, J., Sekine, M., Tsuritani, K., Wakaguri, H., Ishii, S., Sugiyama, T., Saito, K., Isono, Y., Irie, R., Kushida, N., Yoneyama, T., Otsuka, R., Kanda, K., Yokoi, T., Kondo, H., Wagatsuma, M., Murakawa, K., Ishida, S., Ishibashi, T., Takahashi-Fujii, A., Tanase, T., Nagai, K., Kikuchi, H., Nakai, K., Isogai, T., & Sugano, S. (2006). Diversification of transcriptional modulation: Large-scale identification and characterization of putative alternative promoters of human genes. *Genome Research, 16*(1), 55-65

Kleffmann, T., Russenberger, D., von Zychlinski, A., Christopher, W., Sjölander, K., Gruissem, W., & Baginsky, S. (2004). The *Arabidopsis thaliana* chloroplast proteome reveals pathway abundance and novel protein functions. *Current Biology, 14*(5), 354-362

Koncz, C., & Schell, J. (1986). The promoter of T L-DNA gene 5 controls the tissue-specific expression of chimaeric genes carried by a novel type of Agrobacterium binary vector. *Molecular and General Genetics MGG, 204*(3), 383-396

Kurakawa, T., Ueda, N., Maekawa, M., Kobayashi, K., Kojima, M., Nagato, Y., Sakakibara, H., & Kyozuka, J. (2007). Direct control of shoot meristem activity by a cytokinin-activating enzyme. *Nature, 445*(7128), 652-655

Le Floc'h, F., & Lafleuriel, J. (1983). The role of mitochondria in the recycling of adenine into purine nucleotides in the jerusalem artichoke (*Helianthus tuberorus* L.). *Zeitschrift Für Pflanzenphysiologie, 113*(1), 61-71

Lecomte, I., & Le Floc'h, F. (1999). Adenine phosphoribosyltransferase of peach tree leaves: Purification and properties. *Journal of Plant Physiology, 154*(3), 289-295

Lee, D., & Moffatt, B. A. (1993). Purification and characterization of adenine phosphoribosyltransferase from *Arabidopsis thaliana*. *Physiologia Plantarum, 87*(4), 483-492

Lee, D., & Moffatt, B. A. (1994). Adenine salvage activity during callus induction and plant growth. *Physiologia Plantarum, 90*(4), 739-747

Leroch, M., Kirchberger, S., Haferkamp, I., Wahl, M., Neuhaus, H. E., & Tjaden, J. (2005). Identification and characterization of a novel plastidic adenine nucleotide uniporter from *Solanum tuberosum*. *Journal of Biological Chemistry, 280*(18), 17992

Li, Y., & Breaker, R.R. (1999) Kinetics of RNA degradation by specific base catalysis of transesterification involving the 2′-hydroxyl group. *Journal of the American Chemical Society, 121* (23), 5364-5372

Logan, D. C., & Leaver, C. J. (2000). Mitochondria-targeted GFP highlights the heterogeneity of mitochondrial shape, size and movement within living plant cells. *Journal of Experimental Botany, 51*(346), 865-871

Miranda, P. V., Brandelli, A., & Tezon, J. G. (1993). Instantaneous blocking for immunoblots. *Analytical Biochemistry, 209*(2), 376-377

Moffatt, B., Pethe, C., & Laloue, M. (1991). Metabolism of benzyladenine is impaired in a mutant of *Arabidopsis thaliana* lacking adenine phosphoribosyltransferase activity. *Plant Physiology, 95*(3), 900-908

Moffatt, B., & Somerville, C. (1988). Positive selection for male-sterile mutants of Arabidopsis lacking adenine phosphoribosyltransferase activity. *Plant Physiology, 86*(4), 1150-1154

Moffatt, B. A., McWhinnie, E. A., Agarwal, S. K., & Schaff, D. A. (1994). The adenine phosphoribosyltransferase-encoding gene of *Arabidopsis thaliana*. *Gene, 143*(2), 211-216

Moffatt, B. A., McWhinnie, E. A., Burkhart, W. E., Pasternak, J. J., & Rothstein, S. J. (1992). A complete cDNA for adenine phosphoribosyltransferase from *Arabidopsis thaliana*. *Plant Molecular Biology (Netherlands), 18*, 653-662

Moffatt, B. A., Wang, L., Allen, M. S., Stevens, Y. Y., Qin, W., Snider, J., & von Schwartzenberg, K. (2000). Adenosine kinase of Arabidopsis: Kinetic properties and gene expression. *Plant Physiology, 124*(4), 1775-1785

Myouga, F., Hosoda, C., Umezawa, T., Iizumi, H., Kuromori, T., Motohashi, R., Shono, Y., Nagata, N., Ikeuchi, M., & Shinozaki, K. (2008). A heterocomplex of iron superoxide dismutases defends chloroplast nucleoids against oxidative stress and is essential for chloroplast development in Arabidopsis. *The Plant Cell Online, 20*(11), 3148

Nada, A., & Soll, J. (2004). Inner envelope protein 32 is imported into chloroplasts by a novel pathway. *Journal of Cell Science, 117*(17), 3975-3982

Nielsen, H., Engelbrecht, J., Brunak, S., & Von Heijne, G. (1997). Identification of prokaryotic and eukaryotic signal peptides and prediction of their cleavage sites. *Protein Engineering Design and Selection, 10*(1), 1-6

Oblong, J. E., & Lampa, G. K. (1992). Identification of two structurally related proteins involved in proteolytic processing of precursors targeted to the chloroplast. *EMBO Journal, 11*(12), 4401-4409

Regan, S. M., & Moffatt, B. A. (1990). Cytochemical analysis of pollen development in wild-type Arabidopsis and a male-sterile mutant. *The Plant Cell Online, 2*(9), 877-889

Reynolds, P. H., Blevins, D. G., & Randall, D. D. (1984). 5-phosphoribosylpyrophosphate amidotransferase from soybean root nodules: Kinetic and regulatory properties. *Archives of Biochemistry and Biophysics, 229*(2), 623-631

Rohmer, M., & Rohmer, M. (1999). The discovery of a mevalonate-independent pathway for isoprenoid biosynthesis in bacteria, algae and higher plants. *Natural Product Reports, 16*(5), 565-574

Ross, C. W. (1981). In Marcus A. (Ed.), *Biosynthesis of nucleotides*. New York: Academic Press

Sakakibara, H. (2006). Cytokinins: Activity, biosynthesis, and translocation. *Annual Review of Plant Biology, 57*, 431-449

Schnorr, K. M., Gaillard, C., Biget, E., Nygaard, P., & Laloue, M. (1996). A second form of adenine phosphoribosyltransferase in *Arabidopsis thaliana* with relative specificity towards cytokinins. *The Plant Journal, 9*(6), 891-898

Schwab, R., Palatnik, J. F., Riester, M., Schommer, C., Schmid, M., & Weigel, D. (2005). Specific effects of microRNAs on the plant transcriptome. *Developmental Cell, 8*(4), 517-527

Seki, M., Carninci, P., Nishiyama, Y., Hayashizaki, Y., & Shinozaki, K. (1998). High-efficiency cloning of Arabidopsis full-length cDNA by biotinylated CAP trapper. *Plant Journal, 15*(5), 707

Senecoff, J. F., McKinney, E. C., & Meagher, R. B. (1996). De novo purine synthesis in *Arabidopsis thaliana* (II. the PUR7 gene encoding 5 [prime]-phosphoribosyl-4-(N-succinocarboxamide)-5-aminoimidazole synthetase is expressed in rapidly dividing tissues). *Plant Physiology, 112*(3), 905-917

Shelp, B. J., Atkins, C. A., Storer, P. J., & Canvin, D. T. (1983). Cellular and subcellular organization of pathways of ammonia assimilation and ureide synthesis in nodules of cowpea (*Vigna unguiculata* L. walp.). *Archives of Biochemistry and Biophysics, 224*(2), 429-441

Smith, A. L. G. (1997). Localization of *Arabidopsis thaliana* (L.) heynh adenine phosphoribosyltransferase. M.Sc. Thesis. University of Waterloo, Waterloo ON

Smith, P. M. C., & Atkins, C. A. (2002). Purine biosynthesis: Big in cell division, even bigger in nitrogen assimilation. *Plant Physiology, 128*(3), 793-802

Smith, P. M. C., Mann, A. J., Goggin, D. E., & Atkins, C. A. (1998). AIR synthetase in cowpea nodules: A single gene product targeted to two organelles? *Plant Molecular Biology, 36*(6), 811-820

Spichal, L., Rakova, N. Y., Riefler, M., Mizuno, T., Romanov, G. A., Strnad, M., & Schmulling, T. (2004). Two cytokinin receptors of *Arabidopsis thaliana*, CRE1/AHK4 and AHK3, differ in their ligand specificity in a bacterial assay. *Plant and Cell Physiology, 45*(9), 1299-1305

Stasolla, C., Loukanina, N., Ashihara, H., Yeung, E. C., & Thorpe, T. A. (2006). Changes of purine and pyrimidine nucleotide biosynthesis during shoot initiation from epicotyl explants of white spruce (*Picea glauca*). *Plant Science, 171*(3), 345-354

Stasolla, C., Loukanina, N., Yeung, E. C., & Thorpe, T. A. (2005). Progression of programmed cell death in tobacco BY-2 cells is delineated by specific changes in de novo and salvage synthesis of purine nucleotides. *Physiologia Plantarum, 123*(3), 254-261

Stitt, M., Lilley, R. M. C., & Heldt, H. W. (1982). Adenine nucleotide levels in the cytosol, chloroplasts, and mitochondria of wheat leaf protoplasts. *Plant Physiology, 70*(4), 971-977

Sukrong, S., Yun, K. Y., Stadler, P., Feldman, G., Kumar, C., Facciuolo, A., Moffatt, B. A., & Falcone, D. L. Improved growth and stress tolerance in the Arabidopsis *oxt1* mutant triggered by altered adenine metabolism, manuscript in preparation

Sun, Q., Zybailov, B., Majeran, W., Friso, G., Olinares, P. D. B., & van Wijk, K. J. (2009). PPDB, the plant proteomics database at Cornell. *Nucleic Acids Research, 37* (Database issue), D969

Terasawa, K., & Sato, N. (2005). Visualization of plastid nucleoids *in situ* using the PEND-GFP fusion protein. *Plant and Cell Physiology, 46*(4), 649-660

Titorenko, V. I., & Mullen, R. T. (2006). Peroxisome biogenesis: The peroxisomal endomembrane system and the role of the ER. *Journal of Cell Biology, 174*(1), 11

Tzfira, T., Tian, G. W., Lacroix, B., Vyas, S., Li, J., Leitner-Dagan, Y., Krichevsky, A., Taylor, T., Vainstein, A., & Citovsky, V. (2005). pSAT vectors: A modular series of plasmids for autofluorescent protein tagging and expression of multiple genes in plants. *Plant Molecular Biology, 57*(4), 503-516

Wachter, A., Tunc-Ozdemir, M., Grove, B. C., Green, P. J., Shintani, D. K., & Breaker, R. R. (2007). Riboswitch control of gene expression in plants by splicing and alternative 3'end processing of mRNAs. *The Plant Cell Online, 19*(11), 3437

Werner, A. K., Sparkes, I. A., Romeis, T., & Witte, C. P. (2008). Identification, biochemical characterization, and subcellular localization of allantoate amidohydrolases from Arabidopsis and soybean. *Plant Physiology, 146*(2), 418

Winkler, W., Nahvi, A., & Breaker, R. R. (2002). Thiamine derivatives bind messenger RNAs directly to regulate bacterial gene expression. *Nature, 419*(6910), 952-956

Witte, C. P., Noel, L., Gielbert, J., Parker, J., & Romeis, T. (2004). Rapid one-step protein purification from plant material using the eight-amino acid StrepII epitope. *Plant Molecular Biology, 55*(1), 135-147

Zhang, C. (2000). The involvement of adenine phosphoribosyltransferase in microsporogenesis of *Arabidopsis thaliana*. M.Sc. Thesis. University of Waterloo, Waterloo ON

Zhang, C., Guinel, F. C., & Moffatt, B. A. (2002). A comparative ultrastructural study of pollen development in *Arabidopsis thaliana* ecotype columbia and male-sterile mutant *apt1-3*. *Protoplasma, 219*(1), 59-71

Zhang, J., Addepalli, B., Yun, K. Y., Hunt, A. G., Xu, R., Rao, S., Li, Q. Q., & Falcone, D. L. (2008). A polyadenylation factor subunit implicated in regulating oxidative signaling in *Arabidopsis thaliana*. *PLoS ONE, 3*(6)

Zrenner, R., Stitt, M., Sonnewald, U., & Boldt, R. (2006). Pyrimidine and purine biosynthesis and degradation in plants. *Annual Review of Plant Biology, 57*, 805-836

Zybailov, B., Rutschow, H., Friso, G., Rudella, A., Emanuelsson, O., Sun, Q., & van Wijk, K. J. (2008). Sorting signals, N-terminal modifications and abundance of the chloroplast proteome. *PLoS One, 3*(4)